Spring 1-1-2013

An Evaluation and Model of the Chinese Kang System to Improve Domestic Comfort in Northeast Rural China

Andrew Porter Yates
University of Colorado at Boulder, porteryates@gmail.com

AN EVALUATION AND MODEL OF THE CHINESE KANG SYSTEM TO IMPROVE DOMESTIC COMFORT IN NORTHEAST RURAL CHINA

By

ANDREW PORTER YATES

B.S., University of Colorado, 2006

A thesis submitted to the

Faculty of the Graduate School of the

University of Colorado in partial fulfillment

of the requirement for the degree of

Masters of Science

Department of Civil, Environmental and Architectural Engineering

2013

This thesis entitled:
An evaluation and model of the Chinese kang system to improve domestic comfort in northeast rural China
written by Andrew Porter Yates
has been approved for the Department of Civil, Environmental and Architectural Engineering

_____

(John Zhai)

_____

(Bernard Amadei)

_____

(Paul Chinowsky)

Date: _____

The final copy of this thesis has been examined by the signatories, and we find that both the content and the form meet acceptable presentation standards of scholarly work in the above mentioned discipline.

Yates, Andrew Porter (M.S., Civil Engineering)

An evaluation and model of the Chinese kang system to improve domestic comfort in northeast rural china

Thesis directed by Professor John Zhai

Many homes in northeast rural China are not heated sufficiently during the winter months. Rural residents use a traditional system of a stove and Chinese Kang to heat their homes. The current system is inefficient and requires high levels of fuel consumption. The kang system was researched with the goal of creating a simplified system modeling program. Using existing literature and data provided by Dalian University of Technology, a computer model was built. The model is modular with the aim to assist in designing and optimizing the domestic kang heating system. A basic model was created using Excel and Microsoft Visual Basic for Applications (VBA). The output of the basic model was calibrated and a sensitivity analysis of the variables was performed. Once the base scenario of the model's output was verified, improvements were modeled and tested. Some of the improvement scenarios tested include: adding a heat exchanger and radiator system to the existing kang set up, increased building insulation and the placement of phase change material on the surface of the kang. The results from a myriad of scenarios were evaluated on their technical ability to increase domestic comfort. Additionally, input from local communities was used to assess rural residents' heating needs and their acceptability of possible solutions. The technical solutions that were developed must be economic, environmentally satisfactory and culturally sensitive. Results from the completed model and information gathered from the rural communities provided a framework of optimization. An economic analysis was used to evaluate the long term feasibility of possible optimized improvements. It was determined that the addition of a room radiator system, consisting of a heat exchanger, water tank, thermostat controls and a panel radiator, delivered the most economical solution in regards to the increasing the resident's comfort per dollar invested. Furthermore, many rural homes in the northeast already have coal fired

boiler and radiator systems installed. Removing the coal boiler and replacing it with a stove heat exchanger, lessens the household's dependence on coal while still providing adequate comfort during the coldest months of the year. This improved solution meets a concord of technical, social and environmental needs and should be investigated further.

Dedicated to S.P. and Estelle Yates

Acknowledgement

I would like to thank Dalian University of Technology and The National Natural Science Foundation of China (Project No. 51178074) for providing me with the opportunity to study in China. The university was extremely accommodating and helpful; I am grateful for the time and effort that went into setting up my visits to the local communities and the hospitality provided during my time at the University.

Particularly, I would like to thank Professor Duanmu for her assistance in creating this project and providing me the opportunity to experience rural Chinese culture, Professor Wong for his technical expertise and his family for their accommodation in Chengde, and Liu Ying for her help translating and sharing her time to teach me about Chinese culture.

Finally, I'd like to thank Professor John Zhai for his guidance and assistance throughout the entirety of this project.

Contents

Table of Tables

Table of Figures

Chapter I: Background Information

1.1 Introduction

The average indoor temperature of a rural home in northeast China often falls below 16 °C, considered the minimum acceptable indoor temperature by the World Health Organization (WHO, 2000). Traditional stove and kang-platform systems are used to heat more than 85% of homes in the northeast region (Yang, 2010). Fuel is burned in the stove and the hot exhaust travels through the kang which acts as a rudimentary heat exchanger. The kang also serves as a bed base for the building's occupants. The current system is inefficient and requires high levels of fuel consumption. Many residents rely on coal fired boilers and radiator systems to achieve a comfortable temperature in their home.

The fuel used in the stove is usually biomass such as corn stalks, corn cobs or wood; sometimes coal is used as well. On average, the stove is used three times per day, early in the morning for breakfast, around mid-day for lunch and once in the evening for dinner. During the firing period and the time period directly afterwards, the kang's body remains warm and transfers energy to the room's air. However, several hours after the stove is fired, the kang and air temperatures drop, sometimes below 10°C, reducing the thermal comfort of the home's residents.

Research was conducted regarding the Kang system and used to develop a simplified system model. The aim of the model is to assist in designing and optimizing domestic heating systems in rural northeast China. Complex and detailed models currently exist, however their use is often limited and restricted. Detailed data are required to obtain meaningful results. The goal of developing a simplified model of the kang system is to create a tool that can quickly evaluate possible improvements without requiring

significant technical data to function. Data from previous field trials conducted by Dalian University of Technology, along with research data from existing literature were used to construct and validate the system model.

Local communities were visited and the residents' needs were assessed through interviews and focus groups. While each community is unique, common issues regarding heating and energy existed throughout. Successful solutions that address shared problems must be sensitive to unique cultural practices. The field visits also provided insight into cultural behavior and possible hurdles that will require more than technical solutions to overcome.

Results from the completed model and information gathered from the rural communities provided a framework of optimization. Some solutions are technically feasible but require significant work to implement due to cultural and behavioral barriers. Conversely, some solutions are supported and encouraged by the studied communities but are technically or economically difficult to implement. An economic analysis was carried out to determine which possible solutions would be most cost efficient for the affected communities.

1.2 Purpose of Study

The country of China has five climate zones: Severe Cold Zone, Cold Zone, Hot Summer and Cold Winter Zone, Mild Zone and Hot Summer and Warm Winter Zone. In the Severe Cold Zone, the region of study, the average outdoor temperature during winter months can be as low as -10 ℃ (Chen, 2007). **Error! Reference source not found.** illustrates the five different climates zones.

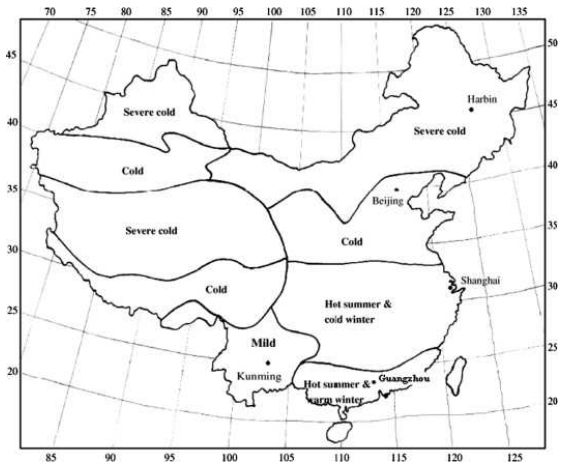

Figure 1 - Climate zones of China

Most of the detached homes in rural areas in the northeast use the traditional kang system for domestic heating.

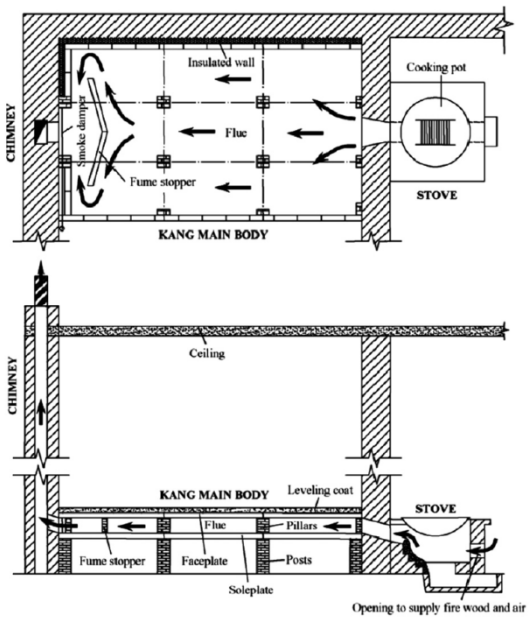

Figure 2 - Structure of the Chinese Kang

The kang is a traditional bed platform made from masonry, adobe and cement. An inner chamber functions as a flue for hot smoke produced from a connected stove. Energy is transferred from the smoke to the kang as smoke travels through the Kang chamber and out a connected chimney, see Figure 2. Heat from the smoke is stored in the thermal mass of the kang. The stored heat is then released into the air of the room containing the kang. Residents sleep on the surface of the kang which will stay warm several hours after the firing of the stove.

Most of the homes do not currently have access to domestic hot water. Solar hot water systems are popular in rural areas but only function well at lower latitudes. The systems are expensive and cost restrictive for most households.

The government of China has recognized the need for efficient, cost effective and renewable energy sources for rural residents. 56% of the population, roughly 750 million people, resides in rural areas. Of this population, nearly 175 million people use the traditional Kang system (Yang, 2010).

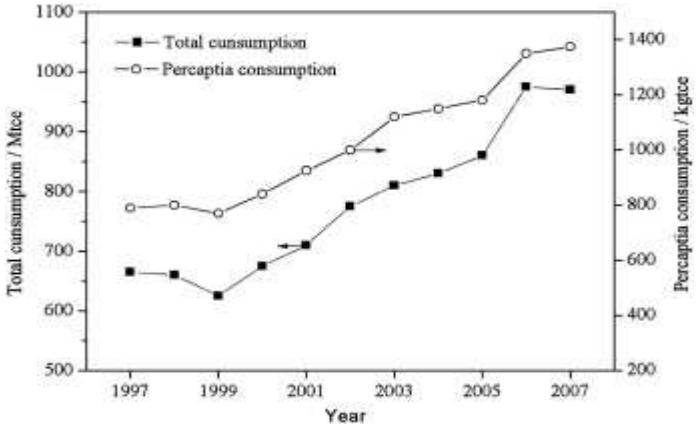

Figure 3 - Total and per capita energy consumption in rural China from 1997 to 2007

The current system is unsophisticated and inefficient; rudimentary kang systems have thermal efficiencies under 20% (Zhuang, 2009). Often, the kang system alone does not provide enough heat to maintain a comfortable indoor thermal environment. Residents often supplement their kang system with coal fired boilers and radiators in order to maintain a level of thermal comfort within the home. The Chinese government has developed a strategy to lessen dependence on fossil fuels and increase renewable energy use. It has recognized the need for improved standards of living for rural residence; the government understands improved living standards require higher levels of energy consumption. However, higher coal use is undesirable due to high usage costs and produced greenhouse gas emissions. Environmentally friendly as well as cost and energy efficient solutions are therefore required to meet the growing needs or rural residents in northeast China (Zhuang, 2007).

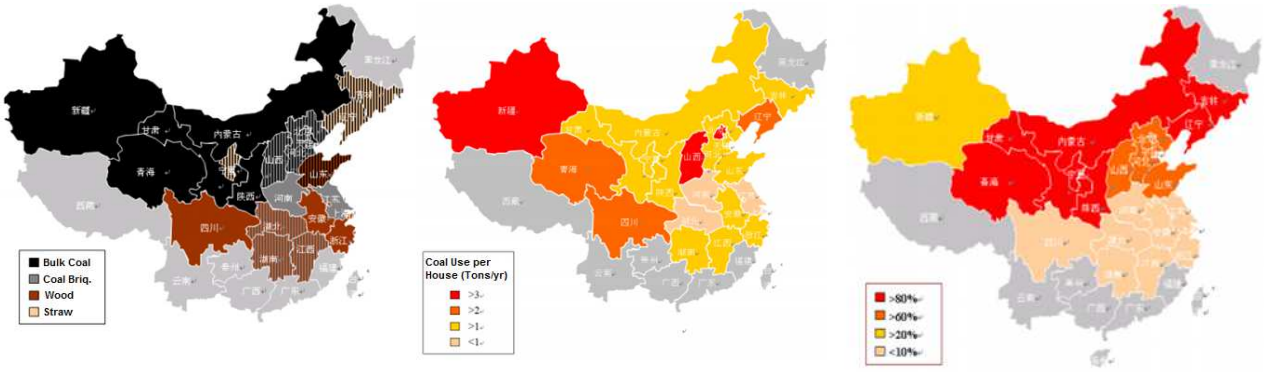

Figure 4 - Type of fuel use, coal use per household and distribution of kang systems in China

Considering there are at least 200 million people live in rural Northern China, if these people lived in the same buildings as the urban population today, then the building energy consumption for home heating alone will increase at least 2—3 folds (Yang, 2010). Adequate solutions that properly address energy related issues faced by rural residents in northeast China must be developed. Much research has already been conducted regarding possible solutions: improved building envelope insulation, coupling the kang with passive solar systems, and the use of phase change materials (PCM) to name a few. However, there is little understanding about which solutions work best or how different technologies

might be complimentarily paired. To understand such issues requires a simplified and modular model that can evaluate and measure the effectiveness of possible technical solutions.

The development of such a model requires the identification of a base case scenario where individual components are molded and modularly connected to other components. Figure 5 depicts a graphical representation of the base scenario of the system model.

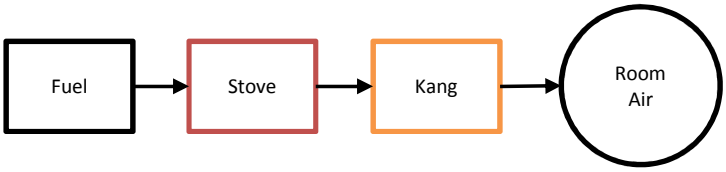

Figure 5 - Diagram of the system model

Once the base case scenario is constructed and validated, additional components representing technical solutions can be integrated. Figure 6 displays the addition of a heat exchanger in the stove that is used to heat water for domestic use. A phase change material (PCM) module has also been added to the model.

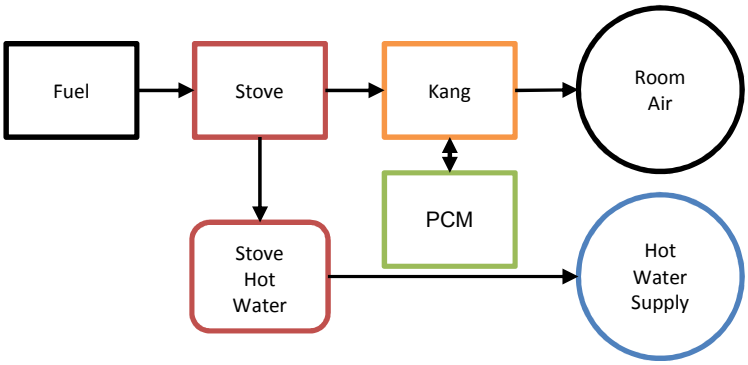

Figure 6 - Diagram of the expanded system model

Figure 7 shows the possible range of module expansion. A system model could evaluate each component's energy and cost effectiveness and would be a useful tool during the decision analysis phase when solutions are evaluated.

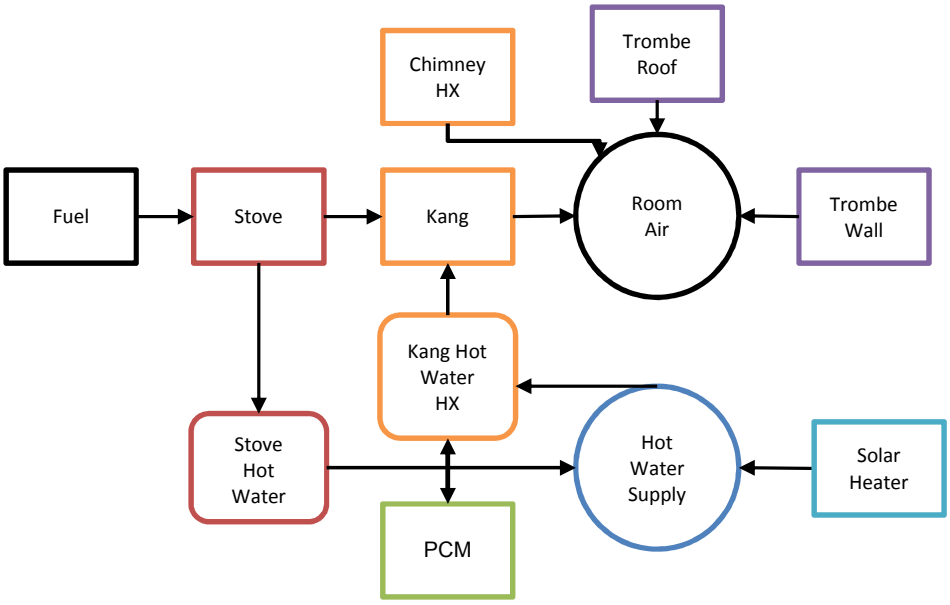

Figure 7 - Diagram of expanded system model

1.3 Literature review & Data Collection

The Chinese kang plays a major role in rural residents' lives, particularly in northeast China. Because of its prevalence in rural life and culture, the Chinese kang system has been extensively studied. *Influence analysis of building types and climate zones on energetic, economic and environmental performances of BCHP systems, Applied Energy* (Jiangjiang, 2011) details energy use in northeast rural China and provides a framework of background information.

Complex models have been developed and used to improve the undeveloped technology of the kang system. Many of the detailed kang studies have focused on particular elements of the system, for instance stove efficiency or smoke flow, and how to accurately model observed data. Due to the objective of designing a simplified model, much of the reviewed literature was used as a guide.

A comprehensive study concerning the heating performance of the kang system was conducted in a paper by Guangyu Cao . In the paper *Simulation of the heating performance of the kang system in one*

Chinese detached house using biomass (Cao, 2011) the dynamic performance of the kang system was simulated using IDA-ICE software. Empirical data from field measurements were collected. Specific data from this study were used to verify model inputs: daily fuel consumption, fuel calorific value, thermal properties of the building and kang material properties and input power.

Much of the data used to construct and verify the model were provided by DUT. In the paper *Experimental Study For The Energy Efficiency Of Hot-Wall Kang* (Wang Z. , 2010), the author details energy flows within the kang system and the efficiency of certain components. The system model was initially created in the same manner, using component efficiency to determine energy flows. The system model was refined but some of the efficiency method is still used, for instance calculated heat flows from the chimney into the room air. The text Principles of Heat Transfer, (Kreith, 2001) provided a guide for many elements of the model. It was used to develop the transient heat transfer of the kang and the radiant heating calculations.

Thermal storage performance analysis on Chinese kangs (Zhuang, 2010) specifically investigated thermal storage in kang systems and was used to incorporate transient heat transfer effects into the system model.

The smoke system developed in the model was created primarily using data from DUT. However, many aspects were verified from the papers, *Measured Heat Transfer and Smoke Flow Performance of a Typical Elevated Chinese Kang* (Zhuang, 2008), and *Simulation of the heating performance of the Kang system in one Chinese detached house using biomass* (Cao, 2011). Both papers used more complex modeling methods to simulate the smoke within the system and both verified the rate of smoke flow that was calculated in the model. The temperature of the smoke at the stove outlet was measured by (Li Y. , 2009) and determined to be in the range of 300-600℃. This value was confirmed by studies

conducted by DUT. The above mentioned literature was used as a guide when constructing the framework for the simplified system model.

A mathematical model for a house integrated with an elevated Chinese kang heating system (Zhuang, 2007) outlined the construction of a mathematical model of the kang system and was used to create the basis of the simplified model. The specifics of the model built by Zhuang were more detailed than what was required for the simplified model. The model developed by Zhuang considered transient heat transfer effects within the building elements which the simplified model only considers for the upper plate of the kang. Additionally, more complex methods of heat transfer were developed for Zhuang's model, specifically for the smoke model and radiant heat transfer. His model determined that the air change rate significantly decreases the indoor air temperature.

(Cao, 2011) created a model of the kang using IDA-ICE software. Some items, such as the periods of room occupancy within a home, were incorporated into the simplified model, however much of the approach to using IDA-ICE software was too complex to be integrated into the simple model.

A thermal comfort model was developed by Cao G 2010 in the paper *Simulation of the heating performance of the Kang system in one Chinese detached house using biomass* (Cao, 2011). It was determined that the comfortable temperature range for the bedroom of a rural home is in the range of 12-16℃. (Guo, 2001) found the optimal range of the surface temperature of the kang to be 25-30℃. The findings of Cao and Guo were used to develop a comparative metric for the model output concerning the air and kang temperatures.

Informal interviews and focus groups with community members provided background information regarding cultural practices and habits in rural northeast China. Research was conducted during a practicum program developed between the University of Colorado and Dalian University of Technology. The practicum lasted six weeks during the summer of 2012. The program began June 4th and finished on

July 13th 2012. Research and work was conducted on campus at DUT. Three field visits were made during the six week period.

Chapter II: Methodology

2.1 Model Background

Since 2007, DUT has been regularly engaged with local communities performing academic research on the Chinese kang. Multiple field trials were carried out in the community of Pulandian, a region of northeast China. A rural home with a ground kang system and unimproved stove was selected as an experimental site. Multiple experiments were conducted and data were collected.

Figure 8- Rural home used for DUT field measurements

Figure 9 displays the layout of the test home. The cooking stove is contained in the east room which functions as a

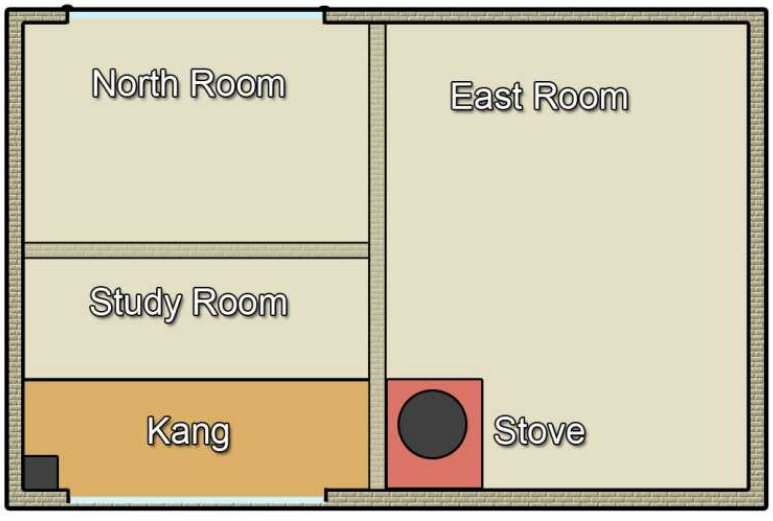

Figure 9 - Floor plan of study house

kitchen and dining room. The kang is located to the west, separated from the stove by a dividing wall. It occupies the southern portion of the room. A chimney is built into the exterior of the west wall. The south wall of the study room contains a large window above the kang. To the north of the study room is another room, cordoned off by an interior wall.

The data from February 19th, 2008 were determined to be the most comprehensive. The data from this testing interval were used to construct and validate the simplified system model. Datasets from supplementary days of study were used to validate and refine variables within the model.

Fuel type was documented and the amount of fuel used per firing in the connected stove was measured. Temperature data were recorded at multiple locations, including but not

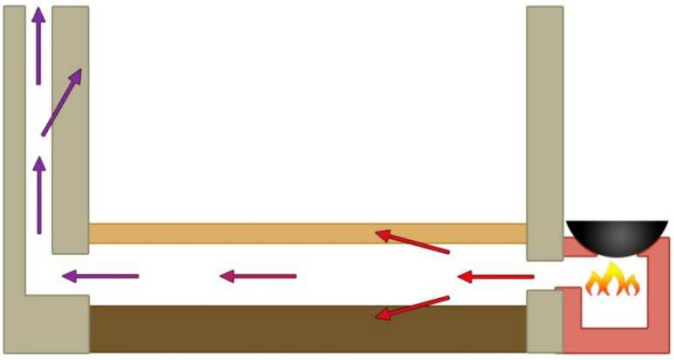

Figure 12- Kang system during stove firing

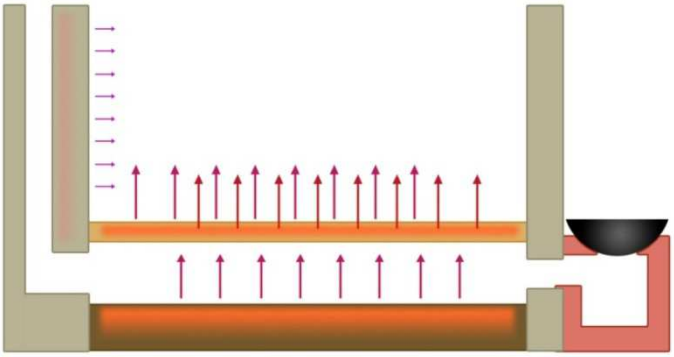

Figure 12 - Kang system after firing

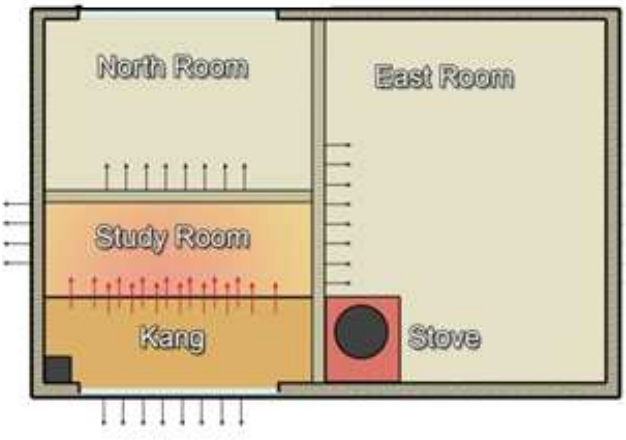

Figure 12 – Diagram of heat transfer of study house

limited to the outlet of the stove, inside the chamber of the kang, inside the attached chimney, the surface of the kang, inside the test room, inside the neighboring rooms, and outside the house. The data were recorded in intervals of two minutes. Each test lasted from several hours to multiple days.

2.2 Base Model Structure

Governing Equations

The simplified system model is structured as follows. Fuel is burned in the stove and energy is released. Some of the energy is used for cooking; the remaining energy is exhausted to the kang chamber. The hot smoke travels through the kang chamber where heat transfer occurs. A portion of the energy from the smoke is transferred into the mud substrate at the base of the kang. Energy is also transferred to the kang's surface plates. The smoke exits the kang's chamber where further heat transfer occurs. Energy is exchanged from the smoke into the wall of the chimney. Finally, the smoke exits the chimney and any remaining energy is expelled to the atmosphere. This process is detailed in Figure 12.

Once the stove firing is complete, energy transfer from the exhaust ceases. Heat transfer occurs between the substrate and the kang plates, the kang plates and the study room and the chimney wall and the study room air. This process is shown in Figure 12.

Heat transfer occurs from the study room air into the surrounding building envelope as well as to the outside air. An illustration of this process is shown in Figure 12 – Diagram of heat transfer of study house. It should be noted that heat transfer between elements is bi-directional. However, assumptions were made to simplify the heat loss mechanism of the building envelope. The north room and east room were both assumed to have constant temperature. While heat transfer occurs between the study room and the north and east rooms, no heat transfer occurs between the north and east rooms or between the outside and the north and east rooms. This will be discussed further in the building model section below.

The model was built using the lumped capacitance method as a basis of heat transfer. The governing equations for each component are listed below:

$$\dot{E}_{In} - \dot{E}_{Out} = \Delta E \qquad 01$$

$$Q = UA\Delta T \qquad 02$$

$$Q = mC_P\Delta T \qquad 03$$

Excluding the kang, thermal gradients within the system's components were not considered; each component's temperature distribution was assumed to be uniform. Transient heat transfer effects were not considered. Although heat transfer due to convection was modeled, fluid behavior of the smoke and room air was not.

A time step (*n*) of twenty seconds was selected for the model. For analysis, a time frame of 24 hours was used. However, upon the refinement of the model, a time frame of 96 hours is possible. The energy flow of each component is calculated at each time step. This data is used to calculate each component's temperature. In an iterative method, component energy flows of the current time step (*n*) are updated based on the component's temperature of the previous time step (*n-1*). Initial conditions of the components were obtained from empirical data.

Figure 13 depicts a graphical representation of the simplified system model's structure and the related energy flow from each component. The

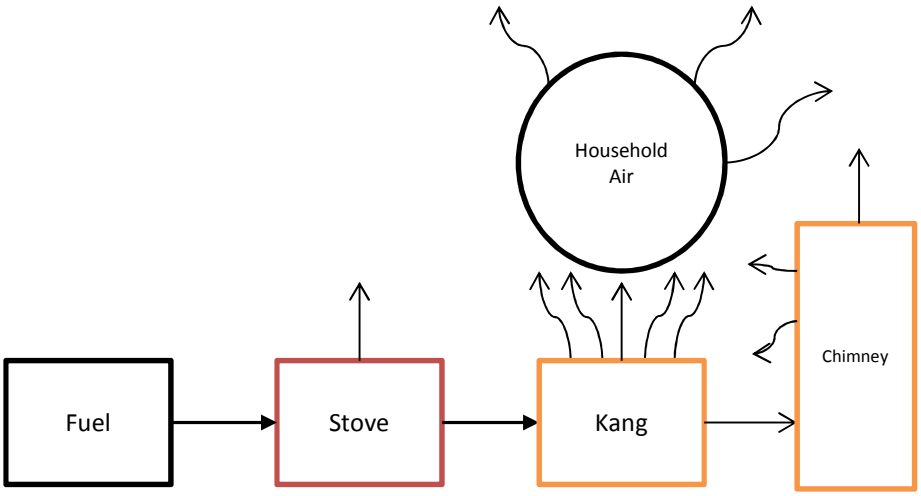

Figure 13 - Simplified diagram of energy flow in the system model

modeling of each component is discussed in detail below.

Fuel

Many different types of cooking fuel are used in the communities of rural northeast China. Biomass was determined to be the most commonly used cooking fuel, specifically corn stalks and corn cobs. The region of study primarily produces corn; therefore the local farms often have a large supply of corn related biomass. The experimental trial conducted on February 19th, 2008 used corn cobs as the cooking fuel. Data from the US department of Energy were used to determine the encapsulated energy of commonly used biomass fuels. The corncobs used as cooking fuel were determined to have 15,190 kJ/kg of encapsulated energy (US Department of Energy).

Table 1- Encapsulated fuel energy

Fuel Type	Heating Energy (kJ/kg)
Hay / Firewood	19,600
Maize Straw	18,000
Straw Briquettes	15,345
Corncob	15,910

Equation 4 was used to obtain the power generation from the combusted fuel.

$$\text{Fuel / firing } (kg) \cdot \text{Fuel Energy / Fuel Mass } \left(\frac{kg}{kJ}\right) \text{ / Firing Time (s) = Power Output } (kW) \qquad 04$$

Literature on the subject suggests typical stoves used in rural northeast China produce 16-40 kW. The model of the fuel established roughly 22 kW of power was produced during the stove firing.

Stove

The stove is where the energy from the fuel is released and exhausted into the kang chamber. Firing times and durations were collected from a DUT study for the day of February 19th, 2009. The stove was fired on three separate occasions. Table 2 shows firing times and firing durations.

Table 2 - Stove firing data

Firing Time Start	Firing Duration (min)
7:34	82
13:54	66
17:56	50

The firing times are displayed in Figure 14. The shaded regions indicate the stove is being fired.

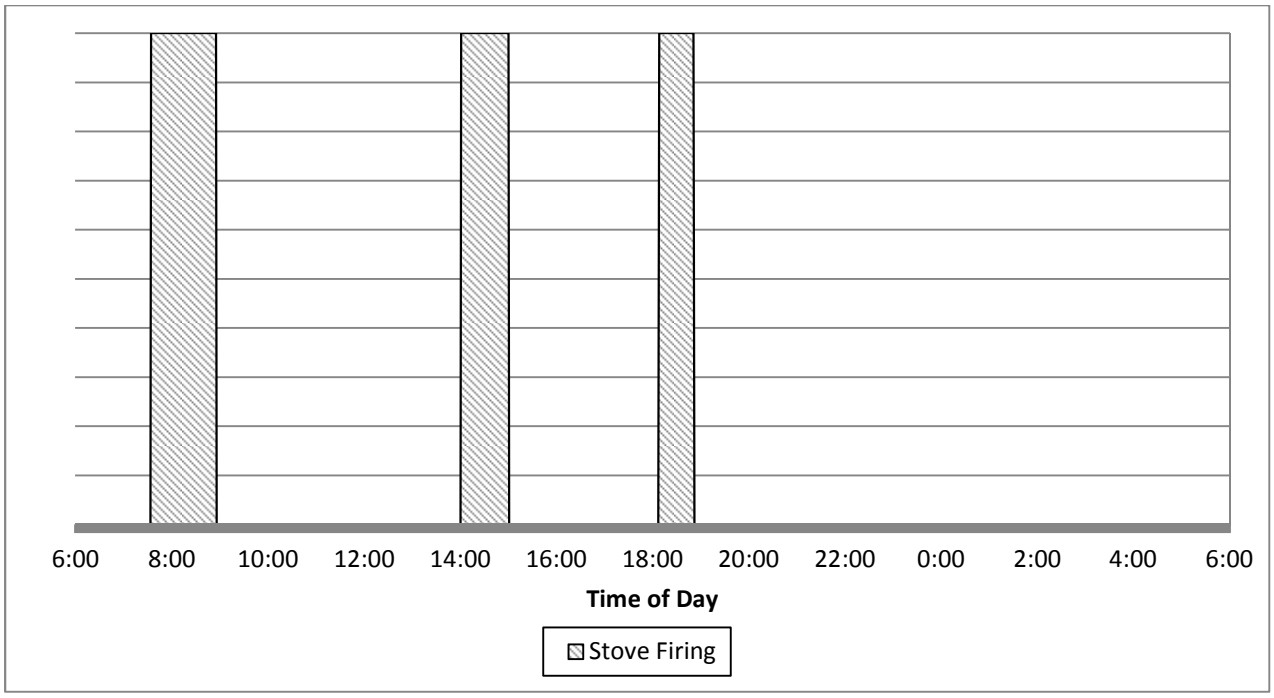

Figure 14 – Graphical representation of stove firing periods

Energy released from the burned cooking fuel is created through combustion in the stove's firing chamber. The ratio of energy used to cook versus energy exhausted from the stove depends on the type of stove. Data from tests conducted by DUT and existing literature indicate that 35% of the energy released from the combusted fuel is used for cooking food. The remaining 65% of the energy provided by the burned fuel is exhausted to the kang chamber. Of the 22kW created from the fuel combustion, 14.2 kW is exhausted to the kang.

Kang

The energy that enters the kang's chamber is either transferred into the kang's substrate, the kang's surface plates or exhausted to the chimney. The thermal efficiency of the kang has been measured and depends on the type of kang. A ground kang has a thermal efficiency of 56 %; of the total energy entering the kang chamber, only 56% is transferred into the room for heating. The thermal efficiency of the kang reduces the power available for heating from 14.2 kW to 8 kW. However, not all of the 8 kW is immediately transferred to the room. The kang's plates and substrate have large thermal storage capacities. The energy flow to and storage within each component was considered. However, this approach was determined to be too complex as there is no data regarding the heat transfer of the substrate. Rather than estimate a ratio to determine how much energy is transferred to the kang plates versus how much energy is transferred to the kang substrate, effects of the substrate were considered by modeling the temperature of the smoke in the substrate. The temperature of the smoke in the kang's chamber is well documented and takes into account the thermal influence of the substrate. Energy from the smoke is transferred to the kang's surface plates according to the equation

$$\dot{Q}_{Kang\ Chamber}{}^{n+1} = (h_{Kang\ Chamber} + Radiation_{Kang\ Chamber}) SA_{Kang} \left(T_{Smoke}{}^{n} - T_{Kang}{}^{n}\right) \quad 05$$

The temperature of the kang plates rises during the stove firing. When the firing stops, the plates transfer energy to the room air. The amount of energy transferred is calculated using

$$\dot{Q}_{Kang\ Surface}{}^{n+1} = \left(T_{Kang}{}^{n} - T_{Air}{}^{n}\right) \cdot (h_{Kang\ Surface} + Radiation_{Kang\ Surface}) \cdot SA_{Kang} \quad 06$$

Heat transfer from convection and radiation was modeled. The convective heat transfer coefficient (h_{Kang}) was measured by DUT and determined to be within the range of 10 and 20 ($\frac{W}{(m^2 \cdot K}$). The coefficient used for radiation was estimated from typical building thermal design and a value of 6 was used. The two coefficients were combined in the model to create an overall heat transfer coefficient with a range from 10-30. A similar process was used to determine the overall heat transfer coefficient of

the interior surface to the kang chamber of the kang plates. The values for both overall heat transfer coefficients were adjusted to match the measured data.

Assuming the temperature of the kang's plate is uniform, the temperature of the kang can be determined using the simplified equation

$$T_{Kang}{}^{n+1} = (\dot{Q}_{Kang\ Chamber}{}^{n+1} - \dot{Q}_{Kang\ Surface}{}^{n+1})/(m_{Kang} \cdot C_{p_{Kang}}) + T_{Kang}{}^{n} \quad 07$$

The modeled temperature of the kang's plates is shown in Figure 15.

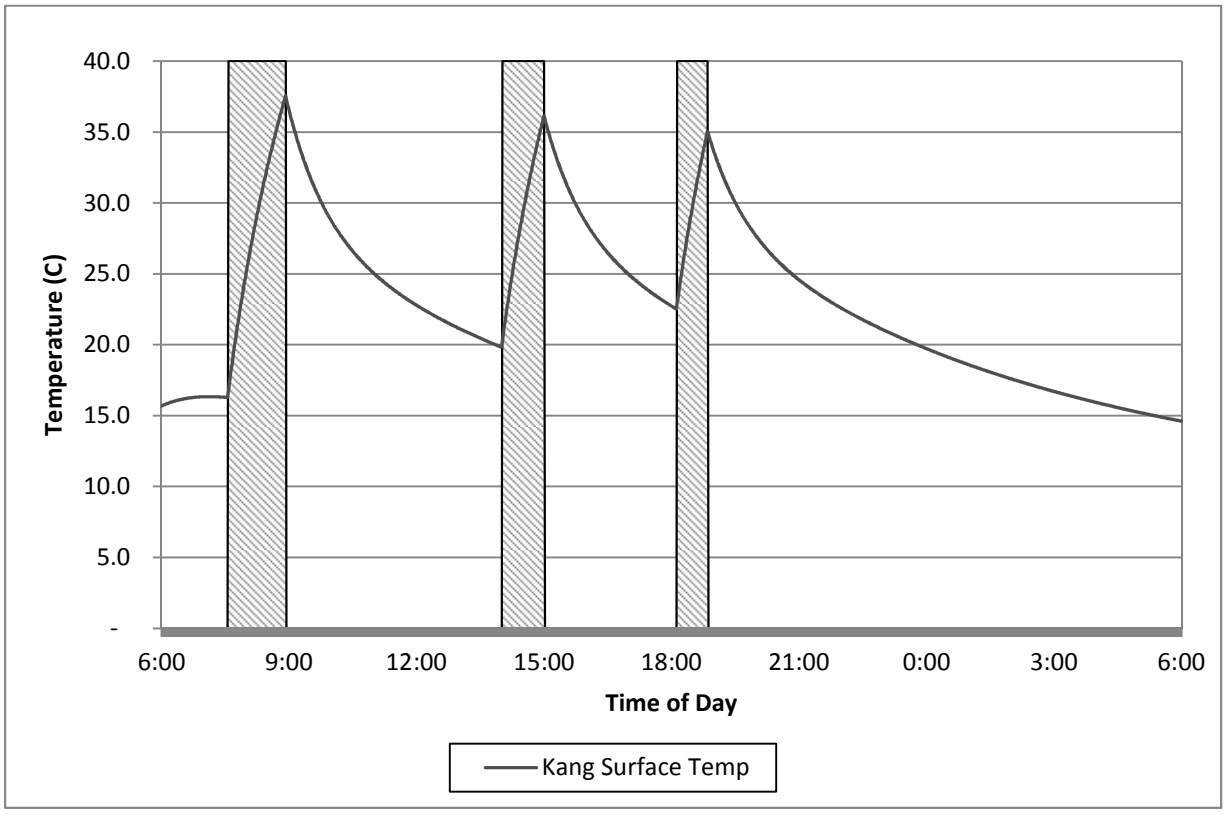

Figure 15 - Modeled kang plate temperature

The modeled temperature of the plates of the kang compared to their measured temperatures is shown in Figure 16.

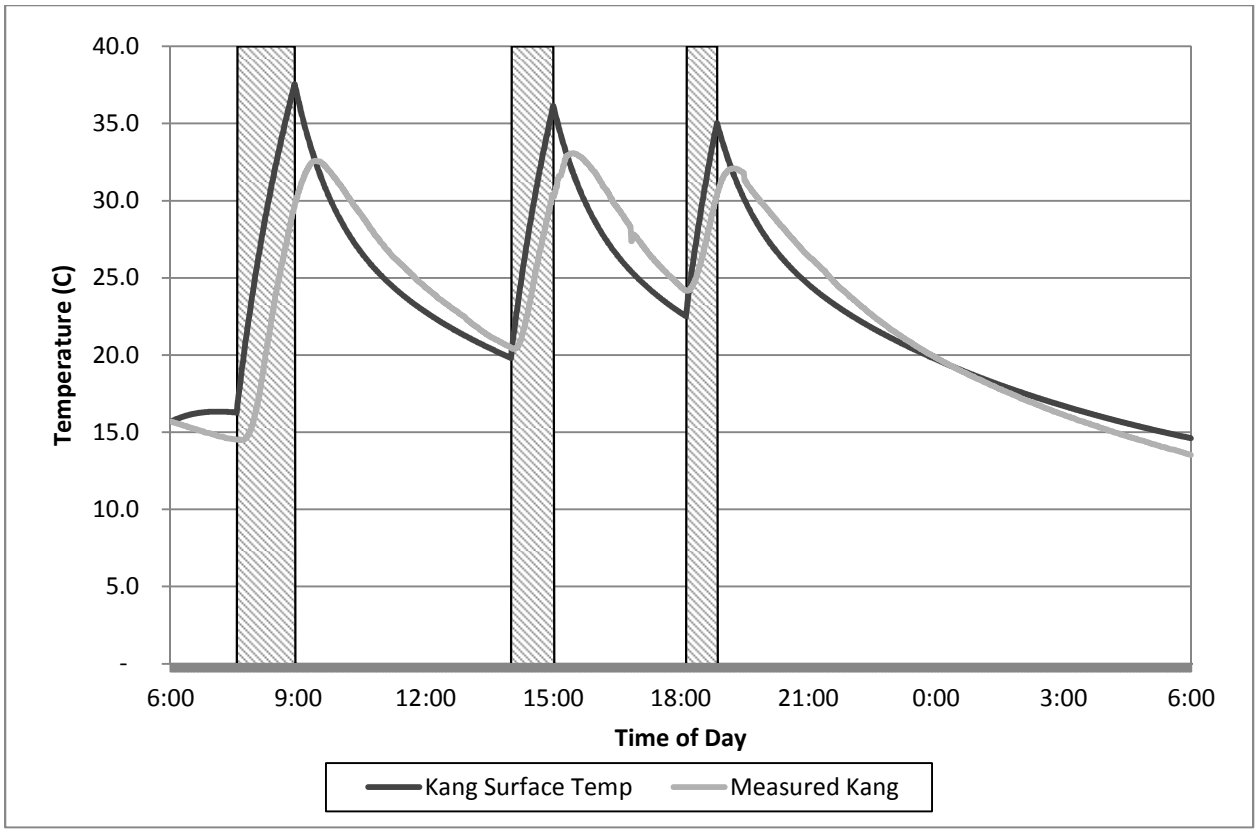

Figure 16 - Modeled and measured kang plate temperature

The general behavior of the two series is similar. However, the calculated maximum temperature for each firing interval is too high. Furthermore, the modeled temperature peaks when the firing of the stove ceases. The measured data peaks roughly 30 minutes after the stove firing stops and the top of the temperature peak is less sharp than the maximum of the calculated temperature. The discrepancy is caused by few factors. First, using the lumped capacitance method to calculate the kang plate's temperature doesn't permit for transient effects and temperature delays to be considered. Second, the smoke from the stove was modeled as a binary element. That is, the smoke was a constant temperature during the firing period, and another constant temperature when the stove was not being fired. In reality the smoke temperature remains elevated after firing and decays over time. Transient effects within the kang and an improved smoke temperature model are discussed in detail below.

Transient Heat Transfer

Transient heat transfer effects need to be considered to increase the model's accuracy. Equation 8 can be used to develop a model of transient heat transfer. In reference to a control volume, the energy balance equation can be written as

$$\dot{q}_{conduction}in + \dot{q}_{generation}\ inside = \dot{q}_{conduction}\ out + \dot{q}_{storage}\ inside \quad 7$$

The temperature of the control volume varies with both space and time indices, *i* and *n.*

$$T_{i,n} \equiv T(x_i, t_n) \quad 08$$

The rate of energy storage within a node during one time step can be written as

$$\rho c \Delta x \frac{T_{i,n+1} - T_{i,n}}{\Delta t} \quad 9$$

Adding equation 9 to equation 10 and solving for the single temperature term with time step *n+1* produces equation 11.

$$T_i^{n+1} = T_i^n + \frac{\Delta t}{\rho c \Delta \mathrm{x}}\left\{\frac{k}{\Delta \mathrm{x}}(T_{i+1}^n - 2T_i^n + T_{i-1}^n) + \dot{q}_{G,i}^n \Delta \mathrm{x}\right\} \quad 10$$

Since $Fo = \frac{\alpha \Delta t}{\Delta x^2}$ and there is no heat generation within the kang plates, equation 11 can be simplified to

$$T_i^{n+1} = T_i^n + Fo\{T_{i+1}^n - 2T_i^n + T_{i-1}^n\} 11$$

Equation 12 is used to calculate the temperature of any internal node. However, separate equations must be developed for the two exterior nodes.

Applying a heat flux boundary condition to equation 12 at the first node produces

$$T_1^{n+1} = T_1^n + \frac{\Delta t}{\rho c \Delta \mathrm{x}}\left\{q"_1^n + \frac{\Delta x}{2}\dot{q}_{G,1}^n + \frac{k}{\Delta \mathrm{x}}(T_2^n - T_1^n)\right\} \quad 12$$

and inserting a convective heat transfer boundary condition at the final node, *L* creates the equation

$$T_L^{n+1} = T_L^n + \frac{\Delta t}{\rho c \Delta \mathrm{x}}\left\{h(T_\infty - T_L^n) + \frac{\Delta x}{2}\dot{q}_{G,L}^n + \frac{k}{\Delta \mathrm{x}}(T_{L-1}^n - T_L^n)\right\} \quad 13$$

There is a constraint on the maximum time step for equations 12-14 to function with stability.

$$\Delta t < \frac{\Delta x^2}{2\alpha} \quad 14$$

Where α is defined as

$$\alpha = \frac{k}{\rho c} \quad 15$$

The model time step is set at 20 seconds so the minimum node thickness can be determined by rearranging equation 15.

$$\Delta x > \sqrt{2\alpha\Delta t} \quad 16$$

Setting Δt equal to 20 seconds and using the kang surface plate materials properties produces a minimum node thickness of 0.0047 meters. The kang plate thickness is 0.07 meters so a Δt of 20 seconds will produce stable results as long as there are fewer than 14 nodes.

The heat transfer within the kang's surface plates can be modeled using a numerical analysis of one dimensional unsteady conduction (Kreith, 2001). A diagram showing a cross section of the kang's plates is shown in Figure 17 – kang Node Diagram.

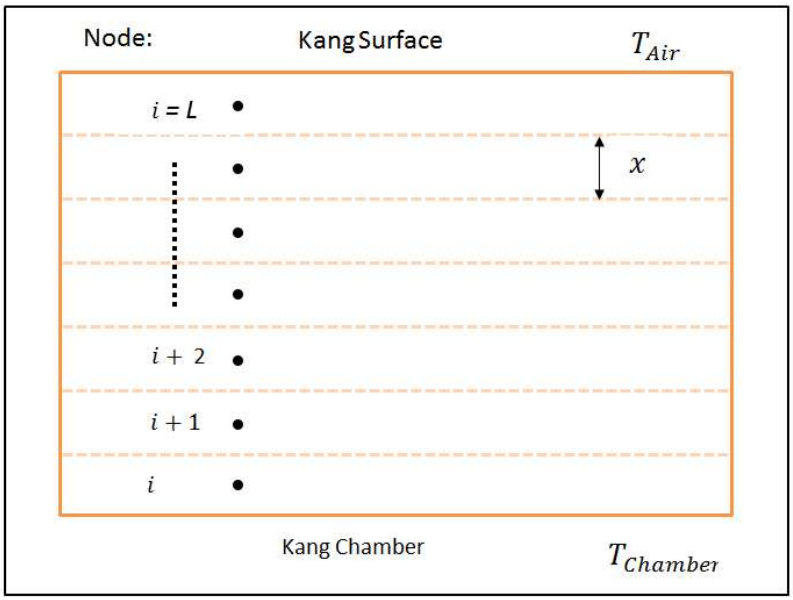

Figure 17 – kang Node Diagram

Model Stability

A balance must be determined between the accuracy of the model, which requires more nodes, and stability which requires fewer. Figure 18 and Figure 19 contrast the difference between stable and unstable model behavior. Small changes in the model and material properties can lead to the calculated temperature of the kang oscillating out of stability. In the case of Figure 19, the instability was caused by increasing the conductivity of the kang's surface plates.

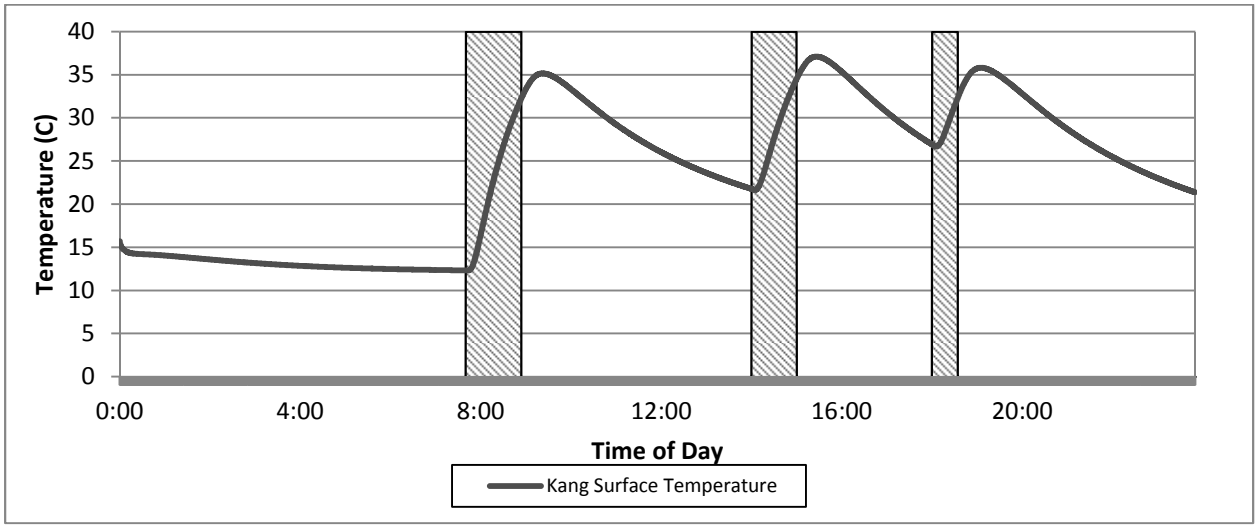

Figure 18 - Stable Model Behavior

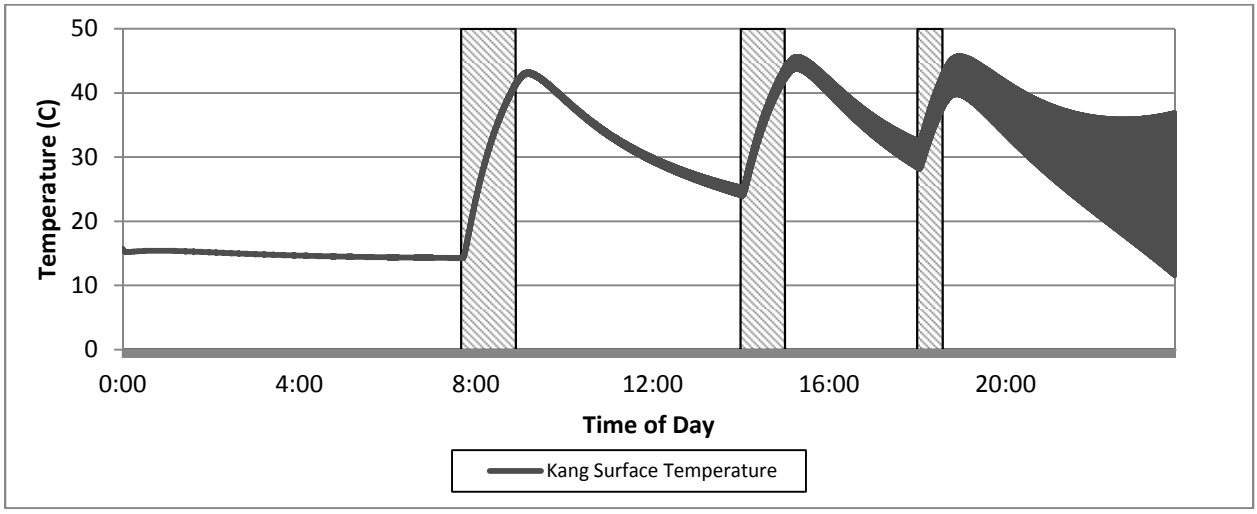

Figure 19 - Unstable Model Behavior

Because of this possible behavior, a stability analysis was performed in which scenarios using different numbers of nodes were tested. The time step was held constant at 20 seconds for three evaluations but changed to 5 seconds for the fourth. This was done to keep the model stable as the corresponding x value; 0.0025m was too small for the model to behave in a stable manner with a time step of 20 seconds. Each analyzed case was subjected to the same conditions. The kang's surface plate, initially at 15℃, transfers heat to a mass of air initially at 10℃. At 1,980 seconds 1,200 Watts of power are exposed to the bottom layer of the kang plates in the kang chamber. The 1,200 Watts of power remains constant until 7,980 seconds into the simulation, after which no further energy is injected into the kang. The temperature of each node is then calculated. The results of the analysis are displayed in Figure 20.

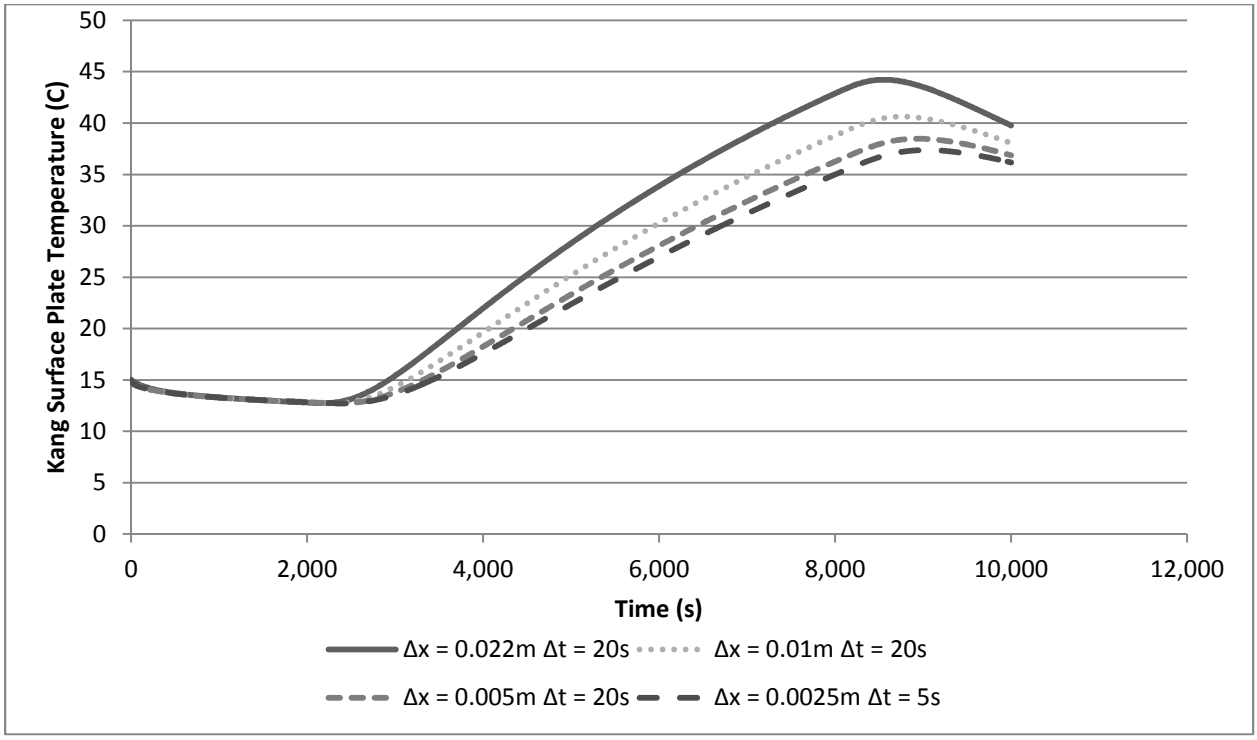

Figure 20 - Node and Model Accuracy

For each analyzed case the kang's surface temperature is compared. Before the stove fires the calculated temperature for each case is nearly identical. However, during and after the stove fires the calculated temperatures diverge. The most accurate scenario is the one with the smallest node size and

time step, Δx = 0.0025m and Δt = 5s. 28 nodes were used in this scenario, and the maximum time step allowed for stability is 5.6 seconds. Increasing the node and time step size to Δx = 0.005m and Δt = 20s produces nearly as accurate results. However, 14 nodes are used and the maximum time step size calculated to achieve stability is 22 seconds. Because the model's stability relies on Δt and α, changing the material properties of the kang (k, ρ, c) could make the model unstable, especially with a time step so near the maximum allowed for stability, 20 vs. 22 seconds. Because of this the node size should be increased. The scenario of Δx = 0.01m and Δt = 20s doesn't create as accurate results as the previous two analyzed scenarios but the maximum calculated time step for stability is 89 seconds. This permits more leeway for the kang's material properties to be adjusted. Finally, analyzing the results produced by the scenario of Δx = 0.022m and Δt = 20s shows significant loss of accuracy.

Because of the reasons stated above, a node size of Δx = 0.01m was selected. Since the kang's surface plate thickness is 0.07m, seven nodes were used for the transient heat transfer analysis.

The updated equations used to calculate the node temperatures are

Node 1

$$T_{Kang}{}_1^{n+1} = T_{Kang}{}_1^{n} + \frac{\Delta t}{\rho c \Delta x}\left\{\frac{Q_{Kang\ Chamber}^{n}}{SA_{Kang}} + \frac{k}{\Delta x}\left(T_{Kang}{}_2^{n} - T_{Kang}{}_1^{n}\right)\right\} \quad 17$$

Nodes 2 -6

$$For\ i = 2\ to\ 6$$
$$T_{Kang}{}_i^{n+1} = T_{Kang}{}_i^{n} + Fo\left\{T_{Kang}{}_{i+1}^{n} - 2T_{Kang}{}_i^{n} + T_{Kang}{}_{i-1}^{n}\right\} \quad 18$$

Node 7

$$T_{Kang}{}_7^{n+1} = T_{Kang}{}_7^{n} + \frac{\Delta t}{\rho c \Delta x}\left\{h_{Kang\ Surface}(T_{Air}^{n} - T_{Kang}{}_7^{n}) + \frac{k}{\Delta x}\left(T_{Kang}{}_6^{n} - T_{Kang}{}_7^{n}\right)\right\} \quad 19$$

Smoke Model

Data from DUT were used to develop a model of the smoke temperature in the stove and interior chamber of the kang. Firing data from the period of 1-18-2009 to 1-21-2009 were analyzed. During this period the stove was fired five times and a summary of the data is shown in Table 3 – Smoke Datasets

Table 3 – Smoke Datasets

Firing #	Start Time	Finish Time	Average Stove Smoke Temperature	Average kang Chamber Smoke Temperature
1	2009-1-18 6:34:31	2009-1-18 7:34:31	278.5	97.5
2	2009-1-18 12:16:31	2009-1-18 13:06:31	310.0	85.0
3	2009-1-19 5:54:31	2009-1-19 7:18:31	287.7	86.2
4	2009-1-19 12:14:31	2009-1-19 13:20:31	295.0	87.9
5	2009-1-19 16:16:31	2009-1-19 17:04:31	289.4	78.6
Average			292.1	87.0
Standard Deviation			65.5	10.1

The temperature of the smoke in the stove was measured at the aperture between the stove and the kang. The average temperature of the smoke in the kang's chamber was calculated by averaging the measured data from the sensors i2, i3, i4, i5, i9, i10, and i11, shown in Appendix A. Sensors i5, i6, and i7 were disregarded as they are inside the hot wall chamber. The i sensors measure the temperature of the top part of the smoke in the kang chamber. Because understanding the heat transfer between the smoke in the chamber of the kang and the interior surface of the kang's plates is desired, the temperature of the top part of the smoke was selected for analysis. The average temperature of the smoke in the stove was determined to be 292.1℃ while the average temperature of the smoke in the kang's chamber was significantly less at 87.0℃.

The relationship between the temperature of the smoke exiting the stove and the top of the kang chamber was investigated. This was carried out to facilitate the use of the program. If a correlation can be determined between the temperature of the smoke in the stove and the temperature of the smoke in the chamber, then only the temperature of the smoke in the stove must be provided as an input to the program. If no relationship can be determined than the user would be required to input average temperatures for the smoke in the stove and the smoke in the kang chamber. It is important to state that the relationship only applies to specific types of kangs. The correlation of the temperature of the smoke in the stove and the temperature of the smoke in the kang's chamber will be different if a ground or elevated kang is studied.

Figure 21 shows the temperature of the smoke in the stove and kang chamber during and after a firing. It is clear that the temperature of the smoke during the firing is significantly higher than that of the smoke in the kang chamber. On average the smoke in the stove is 3.3 times hotter than the smoke in the kang chamber.

Once the firing ceases the difference in temperature narrows and the smoke in the stove is determined to be 1.3 times as hot as the smoke in the chamber. This relationship is shown in Figure 22. While there are clear correlations between the smoke in the stove and the smoke in the kang chamber during the firing period and during the long term decay period after firing has occurred, the relationship breaks down during the period directly after firing, from 0 to 3,000 seconds after firing ceases. This is most likely caused by energy being released by the thermal mass of the kang substrate and support columns.

To create an accurate model of the smoke's temperature further analysis is required.

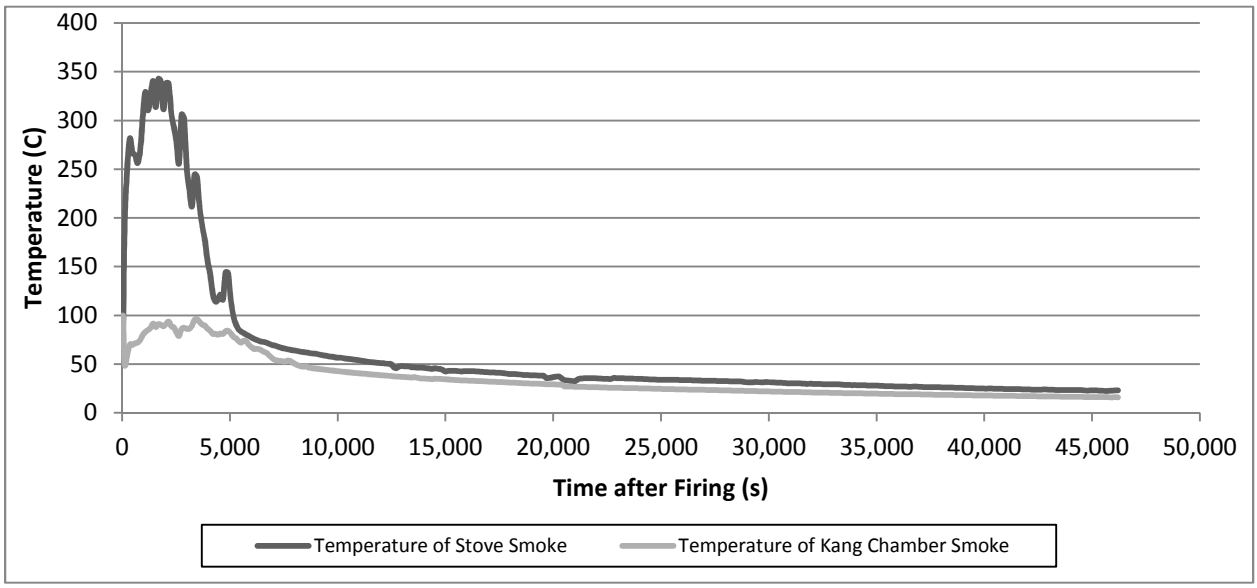

Figure 21- Smoke Temperature Firing and Decay

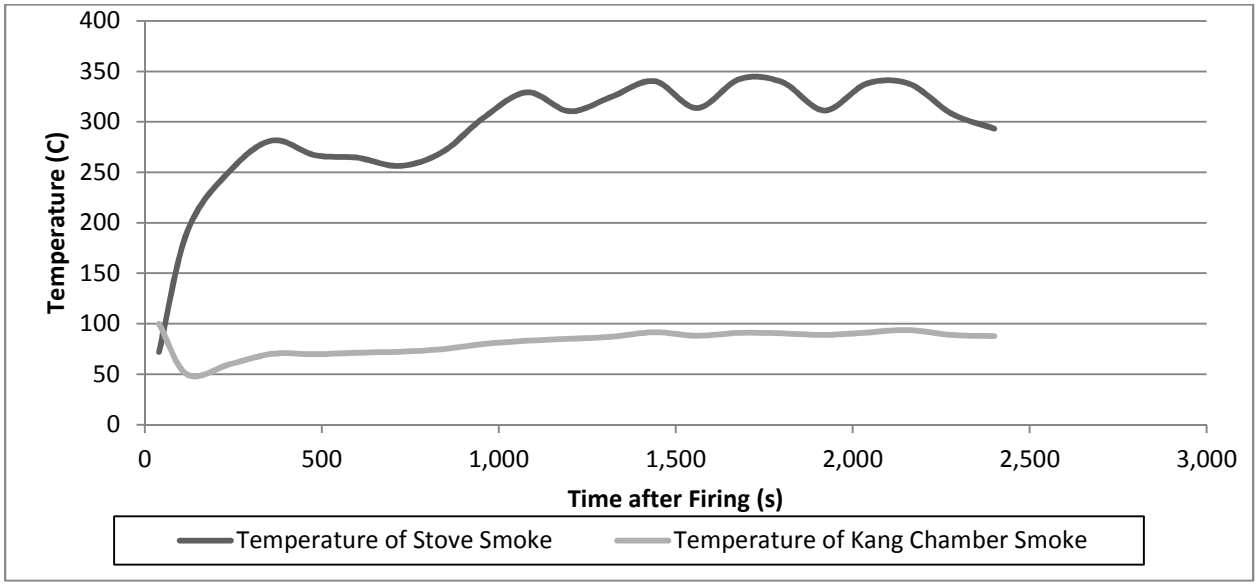

Figure 22 - Smoke Temperature during Firing

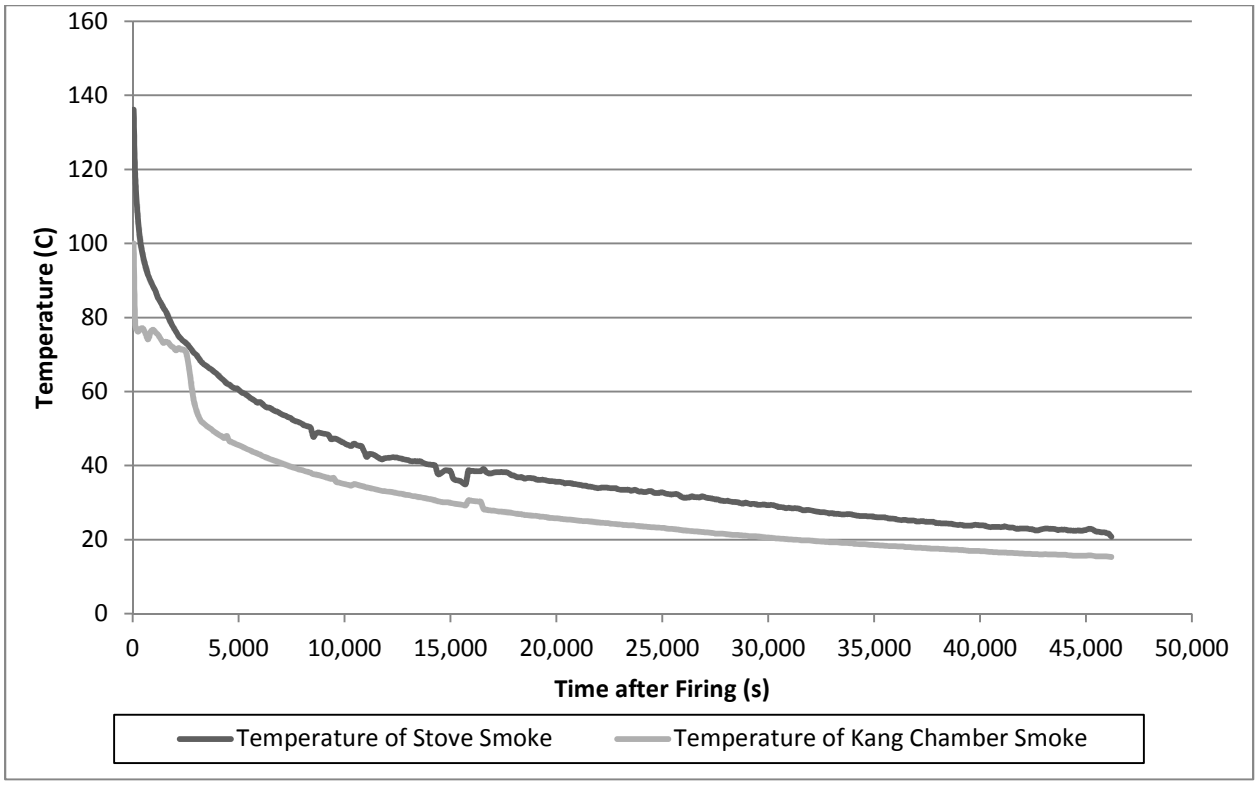

Figure 23 - Smoke Temperature after Firing

The temperature of the smoke in the stove was plotted against the temperature of the smoke in the kang's chamber. This is displayed in Figure 24. Two distinct correlated data sets are seen. When the smoke temperature of the stove is less than 124℃, a linear relationship to the temperature of the smoke in the kang chamber is determined by equation 21. The R^2 value of equation 23 is 0.68

$$T_{Smoke\ Kang\ Chamber} = 0.69T_{Smoke\ Stove} + 7.7 \qquad 20$$

If the temperature of the smoke is greater than 124℃ the linear relationship is defined by equation 24. The R^2 value of equation 22 is 0.22.

$$T_{Smoke\ Kang\ Chamber} = 0.11T_{Smoke\ Stove} + 54.2 \qquad 21$$

The R^2 value of the correlation for the stove smoke temperature greater than 124 degrees is significantly less than that of stove smoke temperatures under 124℃. This is due greater variability in firing temperatures than the temperatures during the decay period. The standard deviation of temperatures

during firing is 65.5℃ compared to only 10.1℃ during the decay period. This is displayed in Table 3 – Smoke Datasets. Using this analysis, the temperature of the smoke in the kang's chamber can be related to the temperature of the smoke that exits the stove. Therefore only one input temperature is required, that of the smoke exiting the stove.

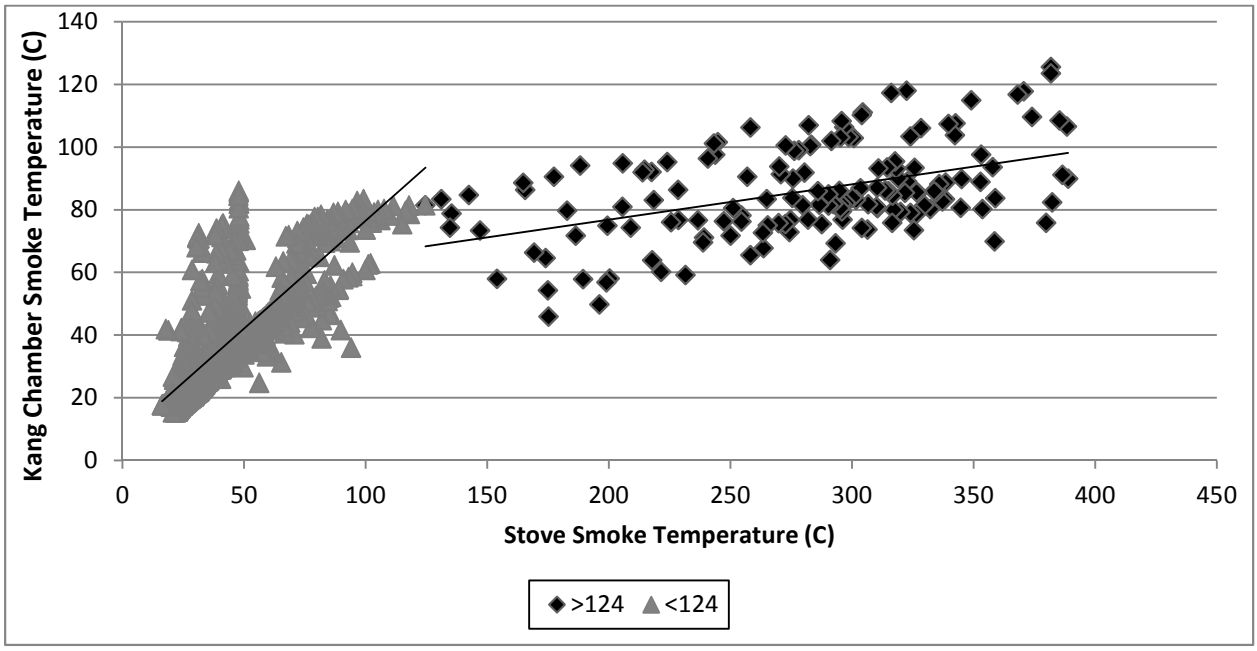

Figure 24 -Stove vs. Kang Chamber Smoke Temperature

It was already stated what the average temperature of the smoke in the stove is during the firing period, 294℃ . Yet to be determined is the temperature of the smoke in the stove during the decay period after the stove has been fired. Analyzing temperature data during the decay period after firing can provide insight into how the temperature of the smoke in the stove changes over time.

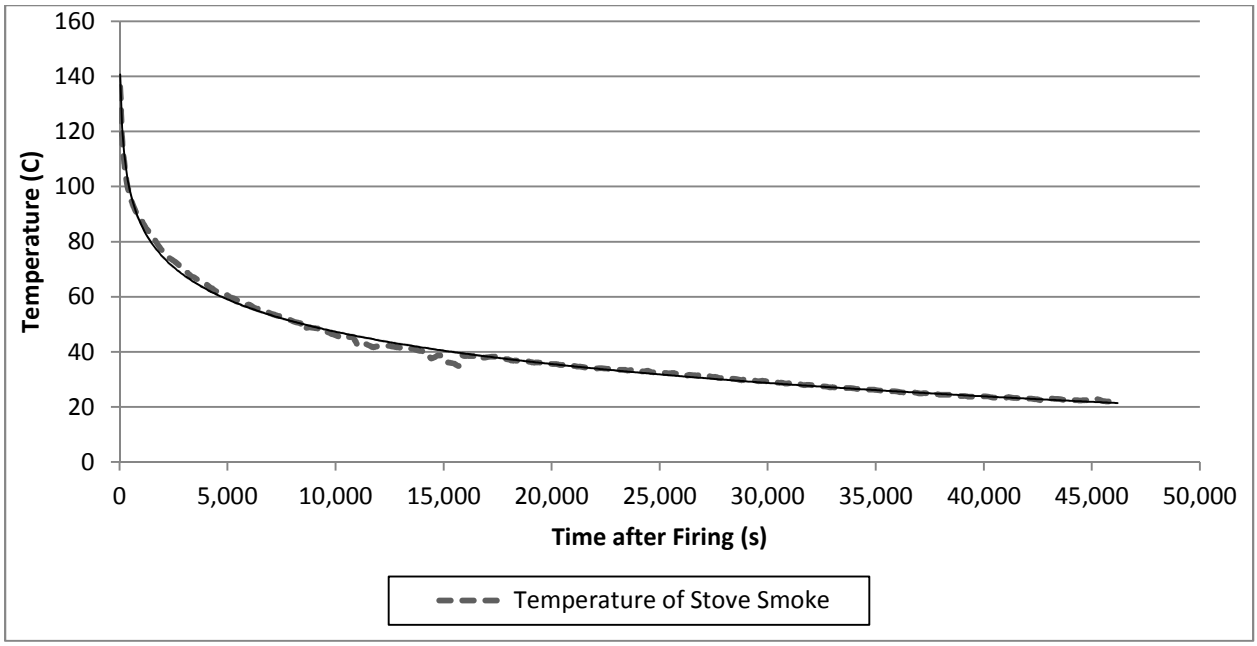

Figure 25 - Average Stove Smoke Temperature after Firing

The start of each decay period was selected when the temperature of the smoke in the stove fell below 150℃. Once a common beginning was selected for all five firing periods the temperatures were averaged and plotted in Figure 25. A logarithmic trend line was added to determine the relationship between the smoke's temperature and time after firing. This relationship is shown in equation 23 and has an R^2 value of 0.99.

$$T_{Smoke\ Stove} = -16.9\ln(t) + 203.2 \qquad 22$$

The t in equation 23 is the time after firing has ceased. With equation 23, a model of the temperature of the smoke in the stove and kang chamber can be created. During firing, the temperature of the smoke is set to a default value of 294℃. This value can be changed by the user of the program. Using equation 22, the temperature of the smoke in the kang chamber is calculated to be 87.5℃ during firing. When the firing period is finished the temperature of the smoke is calculated using equation 23. If the temperature is determined to be greater than 124℃ then equation 21 is used to calculate the temperature of the smoke in the kang's chamber. Otherwise equation 23 is used. Therefore, all required

smoke temperatures can be determined using only one input, the temperature of the smoke in the stove during firing. Figure 26- Smoke and Kang Chamber Temperature charts the temperature of the smoke and the kang chamber over the length of one day. Three periods of the stove firing are indicated by the shaded areas. The smoke in the stove increases to 294℃ during these times. The temperature of the kang chamber is significantly less at 87℃. When the stove firing stops, but temperature profiles decay according to the algorithms defined above.

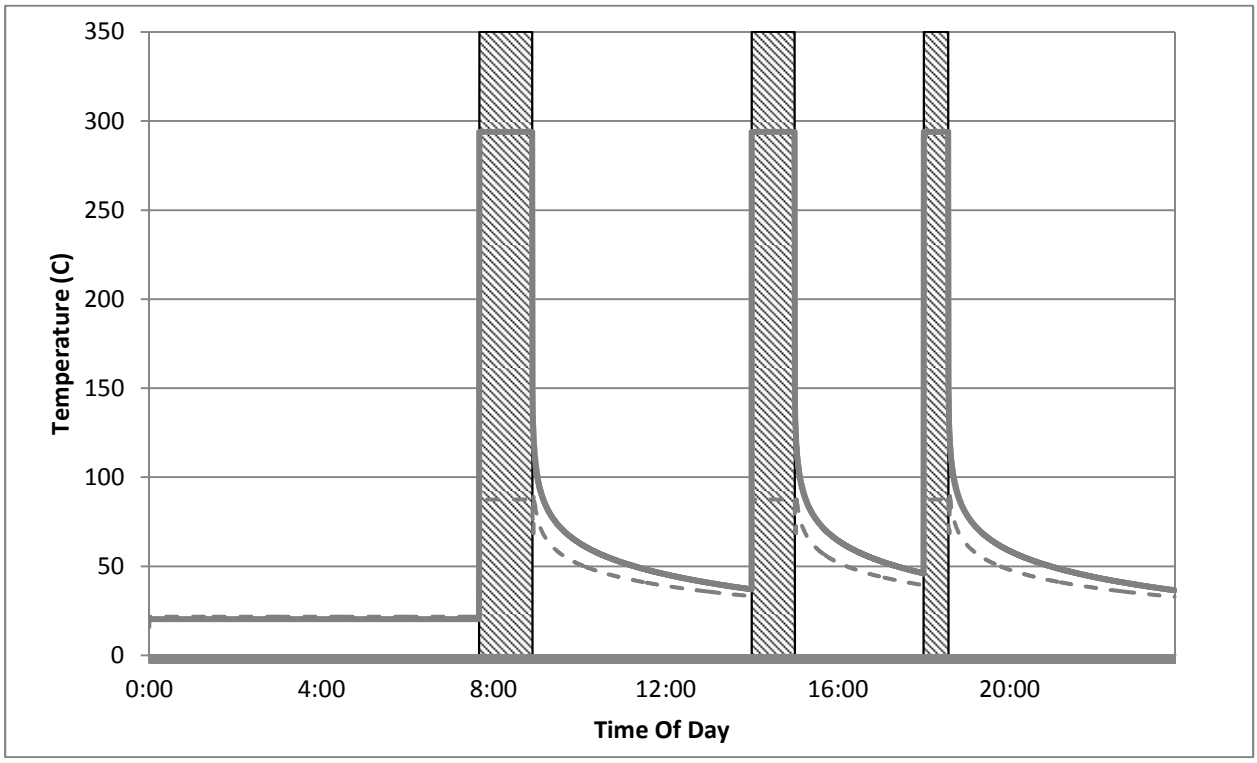

Figure 26- Smoke and Kang Chamber Temperature

Chimney

The smoke that exits the kang chamber enters the chimney. Heat transfer occurs between the smoke and the chimney walls. Some of this heat travels through the chimney wall and enters the study room. The remaining energy exits the system and is considered lost. For a ground kang system, measurements conducted by DUT indicate 35% of the energy that enters the chimney is transferred to the chimney wall. Of this, only 9% is exchanged into the air of the room.

$$\dot{Q}_{Chimney}{}^{n} = \eta_{Chimney} \cdot \eta_{Kang} \cdot \dot{Q}_{Stove}{}^{n} \quad 23$$

$$Q_{Stove} = \dot{m}_{smoke} c_{Air} T_{Smoke} \quad 24$$

Study Room Air

There are multiple energy flows to and from the study room's air. Energy from the kang's plates and the chimney is transferred into the air in the study room. The heat that is transferred causes the air temperature to increase. Some energy is transferred to the room's walls, the air of the surrounding rooms and the outside environment. The energy loss of the air is calculated using equation 26 and 27.

$$\dot{Q}_{Loss}{}^{n+1} = \sum_{i=1}^{i=K} U_i \cdot A_i \cdot \left(T_{Air}{}^{n} - T_{Enviornment_i}{}^{n}\right) \quad 25$$

$\dot{Q}_{Loss}{}^{n+1} = \sum_{i=1}^{i=K} U_i \cdot A_i \cdot \left(T_{Air}{}^{n} - T_{Enviornment_i}{}^{n}\right)$ 25 accounts for the heat loss through multiple surfaces with combined heat transfer coefficients U_i and surface area A_i. The values for *U* and *A* were obtained from data provided by DUT. The surfaces and their corresponding values are listed in Table 4.

Table 4 - Convective heat loss properties

Surface	U (W/m²K)	A (m²)
North Wall	3.42	8.91
South Wall	0.59	4.46
East Wall	3.42	14.98
West Wall	0.59	14.98
Roof (Flat)	0.26	19.80
Window	1.50	3.23
Floor	1.11	14.40

Infiltration induced heat loss from the air to the outside environment was also modeled. Equation 27 was used to calculate the infiltration for the study room. *N* is equal to the number of times per hour the air is cycled in the room.

$$\dot{Q}_{Infiltration}{}^{n+1} = m_{Air} C_{p_{Air}} N \left(T_{Air}{}^{n} - T_{Outside}{}^{n}\right) \qquad 26$$

This value is dependent on variables such as occupant behavior, the quality of door and window seals, and the outdoor wind speed. For a modern building a value of 0.25 to 0.5 is typical. The value measured by DUT ranged from 0.5 to 1.0 depending on which room of the house was considered.

Walls and Outdoor Environment

The walls and ceilings were treated as large thermal mass components. However, each wall's mass was not considered individually and a variable of *additional thermal mass* was used to model the walls' thermal mass. This extra thermal mass is provided as a user input to the model and is used to account for items such as doors, wall mass that is affected by temperature changes, and furniture. The additional thermal mass is coupled to that of the thermal mass of the air in the room. The greater the additional thermal mass, the more thermal momentum the indoor air will have.

Heat transfer occurs between the air of the study room and the surrounding walls. The amount of heat transfer depends on the temperature difference between the air of the study room and the air of the neighboring rooms or outdoor environment. The outdoor temperature, which affects the amount of heat transfer from the outside walls of the study house, was measured by DUT. Heat transfer through the floor was also implemented into the model. However, the floor's temperature was kept static at 8.7℃. This value was also measured by DUT. For the two exterior walls, the west and the south walls of the study room, and the window in the south wall, the heat loss was calculated using the temperature difference of the indoor room temperature and the outdoor temperature. Heat loss through the two interior walls was calculated using the difference between the indoor room temperature and a constant

temperature assigned to the two adjacent interior rooms' air temperatures. In reality, the temperature of the east and north rooms varies with time and energy flows. A constant temperature was used to simplify the model.

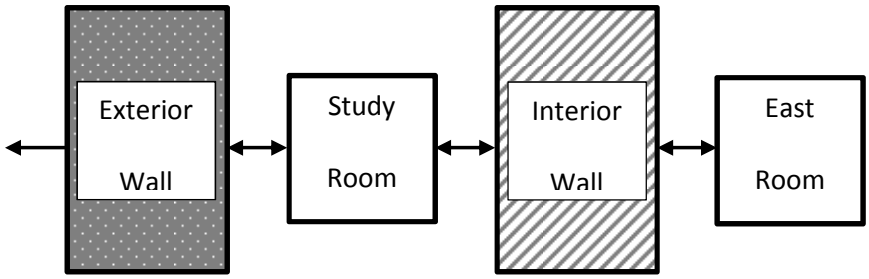

Figure 27 - Diagram of modeled heat flow

Figure 27 shows a simplified graphical depiction of the model's structure. Not all components are shown. The temperature of the study room's air can be calculated using equation 28.

$$T_{Air}{}^{n+1} = (\dot{Q}_{Kang}{}^{n+1} + \dot{Q}_{Chimney}{}^{n+1} - \dot{Q}_{Loss}{}^{n+1} - \dot{Q}_{Infiltration}{}^{n+1})/(m_{Air} \cdot C_{p_{Air}} + m_{Room} \cdot C_{p\,Room}) + T_{Air}{}^{n} \quad 27$$

To determine the accuracy of the modeling techniques discussed above, the calculated values must be compared to measured data. DUT recorded temperature measurements of the kang, air within the study room. and outdoor air. The temperature of the air was recorded in the center of the room. The modeled indoor temperature most closely mimics this curve since the center of the study room is more representative of the average room temperature than that of the air over the kang or air near the floor or ceiling.

2.4 Model Calibration

Data were measured and collected during four separate days of study. The amount of data available varies for each date of study. There is no smoke data for the days of 23rd and 24th of November. This means the smoke temperature for these two days must be estimated. Table 5 - Study Day Data Sets displays a summary of the data available for each day of study.

Table 5 - Study Day Data Sets

Date	Number of Firings	Smoke Data Available	Adjacent Room Temperature Data	24 Hour Data Set
23/11/2008	3	No	No	Yes
24/11/2008	2	No	No	Yes
02/12/208	3	Yes	No	No
19/02/2009	3	Yes	Yes	Yes

Discussed previously, the data sets for the study day 19/02/2009 were the most comprehensive. Due to this, this day was used to initially calibrate the model. The primary variables that were adjusted are listed in Table 6 - Model Variables

Table 6 - Model Variables

Variable	Calibrated Value
$h_{Kang\ Chamber}\ \left({}^{W}/_{m^2K}\right)$	24
$h_{Kang\ Surface}\ \left({}^{W}/_{m^2K}\right)$	16
Additional Thermal Mass $\left({}^{J}/_{K}\right)$	2,500,000
Air Shifts per Hour	0.9
Temperature of Adjacent Rooms (℃)	5
BLC Interior $\left({}^{W}/_{K}\right)$	75
BLC Exterior $\left({}^{W}/_{K}\right)$	18.5
Smoke Temperature (℃)	87

Several variables were used to calibrate the model. Some, like the temperature of the smoke in the kang's chamber, could be modeled from measured data. Others, such as the heat transfer coefficient of the kang's surface plate or the air shifts per hour of the study room had to be adjusted from estimates.

The heat transfer coefficient of the kang's chamber is used to calculate the amount of energy that enters the kang's plates.

$$Q^{n+1}_{KangChamber} = h_{Kang\ Chamber} \cdot SA_{Kang}\left(T^{n}_{Kang\ Chamber} - {T_{Kang}}^{n}_{1}\right) \quad 28$$

The amount of energy that leaves the kang's plates is dependent on the heat transfer coefficient of the plates. It is used to calculate the temperature of the surface node of the kang and the amount of energy transferred from the kang to the air:

$$T_{Kang}{}_7^{n+1} = T_{Kang}{}_7^{n} + \frac{\Delta t}{\rho c \Delta x}\left\{h_{Kang\ Surface}(T_{Air}^{n} - T_{Kang}{}_7^{n}) + \frac{k}{\Delta x}\left(T_{Kang}{}_6^{n} - T_{Kang}{}_7^{n}\right)\right\} \quad 29$$

$$Q_{Kang\ Air}^{n+1} = h_{Kang\ Surface} \cdot SA_{Kang}\left(T_{Kang}{}_7^{n} - T_{Air}^{n}\right) \quad 30$$

The heat transfer coefficient of the kang chamber was assumed to be in the range of 10-30 $\left({}^{W}/_{m^2K}\right)$ based on literature. This value encompasses both convective and radiant heat transfer. The heat transfer coefficient of the kang's surface was assumed to be less than that of its chamber. The initial estimate was between 10 and 20$\left({}^{W}/_{m^2K}\right)$.

The variable *Additional Thermal Mass* was initially calculated from the material properties and mass of the interior walls. The total interior thermal mass was calculated as

$$Interior\ Thermal\ Mass = \sum_{i=1}^{i=k} Mass_i \cdot C_{p_i} \quad 31$$

However, not all of this mass will be affected by temperature changes within the room. Therefore, only a percentage of the *Interior Thermal Mass* was included as *Additional Thermal Mass*. The percentage initially used was 40%.

The number of *Air Shifts per Hour* was initially set in the range of 0.5 to 2.0. Modern buildings in the developed world are usually in the range of 0.25 to 0.5. It is known that the study home has a higher value as the construction and sealing is not as high a quality as buildings in the developed world. However, the exact value was not measured and is dependent on wind speed.

The temperature of adjacent rooms was set as a constant to simplify the model. Because these rooms do not have heating elements and have walls that are exposed to the outdoor environment, a value between the temperature of the air in the study room and the outdoor air temperature was used. This produces a possible temperature range between -5 and 10°C. Measured data were taken in the north and east room during the study period of February 19th. The temperature of the north room ranged

from 3.3 to 5.7 ℃ and averaged 4.4℃. The temperature of the east room ranged from 2.7 to 11.2 ℃ and averaged 6.3℃. No other study days had adjacent room temperature data.

Two Building Load Coefficients (BLC) were developed: one for surfaces exposed to the outdoor temperature and one for surfaces exposed to the adjacent room. Multiplying each BLC by its respective temperature change produces the heat loss for the study room. The BLC is calculated

$$BLC = \sum_{i=1}^{i=K} U_i \cdot A_i \qquad 32$$

Both U and A are measured values provided by DUT.

The model to obtain the smoke temperature in the kang's chamber was discussed above. While the value of the smoke temperature was ascertained from measured data, two of the four days do not have smoke temperature data available. For the two days where smoke temperature data are available, December 2nd and February 19th, the average temperature of the smoke inside the kang chamber was 105℃ and 87℃ respectively. A value of 87℃ was used to model the days of November 23rd and 24th.

The initial values of the variables were entered into the model and the resulting study room air and kang temperature profiles assessed. Modifications were made to each variable until a common set of calibrated values were obtained across the four days of study.

The modeled vs. studied data is shown below in Figure 28- Component Temperature Profile - 02.19 (Feb 19), Figure 29 (Dec 02), Figure 30 (Nov 23), and Figure 31 (Nov 24)

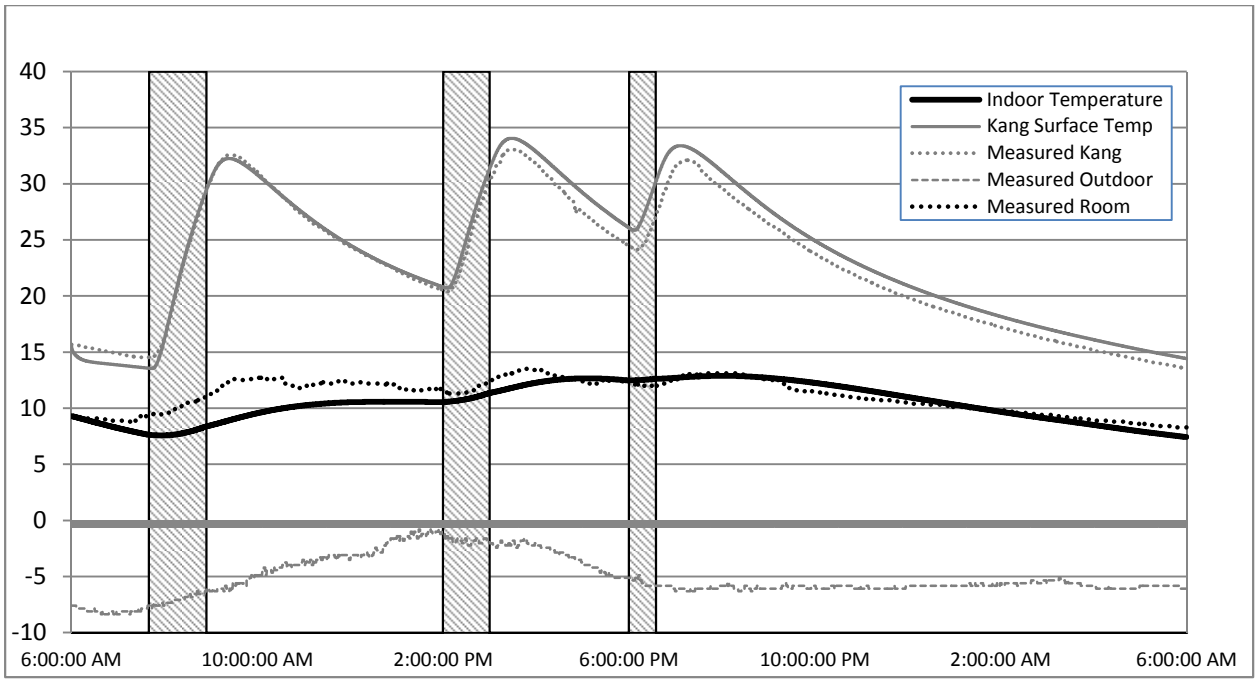

Figure 28- Component Temperature Profile - 02.19

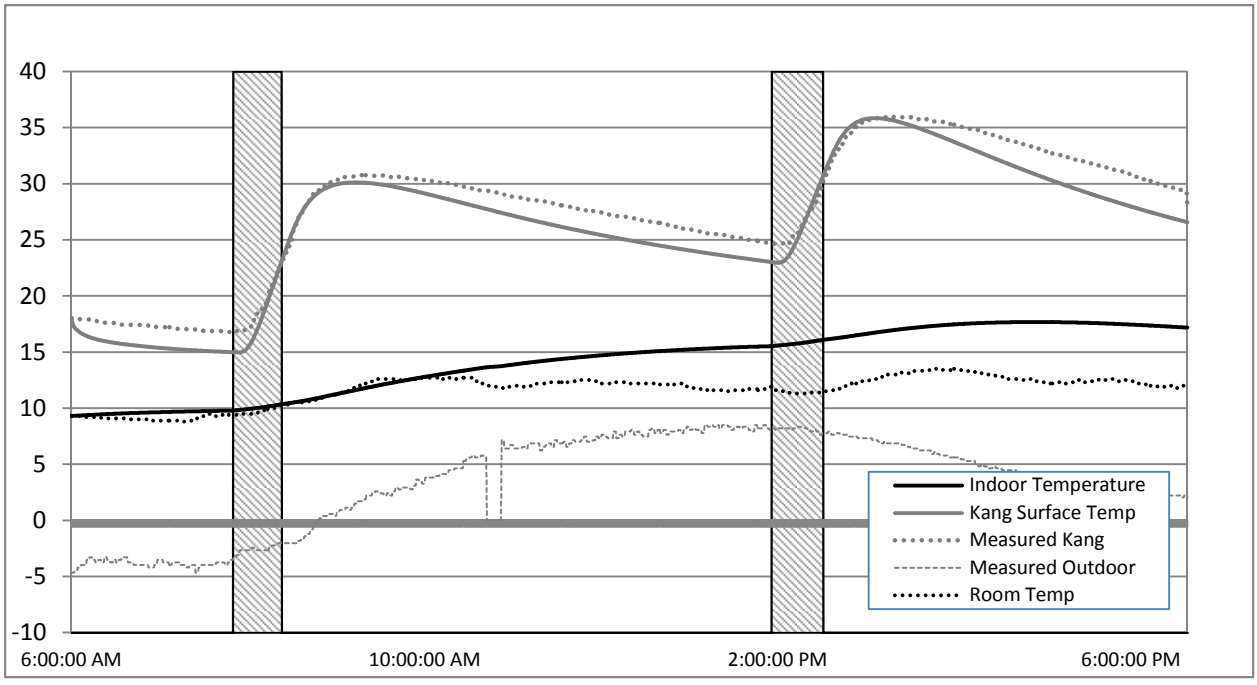

Figure 29 - Component Temperature Profile - 12.02

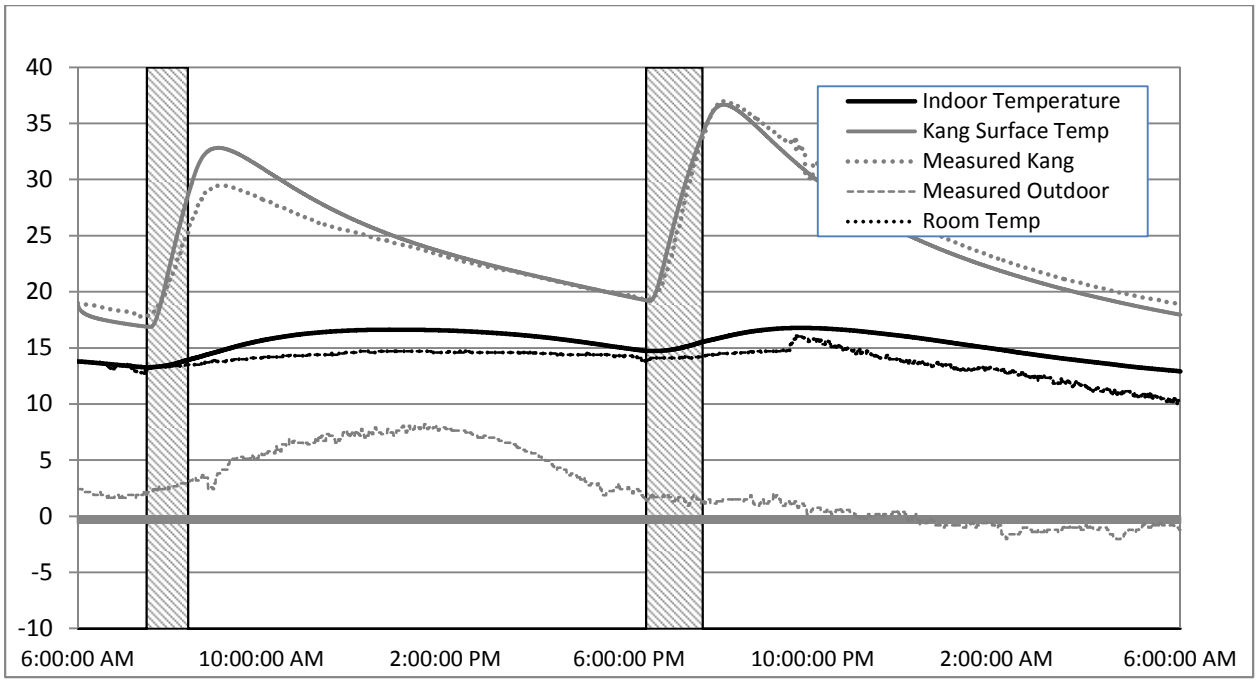

Figure 30 - Component Temperature Profile - 11.23

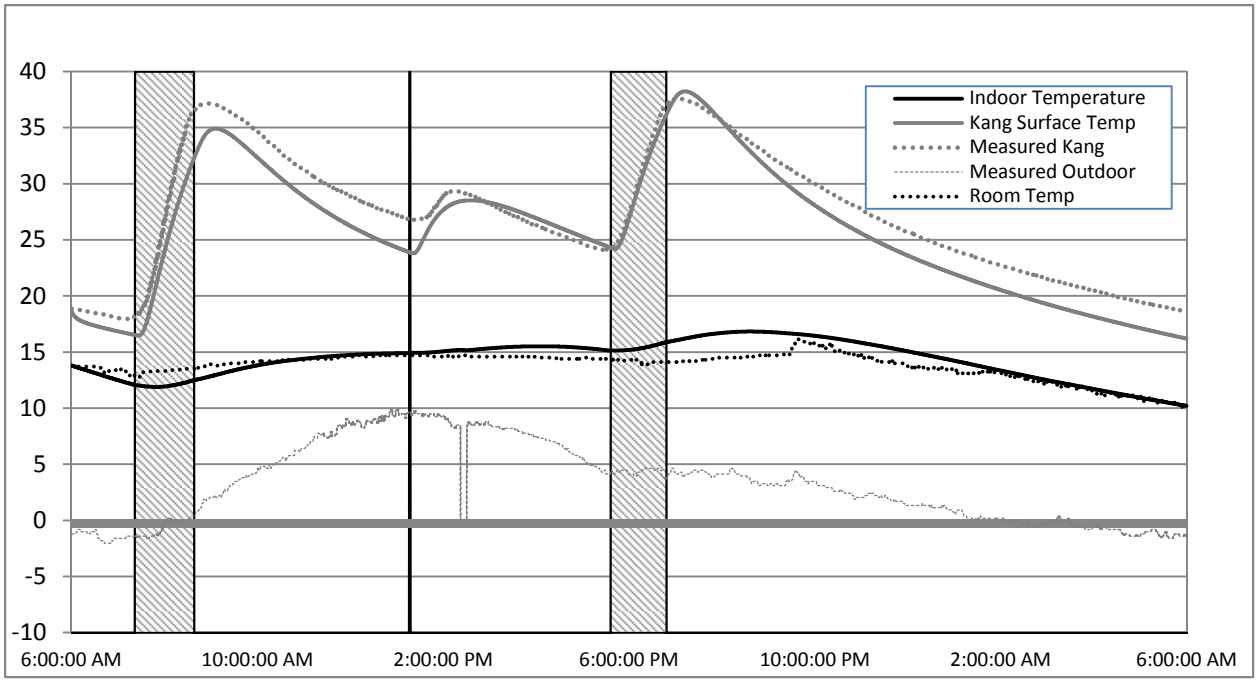

Figure 31 - Component Temperature Profile - 11.24

Sensitivity Analysis

Discrepancies between the measured and modeled data sets are present for each study day. For example: the temperature of the study room air during the morning of February 19th remains too low during the firing period and for several hours after; for the day of December 2nd the temperature of the study room air increases appropriately during the first firing but stays elevated for too long during the afternoon. Additionally, the temperature of the surface of the kang is too cold at the beginning of both firing periods; the kang temperature during the first firing on November 23rd increases too much and the air temperature is slightly too elevated during the entire day; on the day of December 24th the kang temperature during the first firing is too low. There was a small perturbation in the stove that caused a mini firing to occur even though none was recorded by the experiment monitors at DUT.

Despite the discrepancies between study days, the model is able to match the overall trends of the measured data. It is important to understand which variables most greatly affect the model's output so the most sensitive inputs can be more accurately assessed. A sensitivity analysis was performed to ascertain which variables have the greatest influence over the models behavior.

Each variable in Table 6 - Model Variables was altered by 20% and the resulting room and kang temperatures were compared to the room and kang temperatures of the calibrated model. The results are presented in two charts for each altered variable. The change in component temperature from the calibrated model is plotted with the measured data in the first chart. The second chart shows the percent change of component temperature from the calibrated model.

Figures Figure 81 - Figure 94, see Appendix B, display the temperature profile of the kang and room air for the calibrated model, referred to as the base case, and the output of the model with respective variables 20% less than the base case value. The percent change of both components is also charted.

Table 7 displays the change associated changes in the kang and air temperature profiles due to the change in value of the listed variables.

Table 7 – Variable Sensitivity

Variable	Component	Average Change (%)	Standard Deviation (%)
$h_{Kang\ Chamber}\ \left(^{W}/_{m^2K}\right)$	Air	-4.2	1.5
	Kang	-4.5	1.7
$h_{Kang\ Surface}\ \left(^{W}/_{m^2K}\right)$	Air	-6.0	2.0
	Kang	5.0	1.0
Additional Thermal Mass $\left(^{J}/_{K}\right)$	Air	-0.25	2.8
	Kang	-.07	.69
Air Shifts per Hour	Air	**9.5**	3.7
	Kang	2.4	1.4
Temperature of Adjacent Rooms (℃)	Air	-0.91	0.32
	Kang	-0.23	0.12
BLC $\left(^{W}/_{K}\right)$	Air	**13.8**	5.6
	Kang	3.5	2.0
Smoke Temperature (℃)	Air	-4.4	1.9
	Kang	-4.2	3.6

It is clear that the model is most sensitive to changes in the *BLC* and *Number of Air Shifts* per hour. The *BLC* was obtained from measured data provided by DUT. While errors in the measurement of surface area or material properties are possible, the likelihood of them occurring and the magnitude would be small. Discussed previously, the *Number of Air Shifts* is dependent on the estimations of room insulation, air leakage and outdoor wind speed. Many of these values are unknown and using uncertain values to estimate the value of the *Number of Air Shifts per hour* creates uncertainty in the model. Because the model is highly sensitive to this variable, users should do their best to ensure an accurate value is used.

In the paper *A Calculation method for Air Infiltration Energy Loss Based on Climatic Data* (Weber, 2004) a method to calculate the amount of infiltration loss based on climatic data. While the method is generally too complex for the simplified model, it could be implemented if higher accuracy of the infiltration loss is desired.

Chapter III: Improvement Systems

3.1 Introduction

Because of its relatively high specific heat and ability to be transported easily, water functions well as a thermal storage medium. It can store excess energy which can be accessed at a later point in time. A series of improvement components were analyzed and added to the system model; an overview of their setup is diagramed in Figure 32 - Water System.

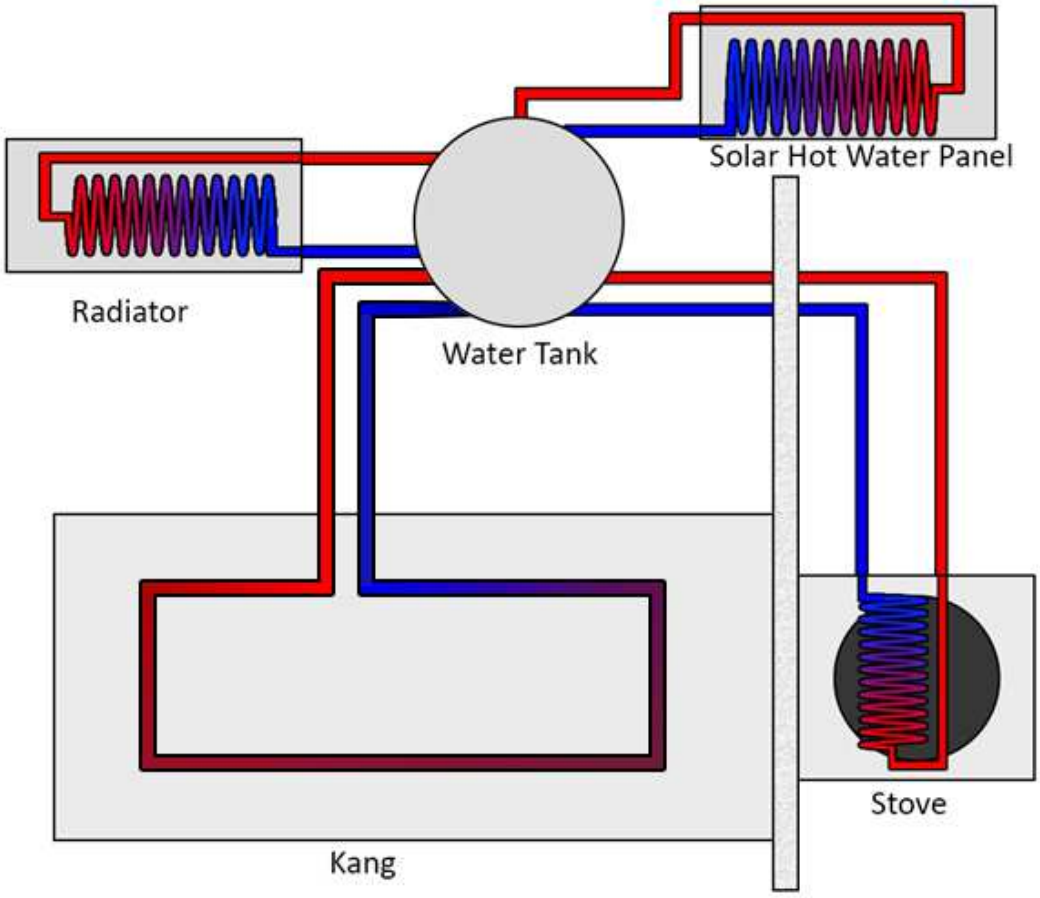

Figure 32 - Water System

Overview

The setup of water based improvements is as follows. Water is stored in a tank inside the house. The size of the tank is variable and can be changed based on the system's efficiency and energy demand. Three components draw water from the tank: a stove heat exchanger, a radiator and a solar hot water panel. The temperature of the water in the tank is uniform and stratification effects were not considered due to the complexity involved. Because of this assumption, the calculated efficiency of the system is less than if temperature stratification effects were considered. Water from the tank is heated in a heat exchanger inside the cook stove. The heated water is returned to the tank and uniformly mixed with the water in the tank. The solar hot water panel operates in a similar manner. Water from the tank is heated in the panel by energy from the sun. It is then returned to the tank where uniform mixing occurs. The radiator acts in the opposite manner of the stove or solar hot water heat exchangers. Water from the tank enters the radiator and energy is exchanged with the indoor air. The cooled water returns to the tank where it is mixed with the remaining water in the tank. Water pipes within the surface slab of the kang act in a similar manner to the radiator. Hot water from the tank flows through the pipes and energy is transferred to the surface plates of the kang. The cooled water then returns to the water tank. Each component is controlled by algorithms within the program which will be discussed in detail below.

Heat Exchanger

The heat exchanger that is used to heat water is located inside the stove. An unmixed cross-flow heat exchanger was selected as the heat exchanger type for the model. An unmixed cross flow heat exchanger restricts both fluid streams to one directional flow, similar to a radiator with tubes and fins. Figure 33 diagrams typical cross flow heat exchangers.

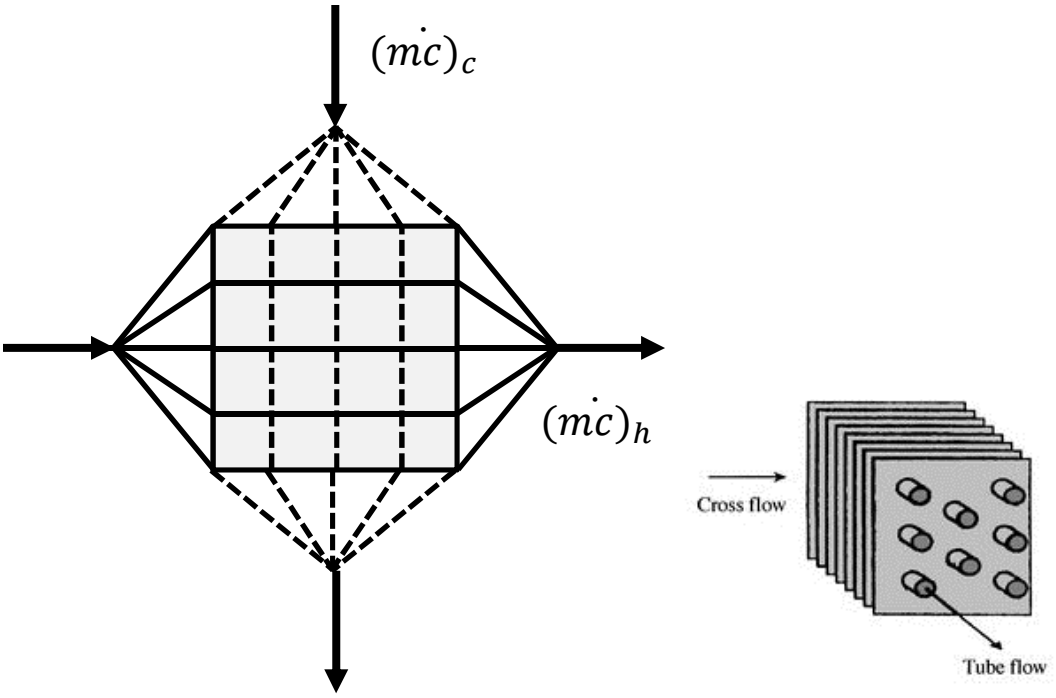

Figure 33 - Cross Flow Heat Exchanger[1]

The temperature of neither outlet flow is known. Because of this, the heat exchanger effectiveness ε must be used. The heat exchanger effectiveness ε is the ratio of actual to maximum possible rate of heat transfer. If the heat exchanger effectiveness ε is known, along with the flow rates of the hot and cold fluid streams, the outlet temperature of the hot and cold streams can be calculated. In this instance, the hot fluid stream is the smoke from the stove and the cold fluid stream is the water from the water storage tank. The heat transfer effectiveness is provided as a user input to the program. The effectiveness is a property that is supplied by heat exchanger manufacturers and will change depending on the model used. The default value in the program is 80%.

Since the heat exchanger is placed in the stove it can be assumed that all energy not used for cooking is available to the heat exchanger. Thus, the inlet temperature of the smoke is the temperature of the smoke in the stove. This was discussed in the section regarding the development of the smoke

[1] (Kreith, 2001)

temperature model. During firing the temperature of the smoke is 294°C, after firing the inlet temperature of the smoke decays logarithmically. Therefore the inlet temperature of the smoke is fully known and varies with time.

The mass flow of the smoke can be determined by the following analysis. Using the equation

$$\dot{m}_{smoke} = \frac{\dot{Q}_{smoke}}{c_{smoke}(T_{smoke} - T_{air})} \quad 33$$

the mass flow rate of the smoke can be calculated. The rate of heat production of the smoke $\dot{Q}_{smoke}$ can be determined from the amount of energy released by the fuel in the stove. Mentioned previously, the combusted fuel releases roughly 22 kW of power. Studies of the typical kang cook stove conducted by DUT have determined that generally 35% of the energy released by the fuel is used for cooking. Therefore, $\dot{Q}_{smoke}$ is equal to just over 14kW. The smoke is assumed to have the same properties as air so c_{smoke} is determined to be the average of c_{air} at 294°C and c_{air} at 10°C, 10°C being the inlet temperature of the air in the stove. Using these data, $\dot{m}_{smoke}$ was determined to be 0.05 kg/s . It is assumed that this mass flow rate is constant, even after firing ceases and the smoke enters the decay regime. A more detailed analysis of the mass flow rate of the smoke was conducted by DUT. Results of the study indicate a smoke mass flow rate between 0.04 and 0.08 kg/s with an average flow rate of 0.054 kg/s (Zhuang, 2008).

The mass flow rate of the water is provided by the program user. It is adjustable, along with the size of the tank so the water in the heat exchanger does not overheat and boil. The default value is 6 liters per minute or 0.1kg/s.

With the mass flow rate of both fluid streams and the effectiveness of the heat exchanger known, the outlet temperature of the hot and cold fluid streams can be determined. Table 8 displays the required data to calculate the outlet temperatures.

Table 8 - Heat Exchanger Properties

Fluid	$c_p(J/kg\ K)$	$\dot{m}\ (kg/s)$	$C_h(W/K)$	$C_c(W/K)$
Water (cold)	4,187	0.1		418
Smoke (hot)	1,024	0.05	50	

The outlet temperature of the water is

$$T_{c,out} = \frac{\varepsilon C_h (T_{h,in} - T_{c,in})}{C_c} + T_{c,in} \quad 34$$

The outlet temperature of the smoke is

$$T_{h,out} = T_{h,in} - \frac{\varepsilon C_h (T_{h,in} - T_{c,in})}{C_h} \quad 35$$

During each time step while the heat exchanger is active, a mass of water is removed from the storage tank $\dot{m}_{hx,water}$, its temperature raised in the heat exchanger, and then returned to the storage tank. The mass of smoke that enters the heat exchanger $\dot{m}_{smoke}$ has its temperature lowered and then enters the kang chamber. The addition of the heat exchanger will lower the temperature of the kang's surface plates as some energy that would be used to heat the kang plates is transferred and stored in the water system.

The heat exchanger is controlled by a simple algorithm. If the temperature of the smoke is greater than the temperature of the water tank, $T_{HX,in}$, then the heat exchanger is activated. If the water temperature at the inlet is greater than that of the smoke, heat transfer would occur in the wrong direction, from the water to the smoke. Additionally, the tank temperature is limited to a maximum user defined temperature which has a default value of 90℃. If the tank temperature is greater than this value, the heat exchanger will be bypassed and no further energy will be added to the water system. This is done so the water in the tank and the lines does not boil and change phase. Figure 34 shows the temperature profile of the inlet and outlet flows of the heat exchanger over the period of 24 hours.

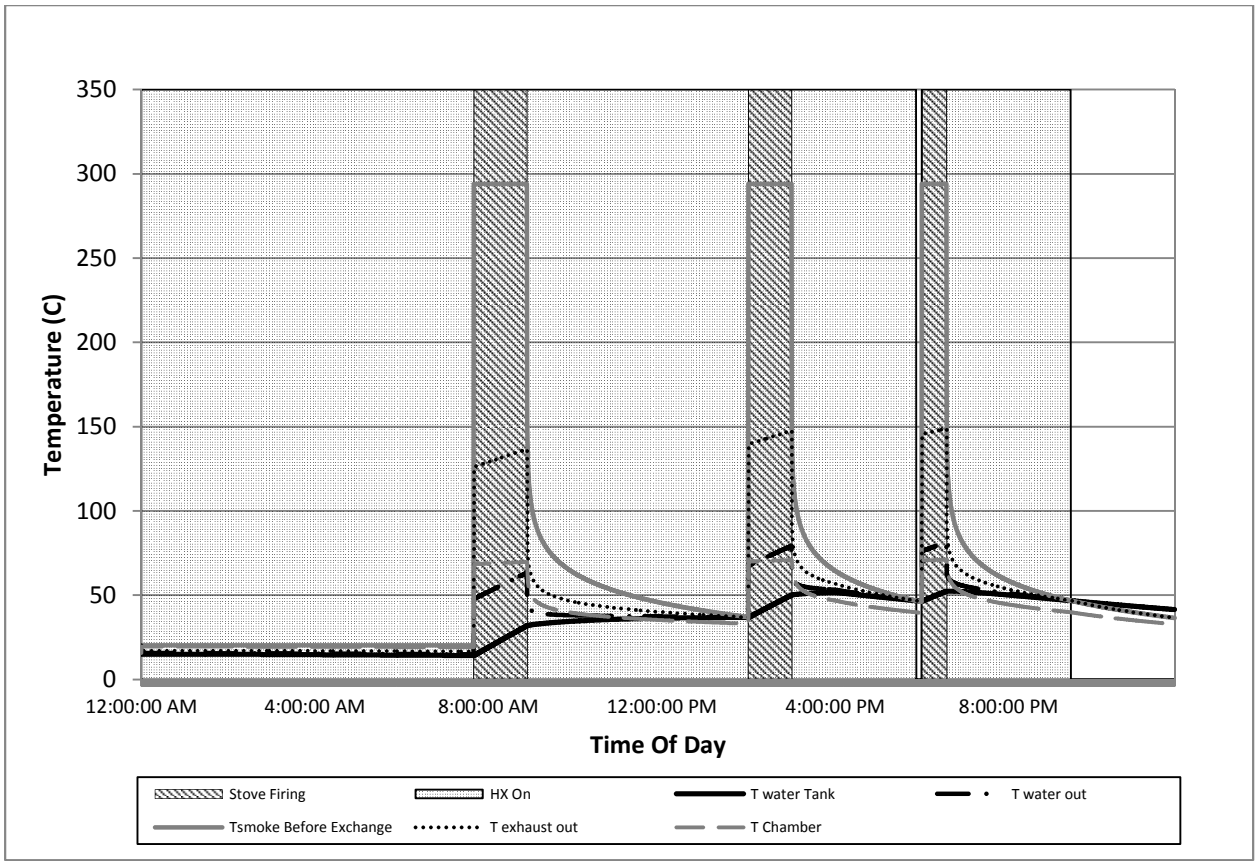

Figure 34 - Heat Exchanger Profile

The solid gray area of the chart indicates the heat exchanger is active. This occurs when the water in the tank is less than the temperature of the smoke in the stove. In Figure 34 the heat exchanger is active until late in the evening. This is partially due to the initial conditions of the program. The initial temperature of the water tank is a user input to the program with a default value of 15℃. The initial temperature of the stove is also a user input and has a default value of 20℃. Because of this temperature difference the heat exchanger will be active at the beginning of the program. The areas shaded with diagonal lines indicate instances when the stove is being fired. During this period the temperature of the smoke in the stove is 294℃. As heat transfer occurs between the cross flowing fluids in the heat exchanger, the temperature of each flow is altered. The temperature of the smoke after the exchange, $T_{h,out}$, drops to roughly 120℃ during the first firing. The temperature of the smoke in the

kang chamber, which, referring to Figure 26- Smoke and Kang Chamber Temperature, was 87℃ when the heat exchanger was not present, is now 69℃; the decrease stemming from energy being transferred to the water flow in the heat exchanger. The surface temperature of the kang will therefore decrease when the heat exchanger is active; some energy that would have entered the kang plates is now stored in the water tank. The temperature of the water tank, $T_{c,in}$ increases from 15℃ to 40℃ during the first firing period. The outlet flow of the water stream increases from 15℃ to 47℃ when the heat exchanger is active. Since the temperature of the water tank increases over the firing period, so does the outlet temperature of the water flow, rising from 47℃ to 63℃.

After the firing period, heat transfer still occurs between the smoke and the water flows and the temperature of the water in the tank continues to rise. This is desired and reflects stored energy that was transferred from the smoke. This energy can be accessed at a later time and put back into the room using a radiator.

Radiator

The radiator is used to transfer stored energy in the water tank into the room. It functions much like the heat exchanger with the exception that energy is transferred from the water to the air rather than from the smoke to the water. If the radiator is active, water from the tank enters the radiator at a determined flow rate. The flow rate is provided as a user input and depends on the type and size of radiator selected. A flat panel, reduced fin, wall radiator was selected and modeled in the program. The panel's dimensions are one meter wide by 0.505 meters tall. According the manufacturer, a flow rate of 8.5 liters per minute should be used. This value was set as the default flow rate, $\dot{m}_{Radiator}$, in the program. The selected radiator is capable of outputting 1,253 Watts at a 50℃ temperature differential between the average temperature of the inlet and outlet flows and the ambient air (Merriott Design Radiators, 2012). This can be summarized as

$$\dot{Q}_{Radiator} = \dot{m}_{Radiator} c_{water} (T_{mean} - T_{air}) = 1{,}253\ W\ @\ \Delta T(50) \qquad 36$$

$$T_{mean} = T_{Radiator,in} - T_{Radiator,out} \qquad 37$$

Equation 37 is only valid for a 50°C temperature differential and must be adjusted for different temperature differentials. The radiator's manufacturer provides an adjustment factor based on different ΔTs. The power adjustment factor is plotted for various temperature differentials in Figure 35 - Delta T Adjustment Factor

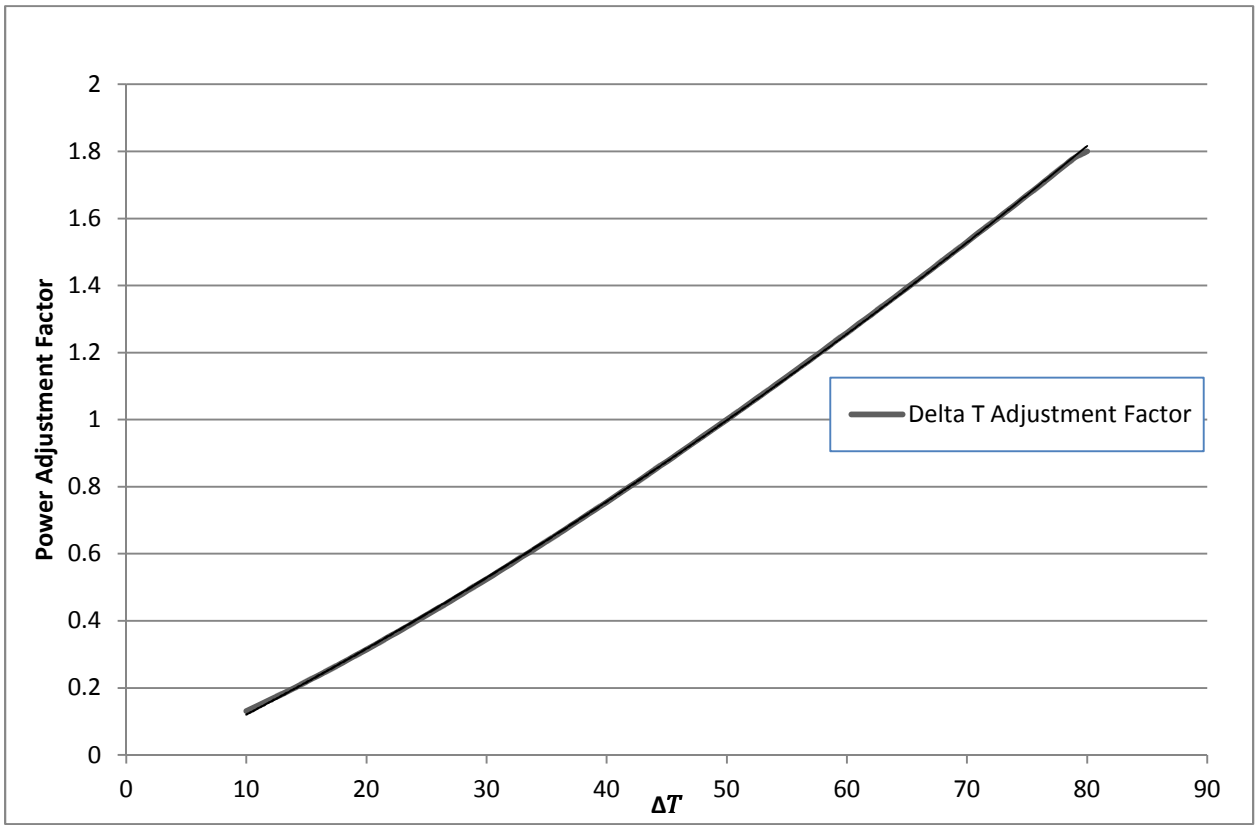

Figure 35 - Delta T Adjustment Factor

At $\Delta T(50)$ the adjustment factor is equal to one so the output power is 1,253 Watts. At @ $\Delta T(80)$ the adjustment factor is 1.8 and the adjusted output power of the panel is 2,255 Watts. The adjustment factor is incorporated into the model. However, while the inlet temperature is known, the temperature of the water in the tank and the outlet temperature of the panel are unknown. Because of this, the power produced by the radiator must be calculated using the outlet temperature from the previous

time step. The number of panels can also be adjusted in the program. The default value is one. If a second panel is desired, the number of panels would be entered as two, and the power output would double. Equation 39 can be updated to accommodate for the time step differential, adjustment factor and number of panels

$$\dot{Q}_{Radiator}^{n+1} = \dot{m}_{Radiator} c_{water} (T_{mean}^{n} - T_{air}^{n}) \cdot AF \cdot n_{panels} \quad 38$$

$$T_{mean}^{n} = T_{Radiator,in}^{n} - T_{Radiator,out}^{n} \quad 39$$

Kang Radiant Heating

The mechanism for transmitting energy into the room is variable. As discussed above, a radiator can be used to transfer energy from the hot water in the storage tank to the room's air, or piping within the kang's surface slab can be used to transfer energy from the water to the surface of the kang. The power output of the radiant heat piping can be determined from equation 41.

$$\dot{Q}_{Kang\ Pipes}^{n} = \dot{m}_{Pipes} c_{water} (T_{Tank}^{n} - T_{Pipes\ Out}^{n}) \quad 40$$

Hot water from the tank flows into the pipes imbedded in the kang's surface slab. The flow rate is specified by the size of the piping used, in this case the flow rate is 3.5 l/m and the pipe diameter (D) is 1 cm. The temperature of the outlet flow is unknown. Because of this, equation 41 is not sufficient to calculate the energy transfer from the water in the pipe to the kang's surface slab. Using a shape factor for a pipe within a slab, the amount of energy released from the pipe can be calculated using equation 42.

$$\dot{Q}_{Kang\ Pipes}^{n} = k_{kang} S \left(T_{Pipe}^{n} - T_{Kang_7}^{n} \right) \quad 41$$

Where the shape factor is calculated as

$$S = \frac{2\pi}{\cosh^{-1}(2z/D)} \quad 42$$

z being the depth of the piping in the slab.

However, equation 43 assumes the temperature of the pipe is constant, which is not the case in the model as the water temperature declines as the water flows through the pipe and transfers heat to the kang. If the pipe is divided into many small sections of length(l), each section can be assumed to have a constant pipe temperature. This allows the amount of energy from each pipe section to be calculated. Furthermore, the temperature of the outlet flow of each section can be determined with equation 44

$$T^n_{Pipe,out_l} = T^n_{Pipe,in_l} - \frac{\dot{Q}_{Pipe_l}}{\dot{m}_{pipe} c_{water}} \quad 43$$

The outlet flow temperature of section one is the same as the inlet flow temperature of section two, represented by equation 45

$$T^n_{Pipe,in_{l+1}} = T^n_{Pipe,out_l} \quad 44$$

Equation 42 can be updated for each section

$$\dot{Q}^n_{Kang\ Pipes_l} = k_{kang} S \left(T^n_{Pipe,in_l} - {T_{Kang}}^n_7 \right) \quad 45$$

and the heat flow and outlet temperature for each section of pipe can be calculated. This process is displayed in Figure 36 - Radiant Piping Nodes below.

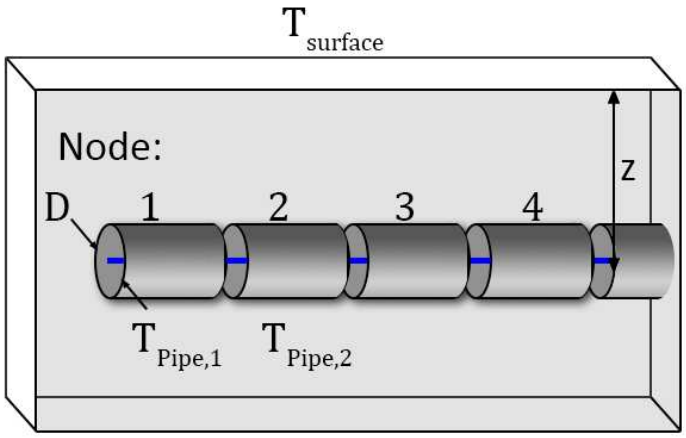

Figure 36 - Radiant Piping Nodes

The heat flow of each section can be summed to determine the total heat flow from the water pipes to the kang surface slab.

$$Q^{n}_{Kang\ Pipes} \sum_{l=1}^{l=m} k_{kang} S \left(T^{n}_{Pipe,in_l} - T_{Kang}{}^{n}_{7} \right) \quad 46$$

The smaller the section the more accurate the calculation will be. However, the temperature and energy flow of each section must be calculated for each time step; that is, the section iteration occurs within each time step. An analysis was performed using 10, 20 and 40 sections over a total pipe length of 10 meters and it was determined that there was less than 0.5% difference in results when using 10 or 40 sections. Therefore, 10 sections were used to keep the model from performing excessive calculations.

Some assumptions were made with the above analysis. To use the conduction model and shape factor method, it must be assumed that all energy released by the pipes flows into the kang's surface node and no energy is conducted into the nodes below. The conduction equations do not account for this but the transient heat transfer model of the kang does allow heat to flow bi-directionally. If the surface node's temperature increases above that of the node below it, energy will flow from the surface node into the kang's chamber.

It was also assumed that the temperature of the pipe's surface was equal to that of the water flowing through it. No insulation or conduction effects of the pipe's material were considered. Furthermore, it was assumed that the energy is uniformly conducted into the surface slab of the kang.

Thermostat

The radiator and kang radiant heating is controlled by a thermostat algorithm within the modeling program. The user can input hourly temperature set points in the programs interface. The desired temperature is different depending on the location of the radiator panels. If the radiator is placed on the wall in the room, the thermostat algorithm uses air temperature as an input. If the users selects kang radiant heating, the thermostat algorithm uses the kang's surface temperature as an input. This allows

for different temperature control based on the location of the radiator. If the radiator is in the room, the room air set point can be set to a comfortable indoor temperature, in the range of 15 to 20℃ . If radiant heating is used to heat the kang, a surface temperature set point of 15 to 20℃ is too low and a set point in the range of 25 to 30℃ can be entered.

The thermostat algorithm compares the current set point temperature to the input temperature; air temperature if the radiator is in the room, kang surface temperature if kang radiant heating is selected. If the input temperature is below the desired set point temperature, the radiator is turned on. The radiator will remain on until the input temperature is equal or greater than the set point temperature. At this point the radiator turns off and remains off until the temperature is less than the current set point temperature. In order to keep the radiator from oscillating on and off when the input temperature is at or near the set point temperature, a temperature buffer was introduced to the algorithm. For the radiator to turn on, the input temperature must be less than or equal to the set point temperature minus the temperature buffer. The radiator will remain on until the input temperature is greater than the set point temperature plus the buffer temperature. When this occurs the radiator stays off until the input temperature drops below the set point temperature minus the buffer temperature. Adding this buffer permits for smoother operation of the physical system.

Figure 37 - Thermostat Control shows an example of the thermostat algorithm of the course of three days.

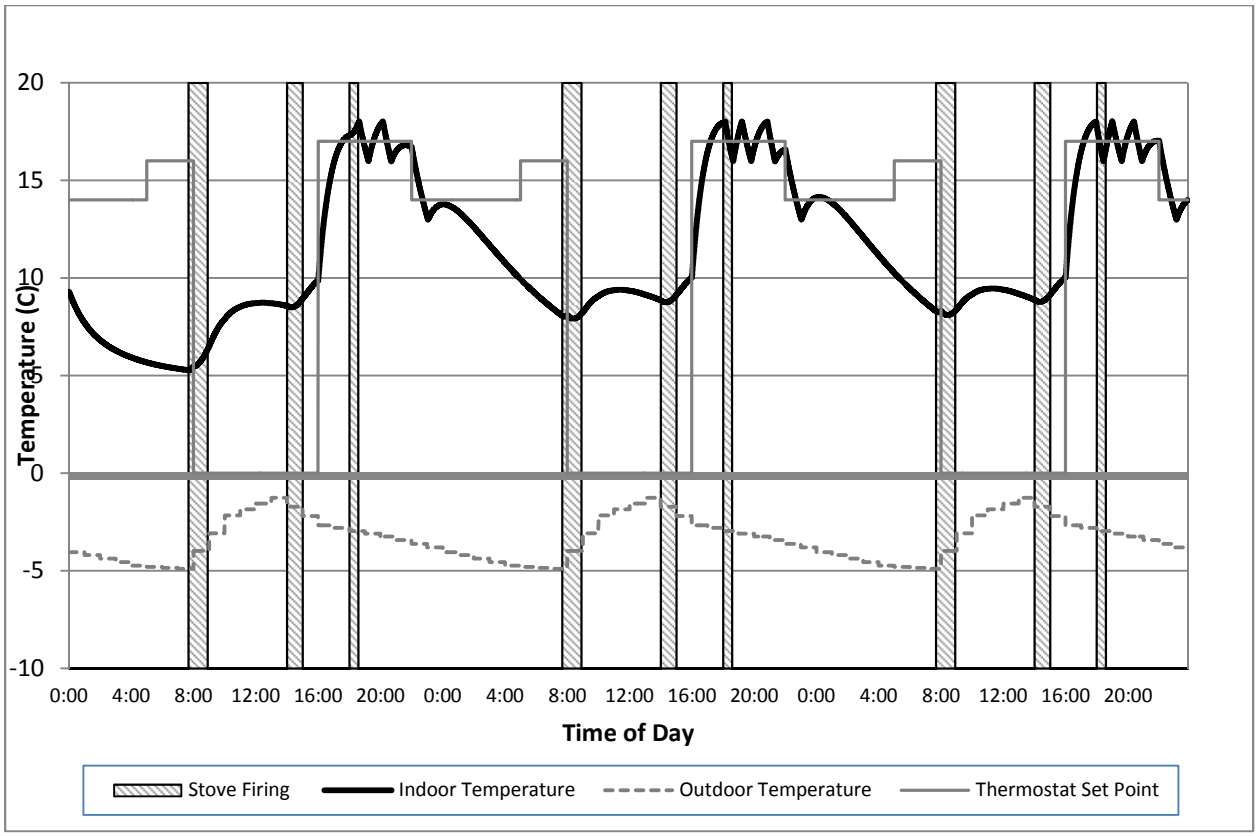

Figure 37 - Thermostat Control

In this instance, the thermostat uses the room air temperature as an input and the radiator is located in the room. The thermostat set point changes throughout the day. Table 9 shows the hourly set points.

Table 9 - Thermostat Program

Hour	Radiator Set Point (C)
12:00 – 06:00	14
06:00 – 08:00	16
08:00 – 17:00	Off
17:00 – 23:00	18
23:00 – 24:00	14

The radiator functions well in the evening but cannot meet the temperature set point of 14 degrees during the night. There is not enough stored energy in the water tank to release into the room to overcome the heat loss.

Solar Hot Water

The solar hot water heater is used to add energy collected from the sun to the indoor environment. Solar and environmental data was gathered from NREL's Typical Meteorological Year (TMY) database for the region of study near Dalian, China (NREL, 1991-2005). A panel that is tilted to receive direct incidental radiation was selected for the model. A tilted panel can receive more solar radiation than one that is flat. Two environmental factors that affect the efficiency of the collecting panel are the direct normal radiation (DNR) and the outdoor ambient temperature. The DNR is defined as the "Amount of solar radiation in $W\ h/m^2$ received within a 5.7° field of view centered on the sun". Incidental radiation is not accounted for. Both the DNR and the outdoor ambient temperature were collected from TMY data provided by NREL. Hourly data was gathered for each day in January and then averaged. The month of January was selected as the outdoor temperature is very cold and there is little solar radiation. The model must be able to optimize the heating systems during the coldest and darkest months. Both series of data are charted in Figure 38.

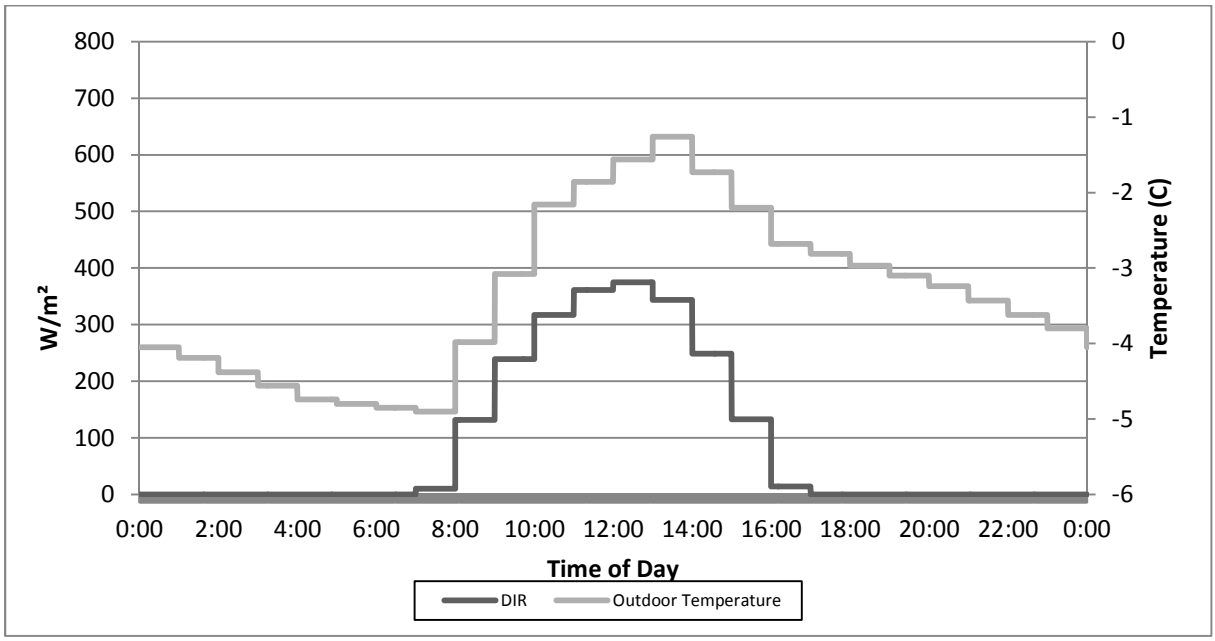

Figure 38 - DNR & Outdoor Temperature - 24 hrs

Because of the month selected there is very little solar radiation available for heating. The solar panel can only collect energy from the hours of 8:00 to 16:00. The DNR reaches a maximum value of just under 400 Watts per square meter slightly after 12:00 pm. The outdoor temperature reaches a minimum of -5℃ slightly before sun rise. The temperature climbs to a maximum of – 1.2℃ around 14:00 before steadily falling through the evening and night.

An evacuated tube solar panel was selected for the model. The area of the panel and the flow rate of the fluid were left as user inputs for the program. The manufacturer of the panels suggests a flow rate of 0.8 gallons per minute or 2.1 liters per minute. The efficiency of the panel is dependent on the mean temperature of the inlet and outlet and the ambient outdoor temperature. A chart of the panel's efficiency is shown in Figure 39.

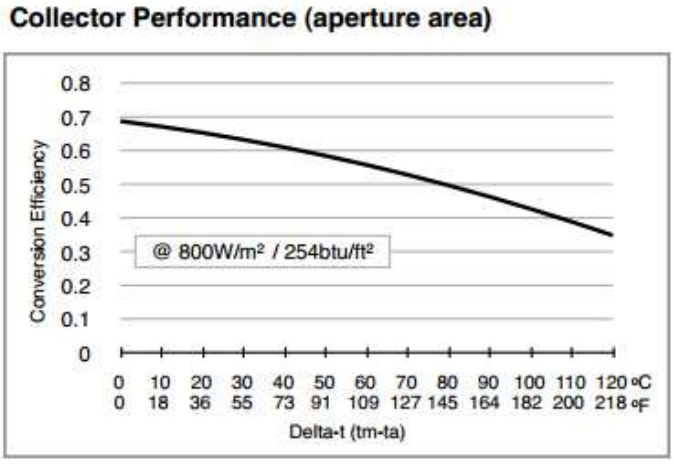

Figure 39 - SHW Collector Performance[1]

The panel's efficiency is accounted for in the model and used to calculate the energy captured from solar radiation. This is done using equation 48

$$\varepsilon_{SHW}^{n} = AF \cdot (T_{SHW,mean}^{n} - T_{Outdoor}^{n}) \quad 47$$

The outlet temperature of the solar hot water heater is calculated as

[1] (Apricus Solar Hot Water, 2011)

$$T_{SHW,out}^{n+1} = \frac{\varepsilon_{SHW}(DNR)A}{\dot{m}_{SHW}C_{p,water}} + T_{SHW,in} \quad 48$$

This is calculated for the succeeding time step due to the solar hot water panel's efficiency relying on the mean temperature which is dependent on the outlet temperature. With the outlet temperature known, the amount of heat collected by the solar panel can be determined.

$$\dot{Q}_{SHW} = \dot{m}_{SHW}C_{p,water}(T_{SHW,out} - T_{SHW,in}) \quad 49$$

Water Tank

The water tank is the unifying element of the heat exchanger, radiator and solar water panel. The size and dimensions of the tank are customizable and provided as user inputs of the program. The shape of the tank is assumed to be a cylinder. Because of this assumption, if the tank volume and height are provided by the user, the diameter and corresponding surface area can be calculated. Heat loss from the tank is calculated as

$$\dot{Q}_{Tank}^{n+1} = U_{Tank}A_{Tank}(T_{Tank}^{n} - T_{Air}^{n}) \quad 50$$

The tank is assumed to be insulated. U_{Tank} is provided as a user input to the program with a default value of 0.35 (W/m^2K). The heat loss from the tank is an energy input to the room's air.

The temperature of the water tank is evaluated at each time step and varies on the amount of energy that is added or subtracted by each attached component. A diagram of the tank and each component is shown in Figure 40.

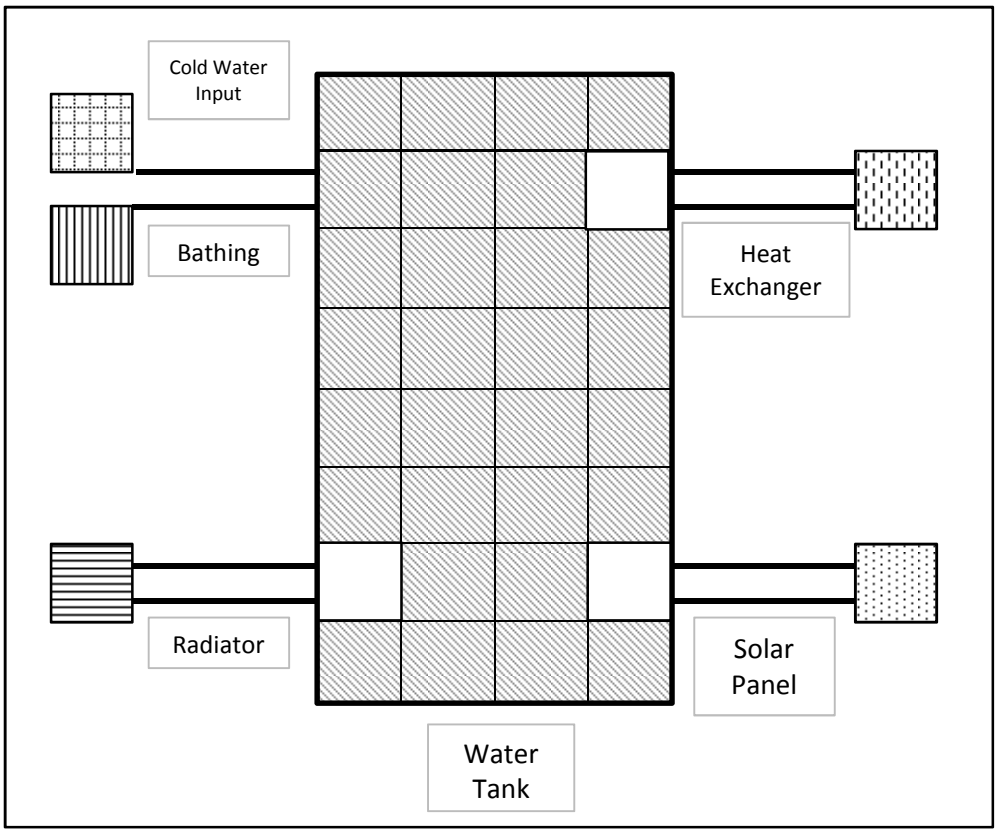

Figure 40 - Water Tank and Attached Components

During each time step, a given amount of water is withdrawn from the tank by each active component, its temperature altered and then replaced into the tank. The tank's temperature is then recalculated according to the amount of energy that has been added or subtracted to the tank's water mass. Other than the bathing algorithm, which will be discussed tin the following section, the tank is a closed system and it is assumed the water mass within the tank does not change. The tank's temperature can be calculated as

$$T_{Tank}^{n+1} = \frac{(m_{Tank} - m_{Stove\,HX} - m_{Radiator} - m_{SHW}) T_{Tank}^{n} + (m_{Stove\,HX} T_{hx,out}^{n} - m_{Radiator} T_{Radiator,out}^{n} - m_{SHW} T_{SHW,out}^{n})}{m_{Tank}} \quad 51$$

If a component is inactive the mass of water within the component is considered to be zero. As mentioned previously, the mixing model for the tank assumes the temperature is uniform and distributed at each time step. This produces lower efficiency in the attached components. Ideally, the

heat exchanger and solar panels would draw cold water from the bottom of the tank and return hot water to the top. The radiator would pull hot water from the top and return cold water to the bottom. This would ensure the ΔT was maximized for each component. However the complexity required to model tank stratification is beyond the scope of a simplified model.

Bathing

A bathing or hot water use algorithm was implemented into the model. The primary focus of this project is improving thermal comfort for rural residents, and much effort has been spent on increasing the kang or air temperature. However, many residents that were interviewed expressed a desire for readily available hot water for bathing. Because of this, improvements that allow for hot water bathing should be evaluated.

The average hot water use of a rural household in northeast China was determined from literature and community interviews and found to be 25 liters of 40℃ water per day. A bathing schedule was developed such that four occupants bathe for 15 minutes each day between the hours of 17:00 and 18:00. These hours were selected for two reasons. First, this time period is when the occupants would have finished work and be ready to wash before dinner. Second, the water temperature of the tank is higher during this period than in the morning before the first and second firing have occurred.

Therefore, 100 liters of 40℃ is used for bathing each day and this occurs during one hour. The flow rate of the water used for bathing is therefore known, $\dot{m}_{bathing}$. The water tank supplies all the hot water that is used for bathing. However, the tank temperature is greater than 40℃, so cold water must be mixed with the hot water of the tank. The ratio depends on the temperature of the tank which is variable. Using equations of mass and energy balance the flow rate of the hot water, that is water from the tank, and cold water can be determined.

$$\dot{m}_{bathing} = \dot{m}_{hot} + \dot{m}_{cold} \quad 52$$

$$\dot{m}_{bathing}T_{bathing} = \dot{m}_{hot}T_{tank} + \dot{m}_{cold}T_{cold} \quad 53$$

The temperature of each stream is known, $T_{bathing}$ is set at 40°C, T_{tank} is variable but known, and T_{cold} is a user input of the program and is set at 10°C as default. Equations 53 and 54 can be reconfigured as

$$\dot{m}_{hot} = \dot{m}_{bathing} - \dot{m}_{cold} \quad 54$$

and

$$\dot{m}_{cold} = \dot{m}_{bathing}\left(\frac{T_{bathing}-T_{tank}}{T_{cold}-T_{tank}}\right) \quad 55$$

The flow rate of hot water from the tank is known; therefore over the hour of bathing a total amount of hot water used for bathing can be calculated. To keep the tank from being drained, an equal amount of cold water is used to replace the amount of hot water used for bathing. This added cold water lowers the temperature of the tank and will affect the performance of the other components attached to the tank. Equation 52 can be updated to accommodate bathing water use. The temperature of the tank is now calculated as:

$$T_{Tank}^{n+1} = \frac{(m_{Tank}-m_{Stove\,HX}-m_{Radiator}-m_{SHW})T_{Tank}^{n}+(m_{Stove\,HX}T_{hx,out}^{n}-m_{Radiator}T_{Radiator,out}^{n}-m_{SHW}T_{SHW,out}^{n}-m_{hot}T_{Tank}^{n}+m_{hot}T_{hot}^{n})}{m_{Tank}} \quad 56$$

Phase Change Material

Phase Change Material functions as a large thermal mass within the model. The PCM absorbs, stores and releases energy. However, rather than absorbing and releasing energy as a function of its sensible heat, the PCM absorbs and releases energy during phase change. Unlike sensible heat storage, the temperature during latent heat storage remains relatively static. This process is governed by the latent heat of the material which is significantly greater than the specific heat. In reality, a PCM will have a melting and freezing temperature. When the material's temperature is between these two temperatures it will be in phase change. When the material is in phase change, it can absorb or release energy related to its latent heat. When the material's temperature is less than its melting point or

greater than its freezing point, it absorbs or releases energy related to its sensible heat. This process is shown in Figure 41. When the temperature of the PCM is within the latent heat temperature range it takes significantly more energy to raise the material's temperature than it does when the temperature of the PCM is in the sensible heat temperature range.

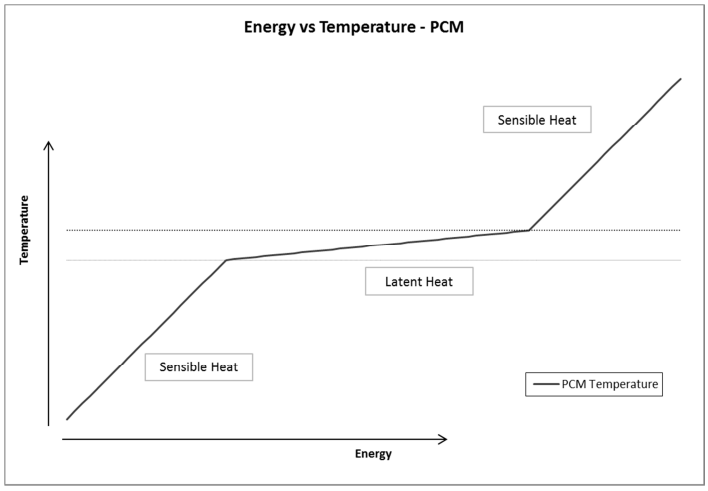

Figure 41 - PCM Behavior

For simplicity, the PCM in the simulation was modeled to change phase at one temperature rather than over a range. This is shown in Figure 42

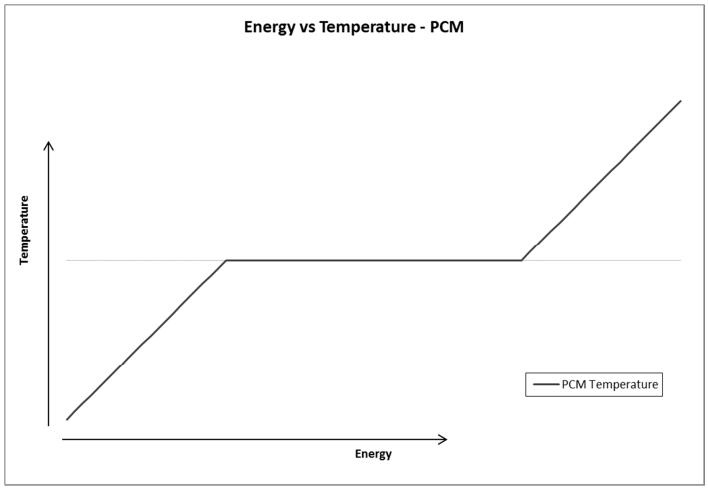

Figure 42 - PCM Behavior Simplified

Furthermore, the sensible heat of the material was disregarded in the model due to its minimal ability to store and release in comparison to the material's latent heat. For example, the PCM, Suntech's P116 paraffin wax has a solid specific heat of 2.95 $(kJ/kg\,K)$ and a latent heat of fusion of 266(kJ/kg) (Hirman , 2003). The latent heat of fusion is nearly 100 times as large as the materials specific heat.

The PCM is modeled on top of the outer surface of the kang. When it is active, it will absorb energy when the kang's surface temperature is equal to the melting temperature, which is provided as a user input to the model. The default value is 28℃. As long as there is a net input of energy into the PCM, defined as

$$Q_{PCM}^{n} = \left\{h_{Kang\ Surface}\left(T_{Air}^{n} - {T_{Kang}}_{7}^{n}\right) + \frac{k_{Kang}}{\Delta x}\left({T_{Kang}}_{6}^{n} - {T_{Kang}}_{7}^{n}\right)\right\}\Delta t \qquad 57$$

Equation 58 is the balance of: energy being conducted into and energy being lost through convection from the surface node of the kang. The reason the surface node of the kang is used, is this is where the PCM is contained. If the $Q_{PCM,in}^{n}$ remains positive, then the temperature of the kang's surface, ${T_{Kang}}_{7}^{n}$, is held constant at the melting point of the PCM. Each iteration of the model, the $Q_{PCM}^{n}$is cumulated and the total stored energy within the PCM tallied.

$$E_{PCM}^{n+1} = E_{PCM}^{n} + Q_{PCM}^{n} \quad 58$$

The E_{PCM} is limited by the amount of energy the PCM can physically absorb. This is defined by

$$E_{PCM\ Max} = m_{PCM}L_{PCM} \qquad 59$$

where L_{PCM} is the latent heat of fusion of the PCM. If the input of energy into the PCM is positive and the E_{PCM} is less than $E_{PCM\ Max}$ the PCM will continue to absorb energy. However, if E_{PCM} exceeds $E_{PCM\ Max}$ then the PCM is considered thermally saturated and no more energy will be stored. The temperature of the kang's surface is no longer held at the melting temperature of the PCM and is again calculated using equation 20.

If at some point the Q_{PCM}^{n} becomes negative, that is more energy is lost through convection than energy that is conducted into the surface node, the PCM begins to release energy. As long as theQ_{PCM}^{n} is negative and total stored energy, E_{PCM}, is greater than zero, energy will continue to be released and the surface temperature of the kang is held constant at the melting point of the PCM. Once there is no more stored energy in the PCM, the kang's surface temperature is calculated using equation 20.

3.2 Program Inputs & Running the Program

Program Input

The model was designed and written in Microsoft Excel and Visual Basic for Applications (VBA). The use of Excel as a front end for the model ensures a wide range of users will be able to access and use the program.

The model is initiated by the user calling the program by pressing a button titled *Run Program.* The button is contained within the sole worksheet titled *Output Data*. When the program is launched a user form is displayed, permitting the user to input simulation data. The input form is divided into seven sections, each contained within a separate tab on the user form. See Appendix C for figures of the program input tabs.

The first tab is the *Room Data* tab. It contains user input boxes regarding the initial room temperature conditions, inputs and options pertaining to the BLC and specifics regarding the physical properties of the building and room air.

The second tab contains user input boxes regarding the fuel. There are only two user inputs on the *Fuel Data* tab*, encapsulated energy* and the *rate of fuel combustion*. The encapsulated energy has a default value of 15,910 (kJ/kg).

The third tab is the *Stove Data* tab. This is where the user enters information regarding firing times and durations, smoke properties and stove data such as the initial temperature of the stove and the stove efficiency.

Next is the *Kang Data* tab, containing user input fields for the variables pertaining to the kang. The user can enter the dimensions of the kang and the heat transfer coefficients of the kang chamber and surface. The efficiency of the kang and the chimney can be entered and are used to calculate the energy output of the chimney to the room. Finally the material properties of the kang can be filled out by the user.

The fifth tab contains data regarding system improvements. The user can enter data for the water storage tank and water properties. Additionally, the user can select which improvements will be active in the model. The stove heat exchanger can be set to on or off. If it is off, the properties of the heat exchanger are grayed out and ignored by the model. If the stove heat exchanger is active the user can select the location of the radiator, either in the room or as radiant piping within the kang's surface slab, along with other radiator properties. The PCM and Solar Hot Water also have drop down boxes that allow the user to turn them on or off. If they are off the related input boxes are grayed out. Finally bathing data can be entered.

The *Climate Data* tab is the sixth tab. Here, the user can enter hourly data regarding the outdoor temperature, the direct normal radiation and the set point of the thermostat. Depending on the location selected for the radiation on the improvement tab, either the room or the kang, the respective thermostat set point input will be enabled. For instance, if the radiator's location is selected as the room, the *Room Thermostat Set point* boxes will be enabled while the *Kang Thermostat Set point* boxes will be grayed out and ignored by the program. If no radiator is present, both the room and kang set point boxes will be grayed out.

The final tab contains variables regarding the simulation. However, only one input box is modifiable, the number of days to run the simulation. The default value is three but can range anywhere from 1 to 4. If the user enters a value greater than four, the simulation will run for only four days. An error message alerts the user to this limitation. The time step of the model is displayed but is not alterable. As discussed in the section regarding transient heat transfer, changing the time step of the model can lead to unstable results. The time the simulation begins, 12:00 AM, is also shown but cannot be changed by the user.

Model Output

Once the user has entered all their data, the *run program button* is pressed and the code is executed. A progress bar is displayed while the program runs, showing the user the percent of the simulation that has been completed.

When the program has finished running, three graphs are produced. The first displays the temperature of the room air and surface of the kang over time. If the stove heat exchanger and radiator are active the thermostat set point will be charted as well. The model output, created using default values and no improvements activated, over the time period of one day is shown in Figure 43.

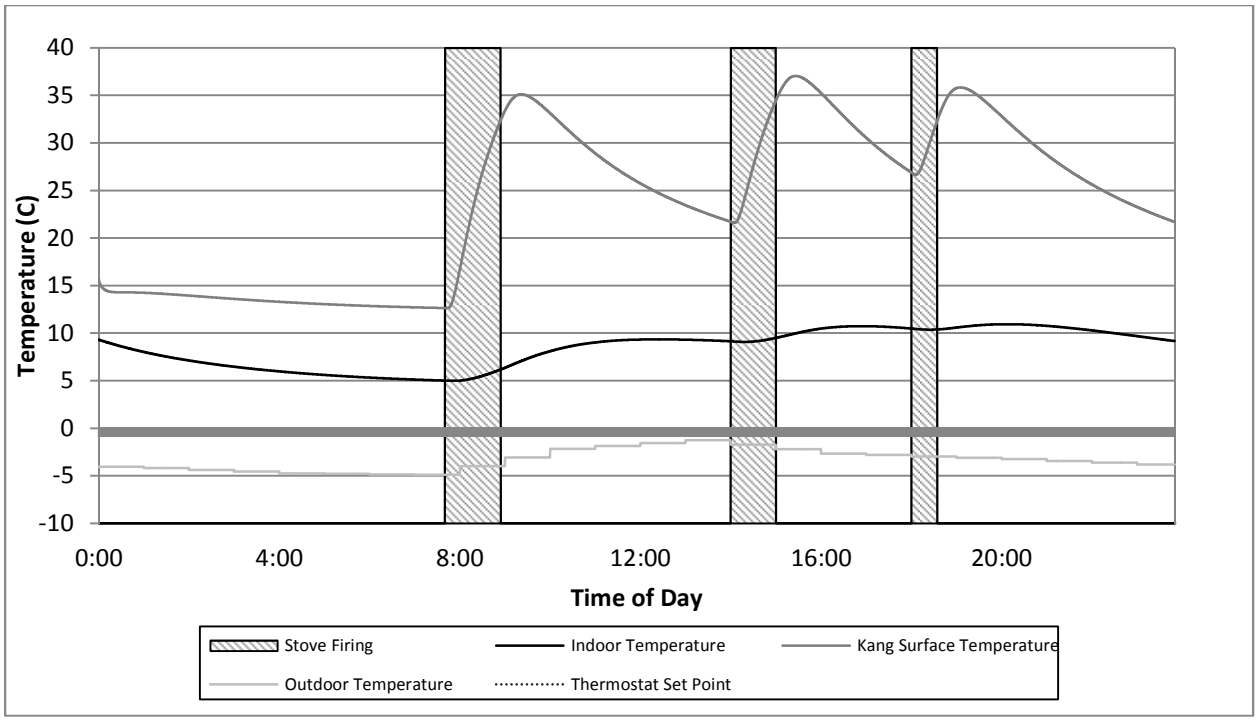

Figure 43 - Model Output - Component Temperature Profile (Base Case)

The temperatures of the kang and room air begin at their respective initial temperatures and slowly cool during the night, from the period of 0:00 until the first firing, shortly before 08:00. During the firing period, the temperature of the kang and room air increases. The sunrise occurs around the same time and the outdoor temperature begins to rise. After the firing, heat from the kang enters the room air for several hours. Around 13:00, heat is lost to the outdoor environment at a faster rate than what is supplied to the room, leading to the temperature declining until the second firing period. This process repeats during the period between the second and third firing and the third firing and the end of the simulation at 24:00. The temperatures of the kang and room air are greater at the end of the simulated day than they were at the beginning. Because of this the model should be run for as many days are required until the temperatures of the kang and room air are equal at the beginning and end of a simulated day. This ensures the elements of the model reach a point of dynamic equilibrium and the results from further simulated days will not vary from those of the day when dynamic equilibrium is

achieved. Figure 44 shows the output of the model using the same initial conditions as were used for the output charted in Figure 43. However, the simulation time was increased from one day to three.

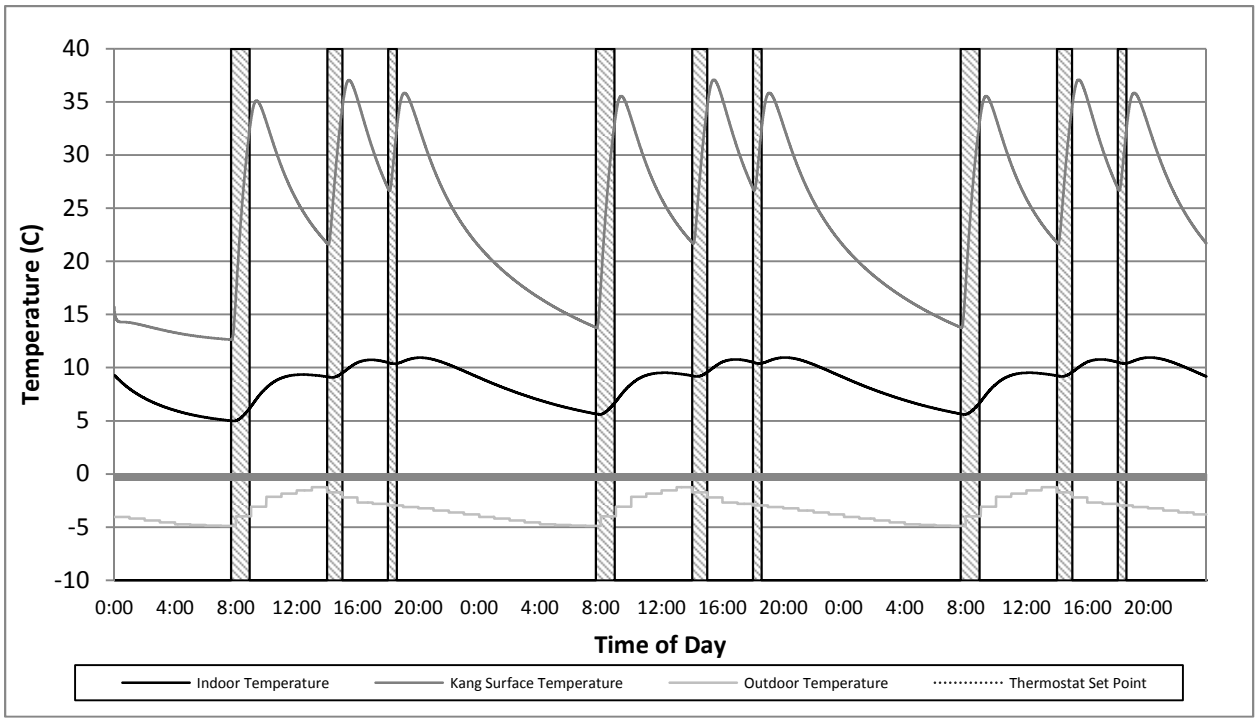

Figure 44 - Model Output - Component Temperature Profile (Base Case) 72 hrs

Equilibrium is nearly achieved on the second day but there is still a small difference between the component temperatures at the beginning of the second day and the beginning of the third day. Dynamic equilibrium is achieved on the third day. The room air and kang temperature for the beginning of each day are shown in Table 10.

Table 10 - Days to Reach Dynamic Equilibrium

Time into Simulation (hh:mm)	Kang Temperature (C)	Room Air Temperature (C)
00:00	15.7	9.3
24:00	21.399	9.0614
48:00	21.402	9.0655
72:00	21.402	9.0655

There is no change in either the kang or room air temperature between the beginning of the third and fourth day. Therefore results from the model must be analyzed through the third day. The amount of days required to reach dynamic equilibrium will vary based on the initial conditions and active improvements selected by the user.

The second chart produced displays the temperature of the smoke and kang chamber along with the temperature of the inlet and outlet temperature of the water flow in the heat exchanger. An output of the modeled components is shown in Figure 45. The same conditions were used to produce Figure 45 as those used for Figure 44.

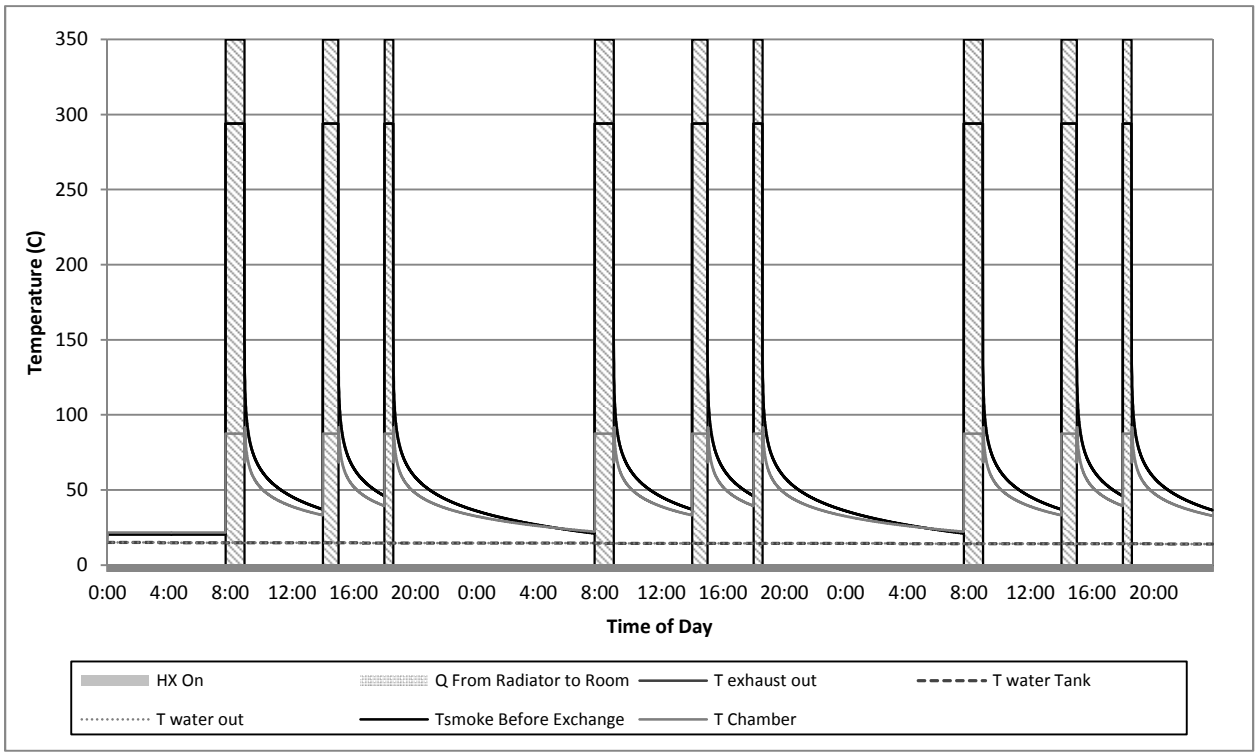

Figure 45 - Variable Temperature Profile

The third and final chart shows the amount of energy produced by each component, shown in Figure 46.

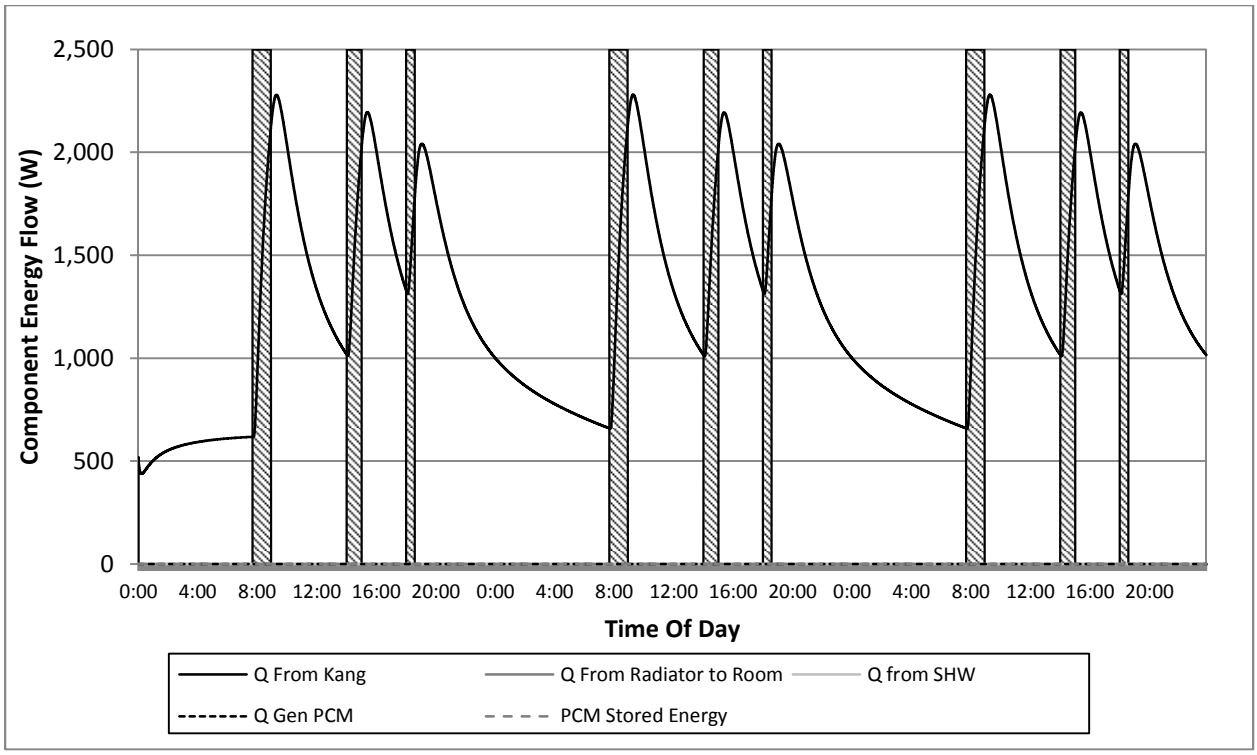

Figure 46 - Heat Flow Profile

In the base case only the kang transfers energy to the air. The amount of power generated by the kang ranges from 500 to 2,200 Watts. This is in the same range as the simulated kang study conducted by Zhuang Z. (Zhuang, Thermal and energy analysis of a Chinese kang, 2010)

Chapter IV: Model Results

4.1 Analysis of Improvements

To analyze the effectiveness of a possible improvement a standard metric must be used for comparison. The primary goal of the model optimization is to increase the comfort of the inhabitants inside their domicile. This can be achieved by increasing the air temperature which would make the indoor space warmer. However, during the night the occupants lie on top of the kang and find comfort sleeping on the warm surface. The model has not been developed to split heating methods between the kang and the room. Therefore it is important to assess the change in temperature of both the indoor air and surface of the kang. Using the model output that is created with the default values as a base case scenario, the percentage change in air temperature and kang temperature can be used to evaluate the effectiveness of each improvement. Only the third day is compared as prior to this period the model has not achieved dynamic equilibrium.

The first scenario tested is to use the heat exchanger in conjunction with the room radiator. The radiator set point is set to a constant value of 16°C and is not varied throughout the simulation period. The

results of this scenario are shown in Figure 47

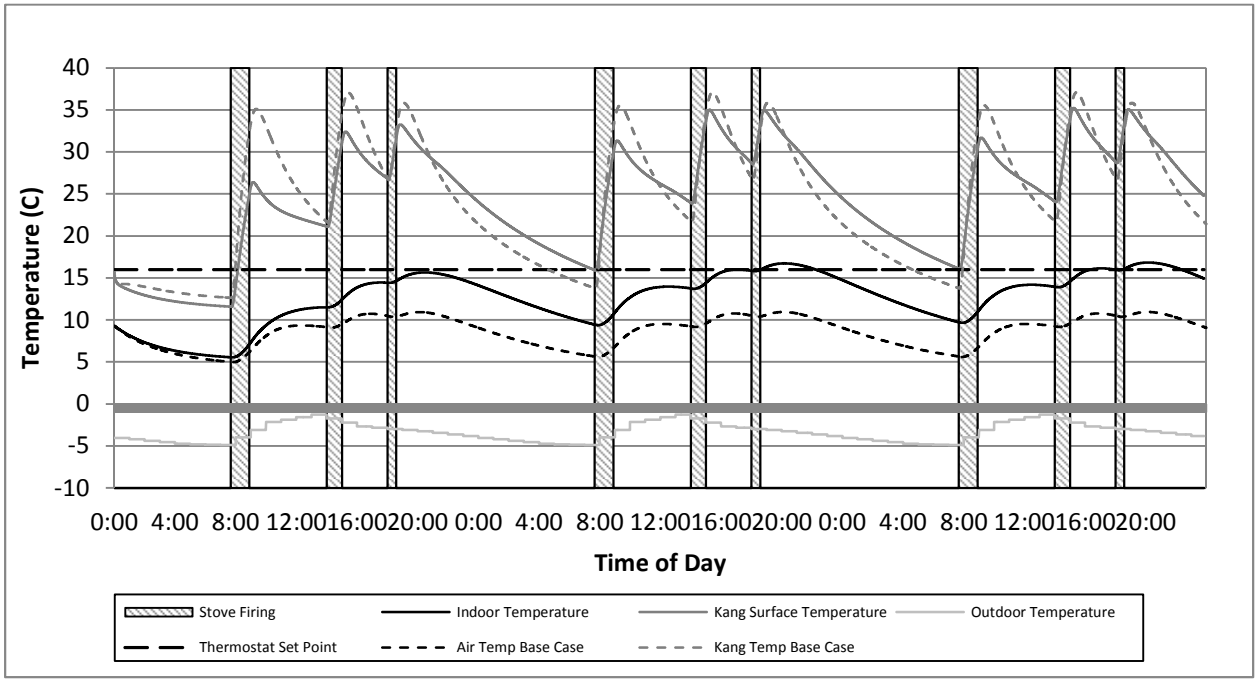

Figure 47 - Heat Exchanger – Room Radiator - Constant Set Point

The room air and kang temperatures are plotted next to their respective series from the base case scenario. The radiator temperature set point is also shown on the chart and is a horizontal line at 16℃. It is clear that the air temperature is significantly higher in this scenario than that of the base case. The kang temperature is sometimes greater but sometimes less than the kang temperature of the base case. For instance, the kang temperature is significantly less during the first firing of the third day than that of the base case. This is due to energy being stored in the water tank that would otherwise enter the kang chamber and raise the temperature of the kang. During decay periods the model shows the kang temperature not dropping as much as that of the base case. This is caused by the room air temperature being warmer and therefore less energy being transferred from the kang to the air. The percent change in the room air and kang temperatures are plotted in Figure 48.

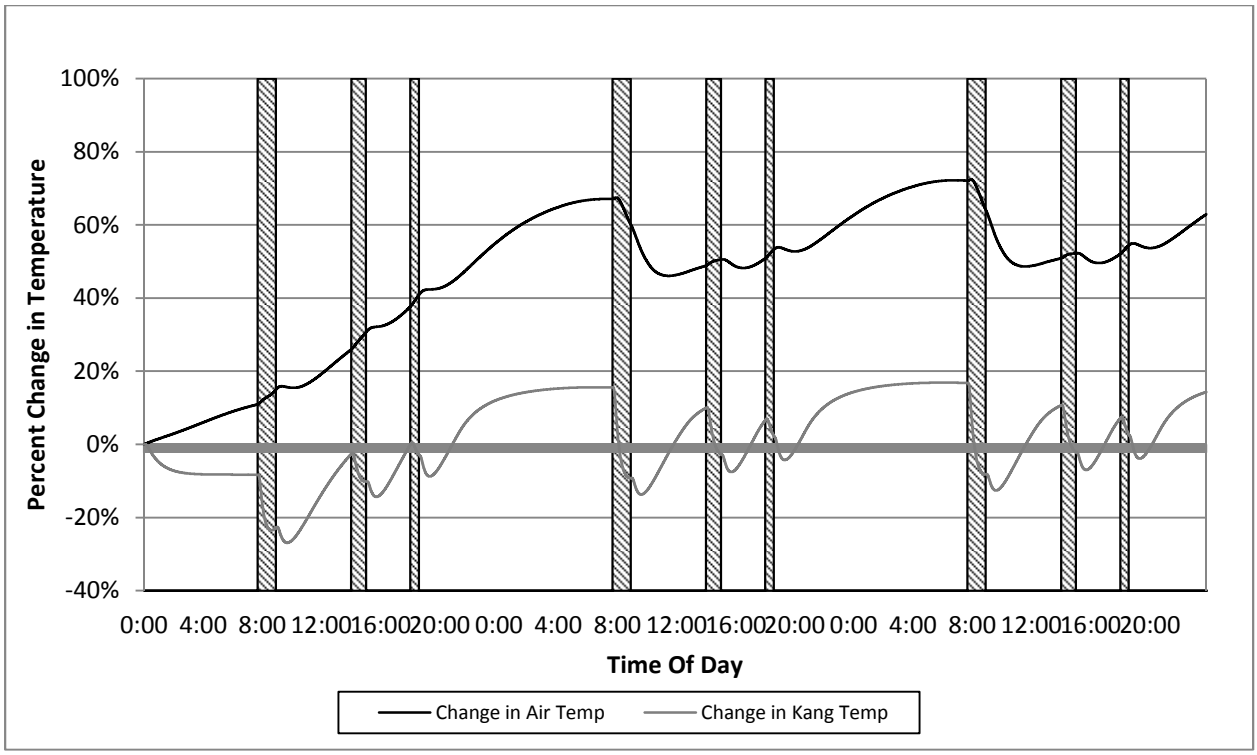

Figure 48 - Improvement Effectiveness - Heat Exchanger – Room Radiator - Constant Set Point

Clearly the air temperature is significantly greater, sometimes 70% more than that of the base case. The kang temperature shows slight improvement, primarily after the evening firing. The percent change in temperatures of the air and kang is displayed in Table 11

Table 11 – Scenario 1 Results

Scenario 1	Air	Kang
Average	58.74%	6.69%

On average the air temperature increased 60% while the kang temperature remained relatively unchanged. However, it is important to note the kang is warmer during the sleeping period.

The next scenario keeps the variables of the first scenario the same with one exception: the thermostat set point is altered throughout the day to better reflect the heating needs of the home's occupants. Cao, G. studied occupant behavior and determined when the bedroom is occupied by the building's

residents. The study room, referred to here as the bedroom is occupied from 0:00– 7:00, briefly from 12:00–13:00 and then from 17:00-24:00. A value of one means the room is fully occupied, a value of half implies the residents partially occupy that room and a value of zero means the room is unoccupied.

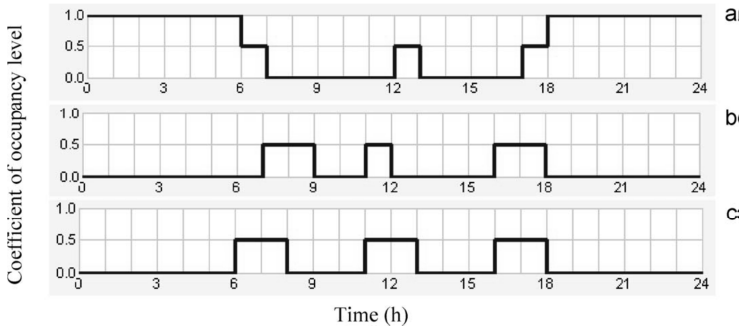

Figure 49- Profiles for the presence of the occupants in the simulation: (a) bedroom; (b) living room; and (c) kitchen[1].

From the hours of 0:00 to 6:00 the thermostat is set at 14℃, from 6:00 to 8:00, the time the occupants get up and occupy the home, the set point it increased to 16℃. From 8:00 to 12:00 the thermostat is set to 0℃ or off. From 12:00 to 13:00 the set point is increased to 16℃ and then turned off from 13:00 to 16:00. The set point is raised to 18℃ during the period from 16:00 to 22:00. The thermostat is set to 14℃ from 22:00 to 24:00 and the daily cycle begins again. Operating the thermostat in this manner keeps the home at its warmest when the occupants are most likely to be home and doesn't waste energy heating the home during hours when the occupants are outside working. A plot of the thermostat and the corresponding temperature series for this scenario are shown in Figure 50 below.

[1] (Cao, 2011)

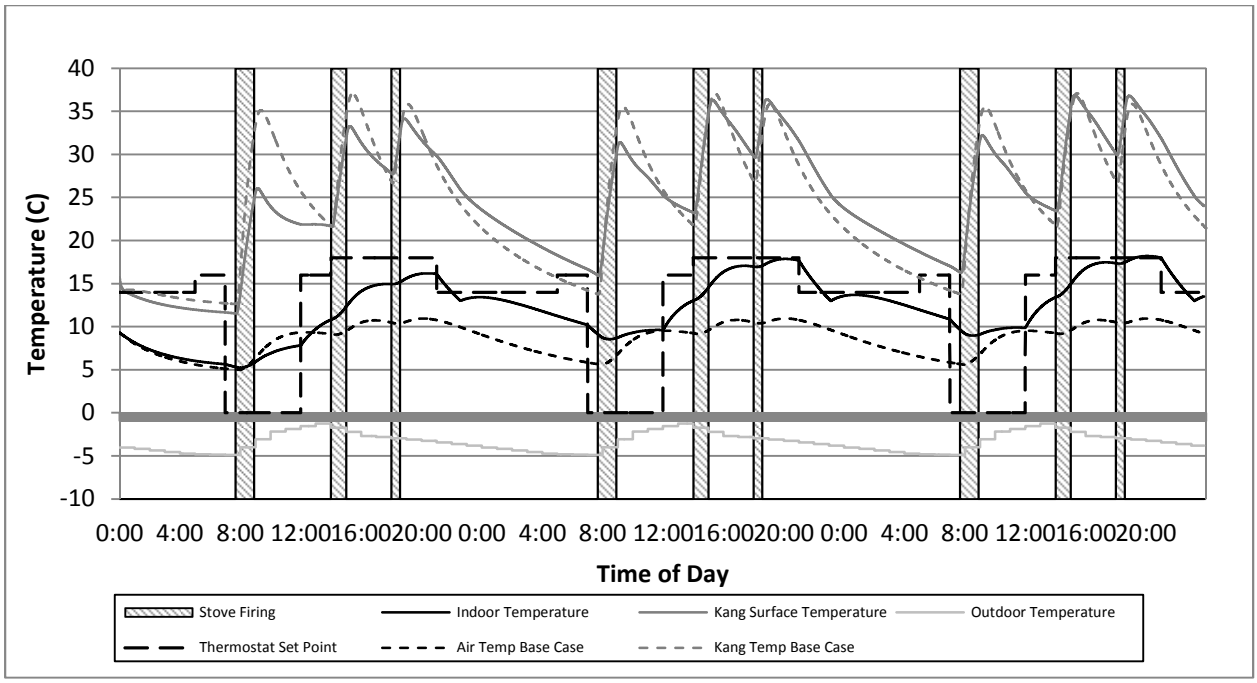

Figure 50 - Heat Exchanger – Room Radiator – Living Set Point

A chart showing the percent increase in room air and kang temperatures is shown in Figure 51

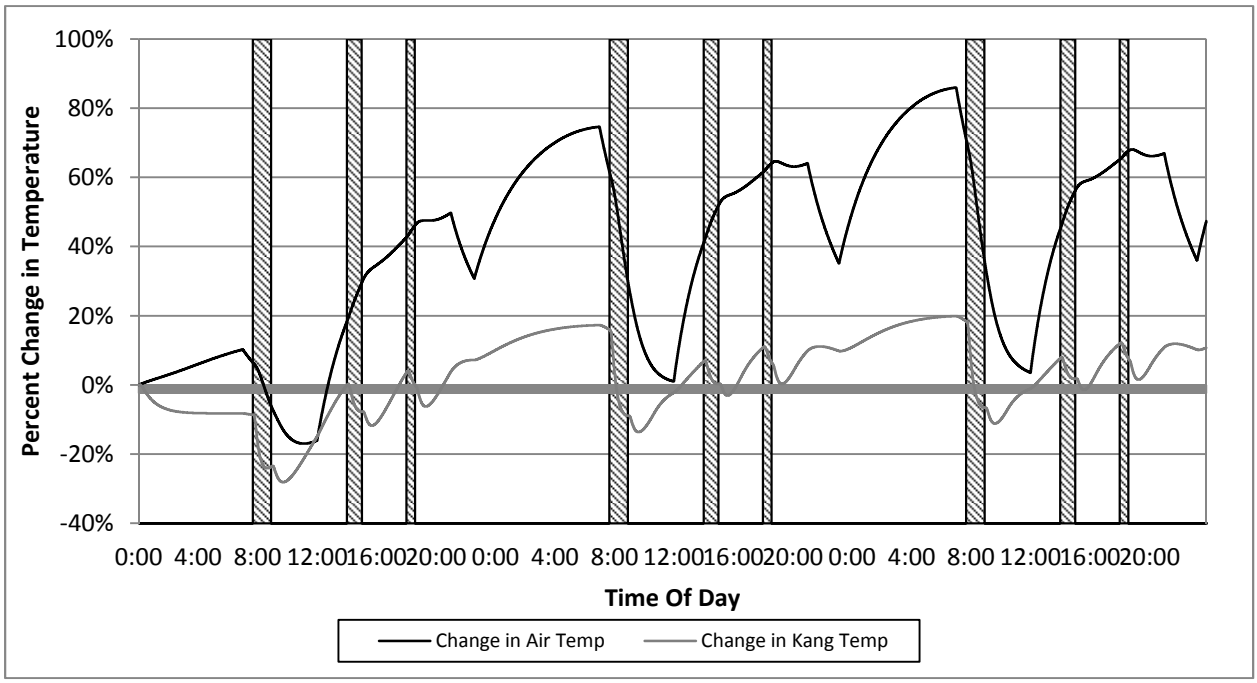

Figure 51 - Improvement Effectiveness -Heat Exchanger – Room Radiator – Living Set Point

The air temperature, at some points during the simulation, rises more than that of scenario one, where the thermostat is kept constant. Table 12 shows the percent change and standard deviation of both the room air and kang temperatures for this scenario compared to the base case.

Table 12 - Scenario 2 Results

Scenario 2	**Air**	**Kang**
Average	54.26%	8.05%

The air temperature, on average, doesn't increase more than the first scenario which experienced nearly a 60% increase over the base case. This is caused by the thermostat turning off during the hours of 8:00 to 13:00 and the thermostat being set lower during the sleeping hours. If the occupants are not in the home during this period than the temperature of the home during this time should not be considered when averaging the percent temperature change. Therefore, only the temperature during the hours from 0:00-8:00, 12:-13:00 and 16:00-24:00 is averaged. If this method is considered, the updated value of the average percent change of the room air and kang temperature is

Table 13 - Scenario 2 Results – Occupied Hours

Scenario 2	**Air**	**Kang**
Average	67.67%	13.75%

The percentage increase would be greater if the thermostat was not set lower during the night. However, by varying the thermostat, energy is not used when it is not needed. It should be understood that saving energy by only heating the room to the necessary temperature, even if the percentage increase over the base case is less, is a desirable outcome. Further research is required to determine what temperature during different hours of the day is comfortable for the home's occupants.

Scenario three investigates the effects of radiant heating within the kang's surface slab. The results are displayed in Figure 52. The thermostat set point of the kang is kept at a constant temperature of 28℃. It is assumed that if the surface temperature of the kang is at this temperature the occupants will be comfortable when they are lying on the top. Like the first two scenarios, the time periods between 8:00 and 12:00 and 13:00-16:00 are not considered when assessing the component temperature change.

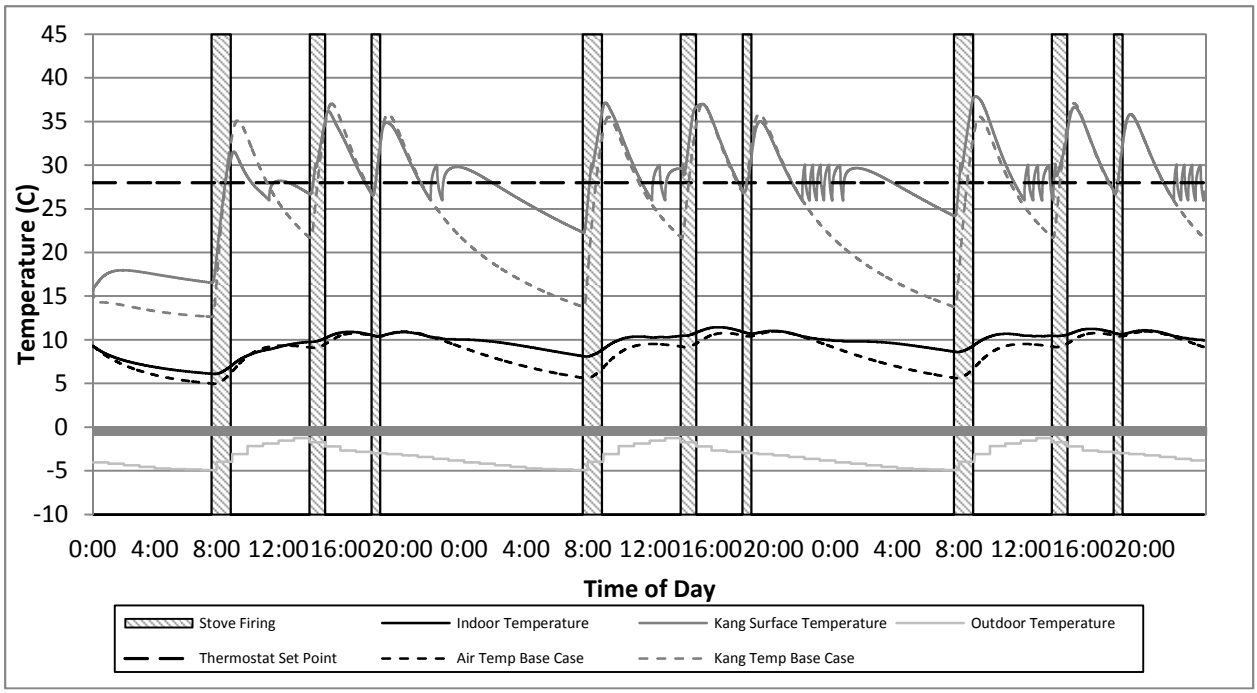

Figure 52 - Heat Exchanger – Kang Radiant – Constant Set Point

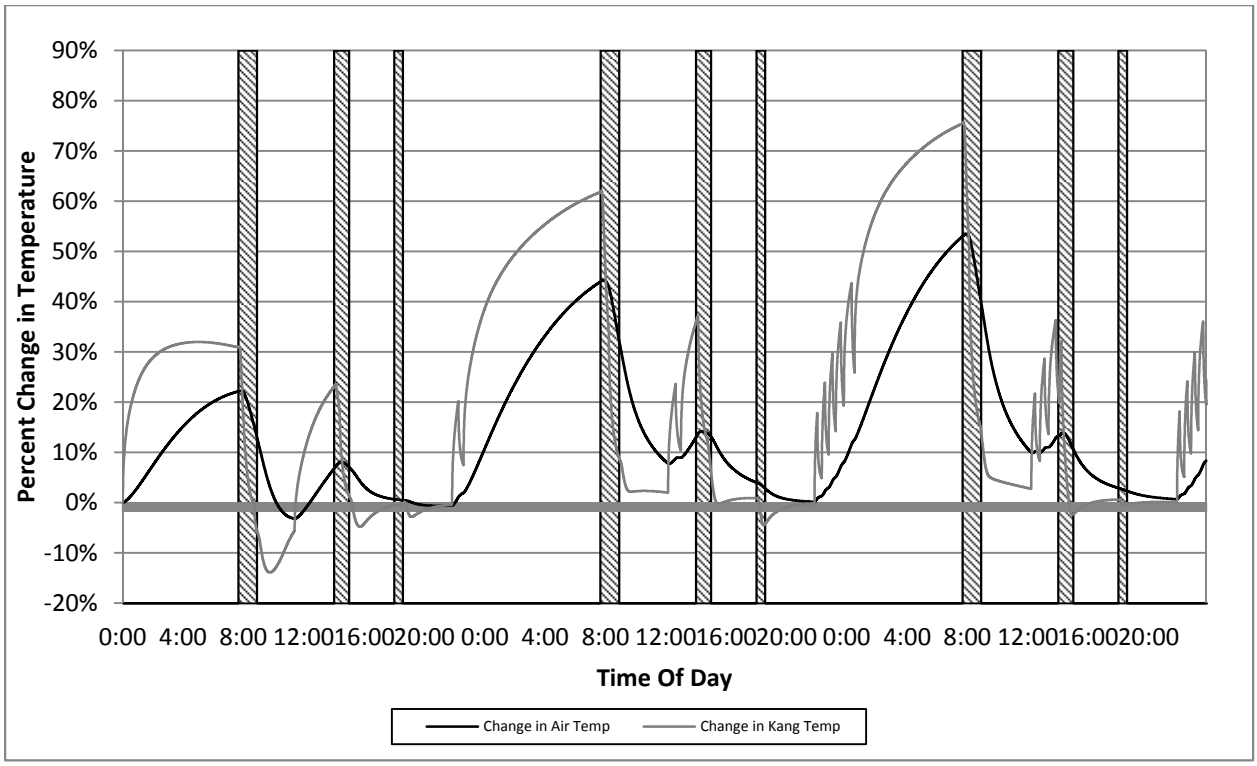

Figure 53 - Improvement Effectiveness - Heat Exchanger – Kang Radiant – Constant Set Point

As can be seen in Figure 53, the kang and air temperatures increase primarily during the sleeping period, from 0:00 to 8:00. However, there is little difference during the later hours of the day. Table 14 displays the average percentage increase of the kang and room air temperatures. The kang surface temperature increases more than it did in the first two scenarios, roughly a 35% increase compared to slightly over 10% in scenario two. The room air temperature changes significantly less, only 19% more than the base case compared to nearly 68% greater than the base case in scenario two. It is clear that the radiator in the room increases the air temperature much more than the radiant heating system in the kang. However, the surface temperature of the kang almost never drops below the set point of 28℃. The occupants might find a warmer kang more comfortable than a room with warmer air, especially while sleeping. Consequently, the kang piping shouldn't be ruled out as a possible technical solution.

Table 14 - Scenario 3 Results

Scenario 3	Air	Kang
Average	19.49%	35.27%

When a variable set point is used, scenario four, shown below in Figure 54and Figure 55, the average percentage change in the kang and room air temperature is actually worse than when a constant set point is used.

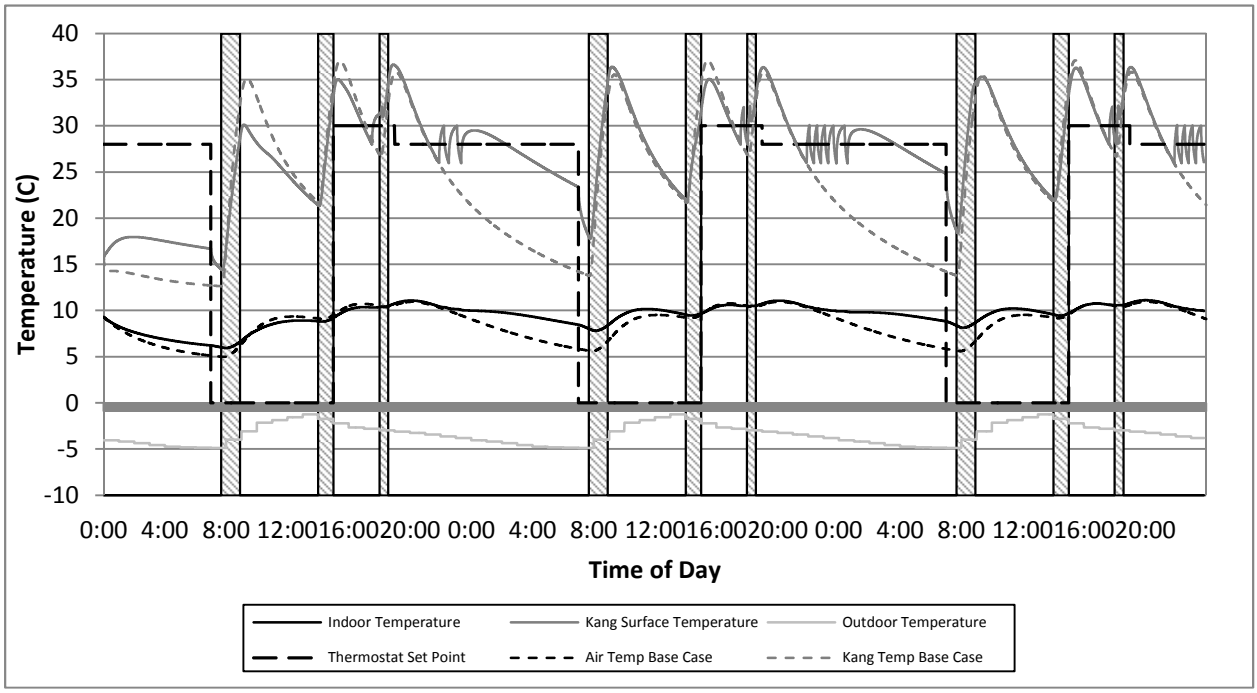

Figure 54 - Heat Exchanger – Kang Radiant – Living Set Point

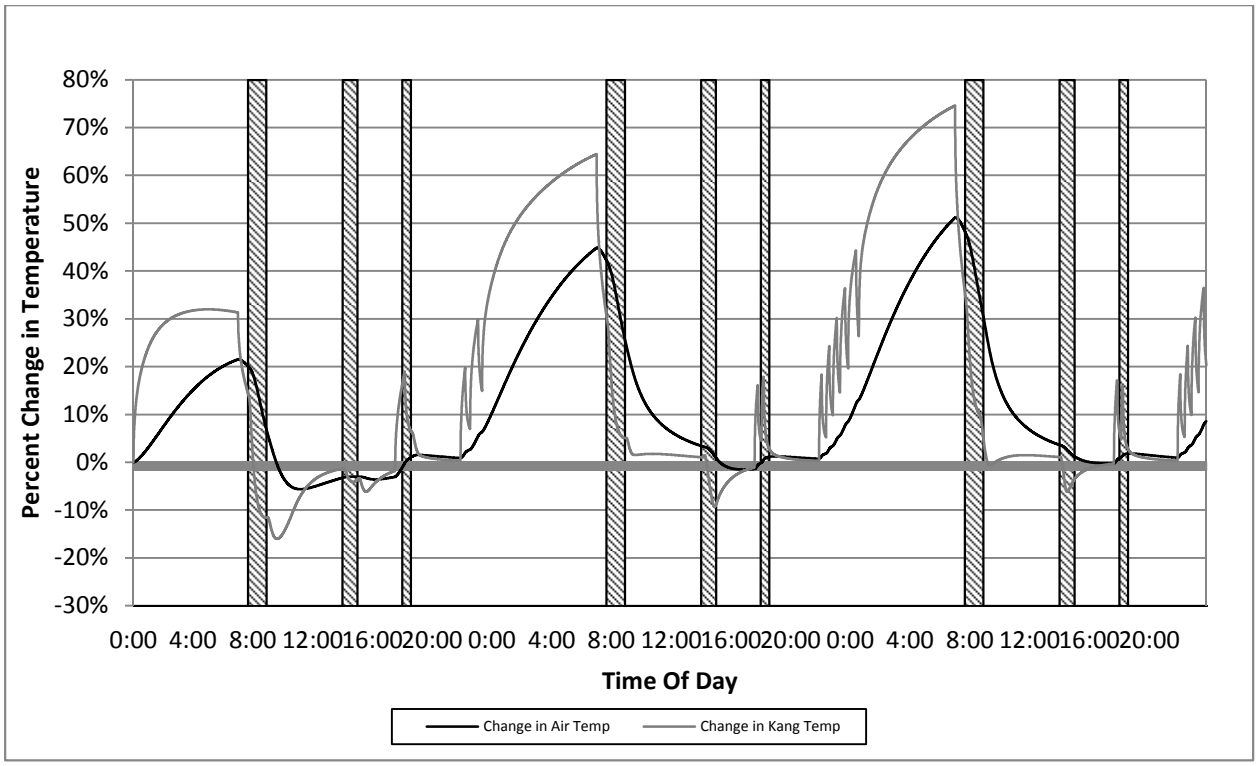

Figure 55 - Improvement Effectiveness - Heat Exchanger – Kang Radiator – Living Set Point

Table 15 - Scenario 4 Results

Scenario 4	Air	Kang
Average	18.82%	33.19%

Some of the ineffectiveness in the radiant heating system inside the kang stems from the fact that the kang's surface temperature exceeds, often by several degrees, the desired set point temperature. For instance, the kang's surface temperature still rises above the set point temperature during firing periods. In fact, the surface temperature only falls below that of the thermostat set point during the sleeping hours, making the period during late night the only possibility for thermal improvement. During the other hours of the day, the model will behave exactly as the base case scenario.

Returning to scenario two, the solar hot water component is turned on and the remaining conditions are kept the same to produce scenario six. The output of the simulation is shown in Figure 56 and Figure 57.

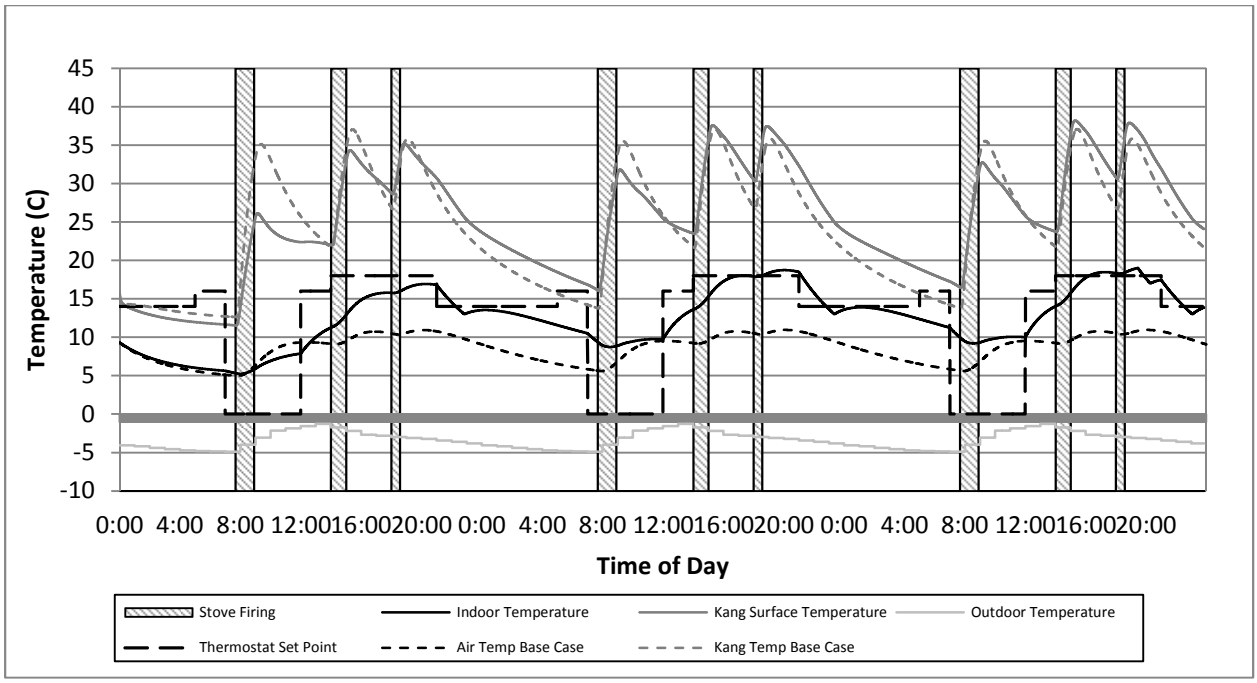

Figure 56 - Heat Exchanger – Room Radiator – Living Set Point - SHW

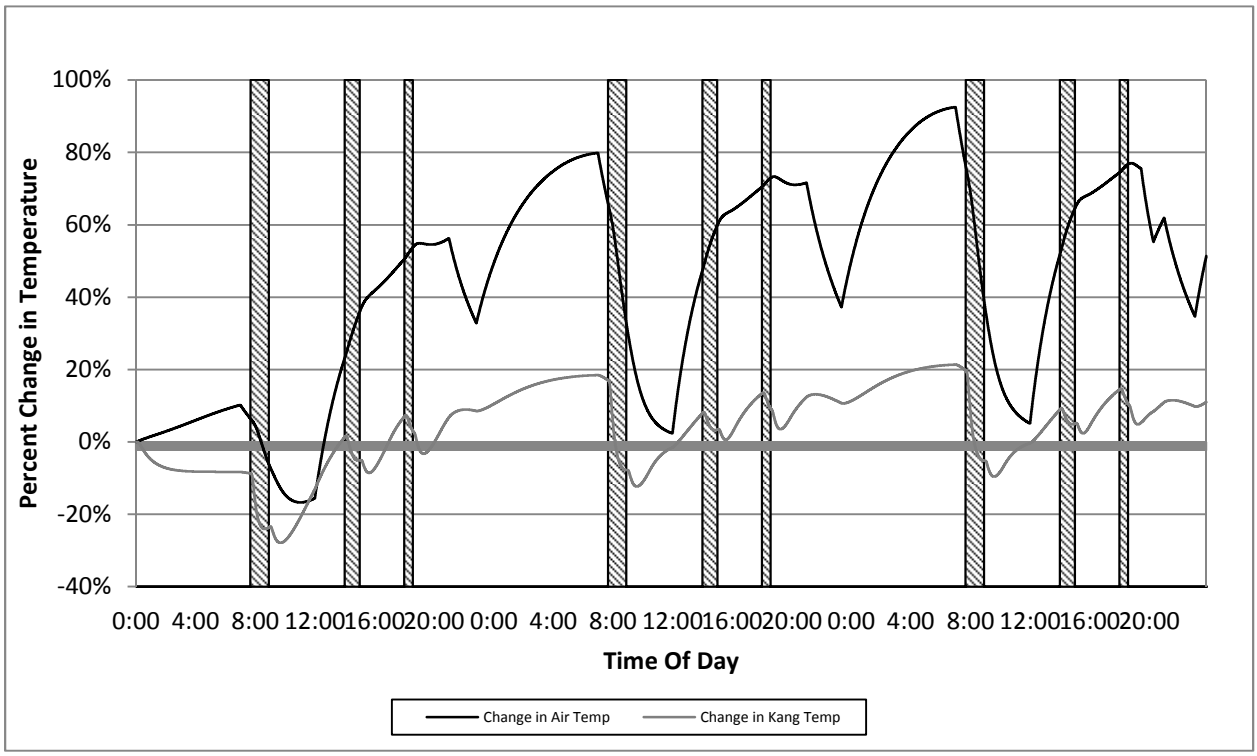

Figure 57 - Improvement Effectiveness - Heat Exchanger – Room Radiator – Living Set Point - SHW

Table 16 displays the percent increase over the base case scenario of scenario 5.

Table 16 - Scenario 5 Results

Scenario 5	Air	Kang
Average	72.83%	15.29%

In the previous scenarios the total energy in the system was constant as the number and length of firings were constant. The solar hot water heater introduces energy into the system. The percent increase in air temperature is over 70% greater than the base case and the kang's temperature increased 15% from the base case. From scenario 2, the solar water heater increased the air temperature an additional 6% and increased the kang temperature an additional 2%. The increase in temperature provided by the solar hot water heater is desirable. An economic analysis will be discussed in a later section to determine if the incremental temperature is worth the added cost of the solar panels.

Scenario six assesses the effects of increasing the building's insulation. The U values for the exterior walls and roof are decreased from 0.417 to 0.2 and from 0.22 to 0.14 W/m^2K respectively. This would be equivalent of adding a layer of rigid foam insular sheathing with a thickness of 75mm and a U value 0.38 W/m^2K to the exterior walls and roof of the home. The new U factors of the exterior walls and roof are calculated using equation 51.

$$U_{Improved} = \frac{1}{\frac{1}{U_{Origianl}} + \frac{1}{U_{Insulation}}} \qquad 60$$

The added insulation will decrease the number of air shifts per hour, which was decreased from 0.9 to 0.25, a value associated with modern construction. No other improvements are active during scenario six. The added insulation significantly reduces the heat loss from the study room resulting in significantly warmer air. Figure 58 and Figure 59 display the temperature profiles for scenario seven.

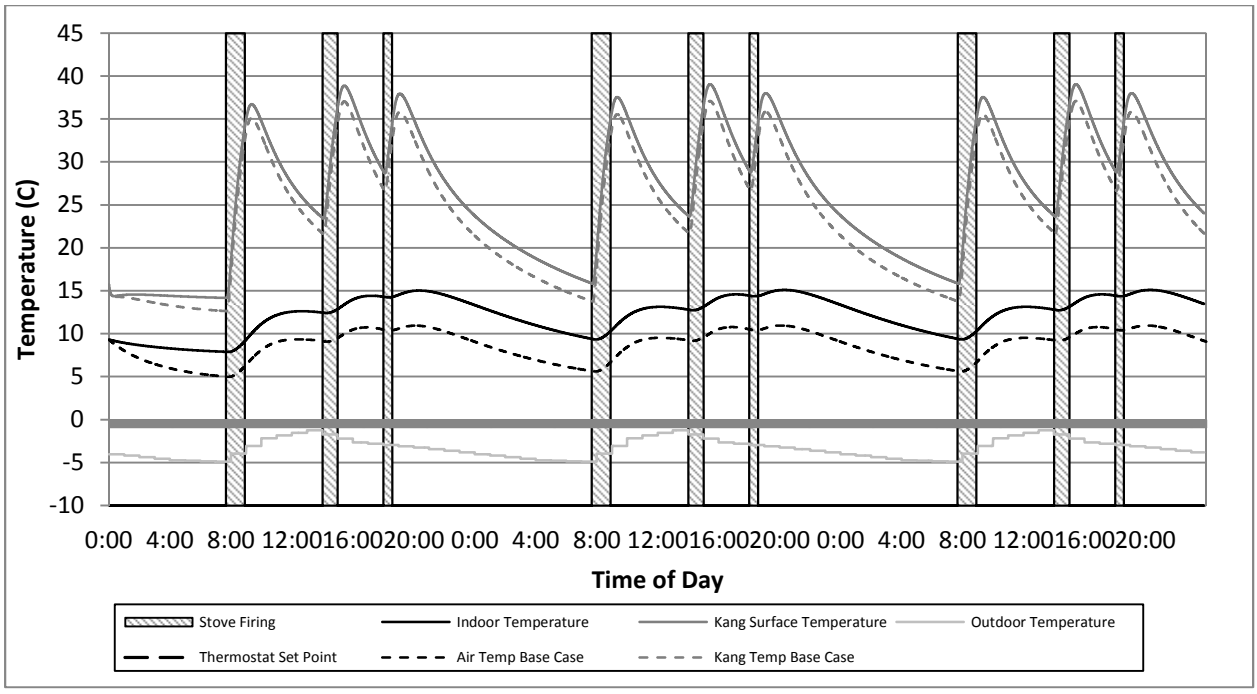

Figure 58 - Improved Building Insulation

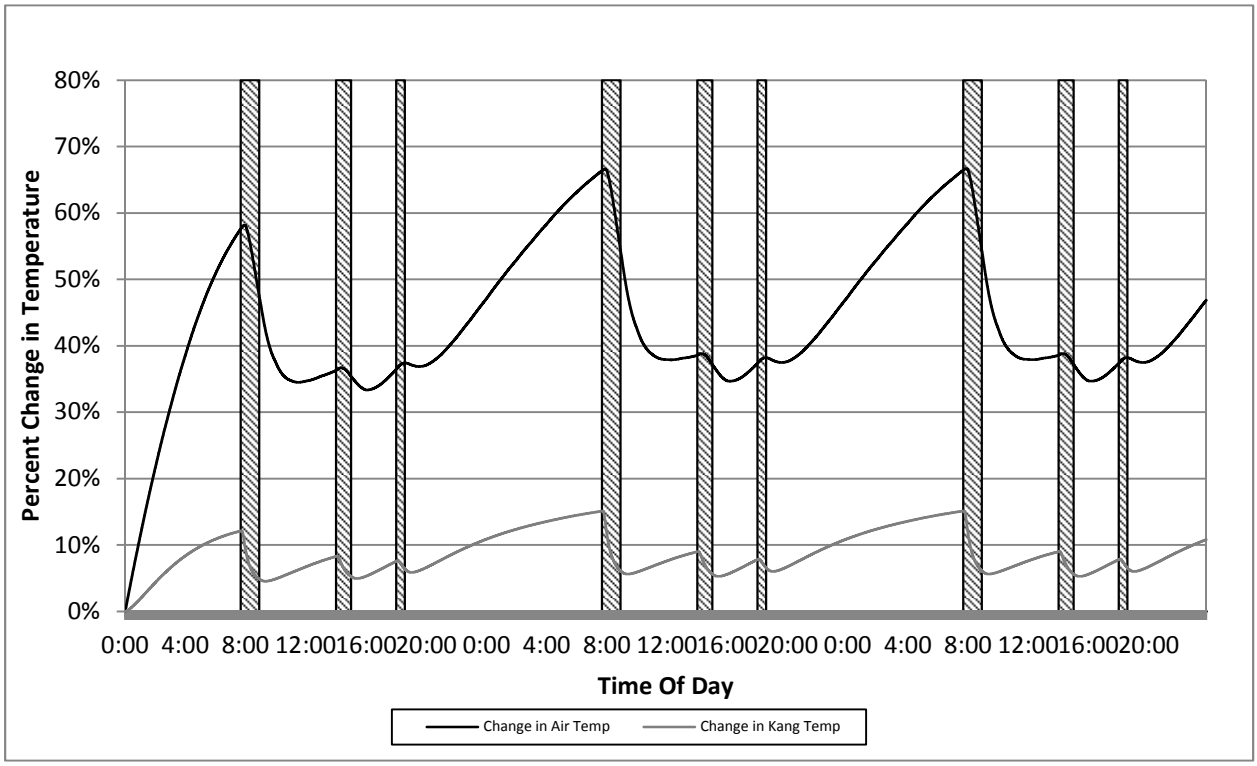

Figure 59 - Improvement Effectiveness - Improved Building Insulation

Table 17 shows the average percentage increase in the room air temperature when insulation is added to the building is over 48%. The average percentage increase of the kang surface temperature over the base case is 10.71%.

Table 17 - Scenario 6 Results

Scenario 6	**Air**	**Kang**
Average	48.87%	10.71%

Adding a room radiator to the kang system has been shown to produce a considerable increase in room temperature. Scenario seven investigates the effects of using a room radiator in conjunction with improved building insulation. Shown in Figure 60, the room air temperature profile is able to follow the thermostat set points. Referring to scenario 2, there is not enough energy in the system for the radiator to raise the room air temperature to the desired set point during the sleeping hours. With added insulation, the radiator can fully meet the temperature set points of the thermostat. The one period this does not occur is before the initial firing when no energy has yet to enter the system.

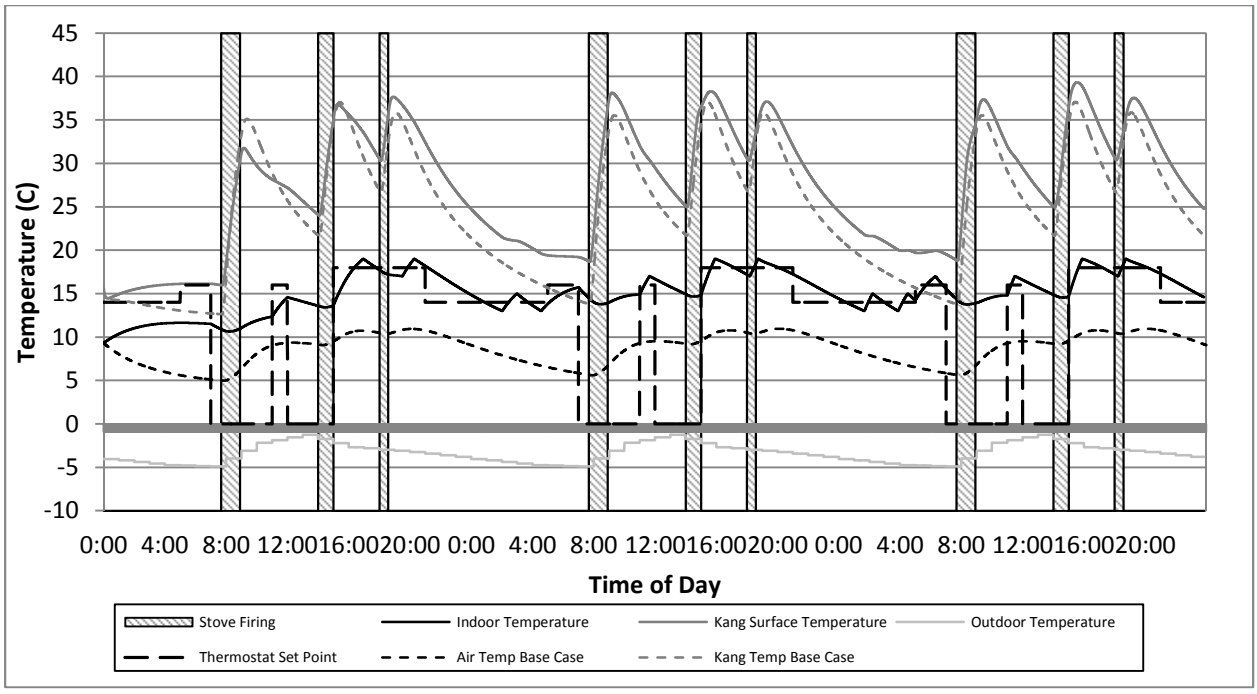

Figure 60 - Heat Exchanger – Room Radiator – Living Set Point- Improved Building Insulation

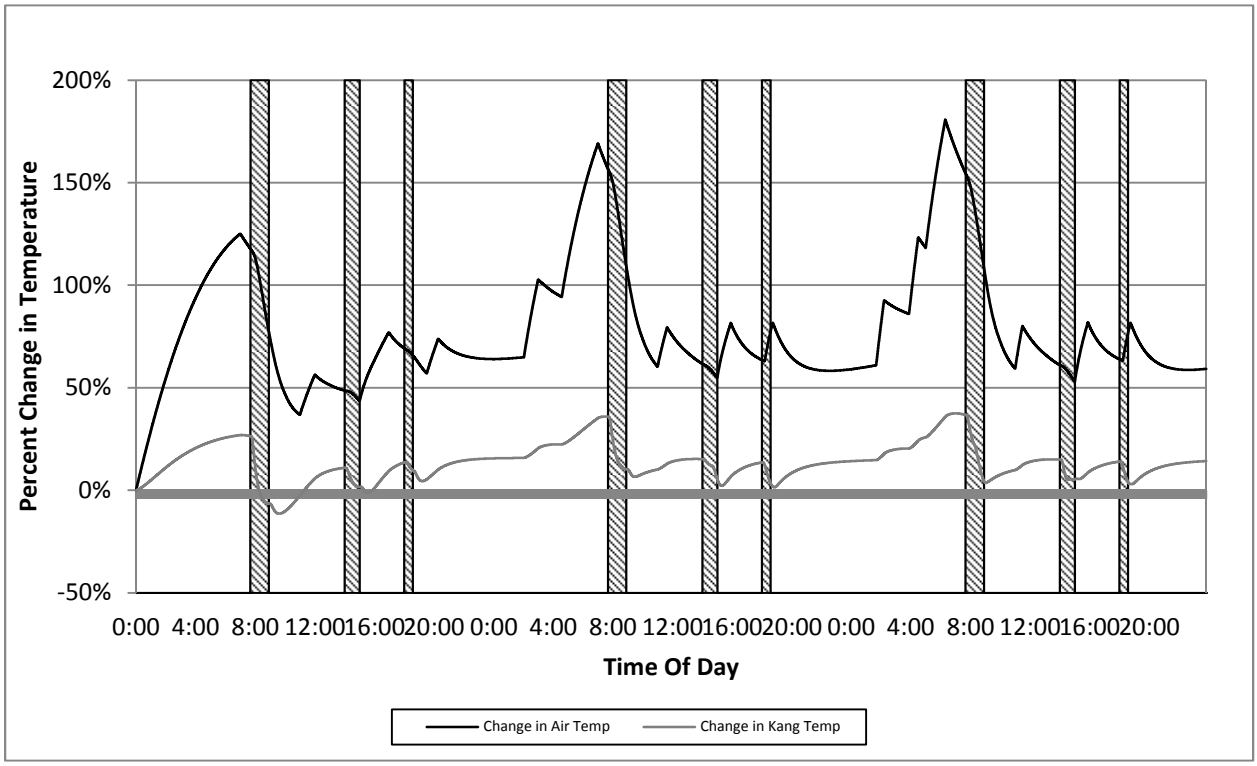

Figure 61 - Improvement Effectiveness - Heat Exchanger – Room Radiator – Living Set Point- Improved Building Insulation

During the early morning period, 4:00 to 7:00, the air temperature is 100 to 200% greater than the base case scenario.

Table 18 - Scenario 7 Results

Scenario 7	Air	Kang
Average	88.15%	17.86%

Table 18 details the percent increase in component temperature over the base case scenario for scenario eight; over 88% for the air and 17.9% for the kang.

Scenario eight looks adding solar heating panels to scenario seven. Little change is produced because the air temperature is able to follow the thermostat program without the panels being present. The added energy is not utilized by the system and either the thermostat set point needs to be raised or less fuel could be used during the firing periods. The solar panels have an average power output of 220 W over 36,000 seconds producing 7,914 kJ/day. The fuel burned has an encapsulated energy amount of 15,910 kJ/kg but only 65% of this energy enters the kang and can be utilized for heating. Only 10,342 kJ of energy is available for heating per kilogram of burned fuel. Therefore, the solar panels would save 0.77 kg of fuel per day. The simulation shows it is possible to fully heat the home without the use of solar hot water panels. Alternatively, a solar heating system could be used to heat water for domestic use. Table 19 shows the average percent increase in component temperature for scenario eight.

Table 19 - Scenario 8 Results

Scenario 8	Air	Kang
Average	88.14%	17.97%

In scenario nine, the thermostat set point is increased to a constant 20℃ during the hours of 0:00-8:00 , 12:00-13:00 and 16:00-24:00. Otherwise the thermostat is turned off. The water tank size is increased to

1 m^3 so the heat exchanger is not shut off due to the water reaching 90℃. This alleviates the constraint of thermostat. Figure 63 and Figure 64 display the results. It is clear that there is not enough energy in the system to meet the thermostat requirement of 20℃, primarily during the sleeping hours. However the air and kang temperatures are significantly elevated above their respective temperatures in the base case scenario.

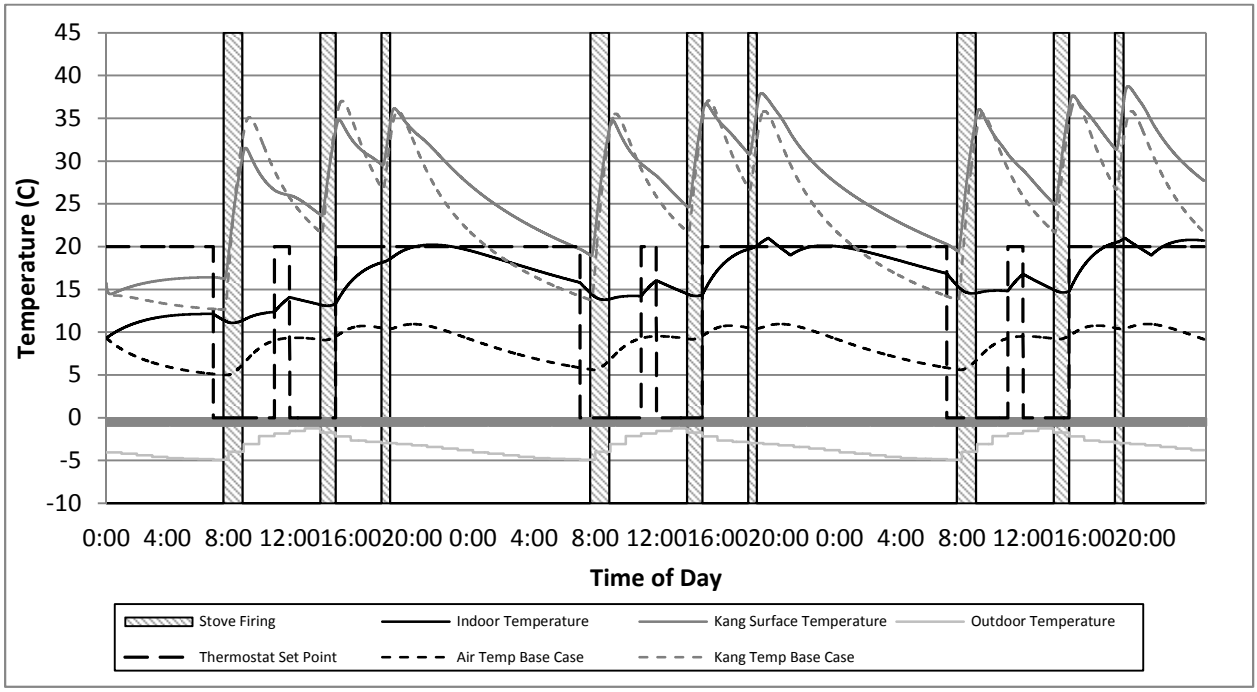

Figure 62 - Heat Exchanger – Room Radiator – Elevated Living Set Point – SHW - Increased Tank Size - Improved Building Insulation

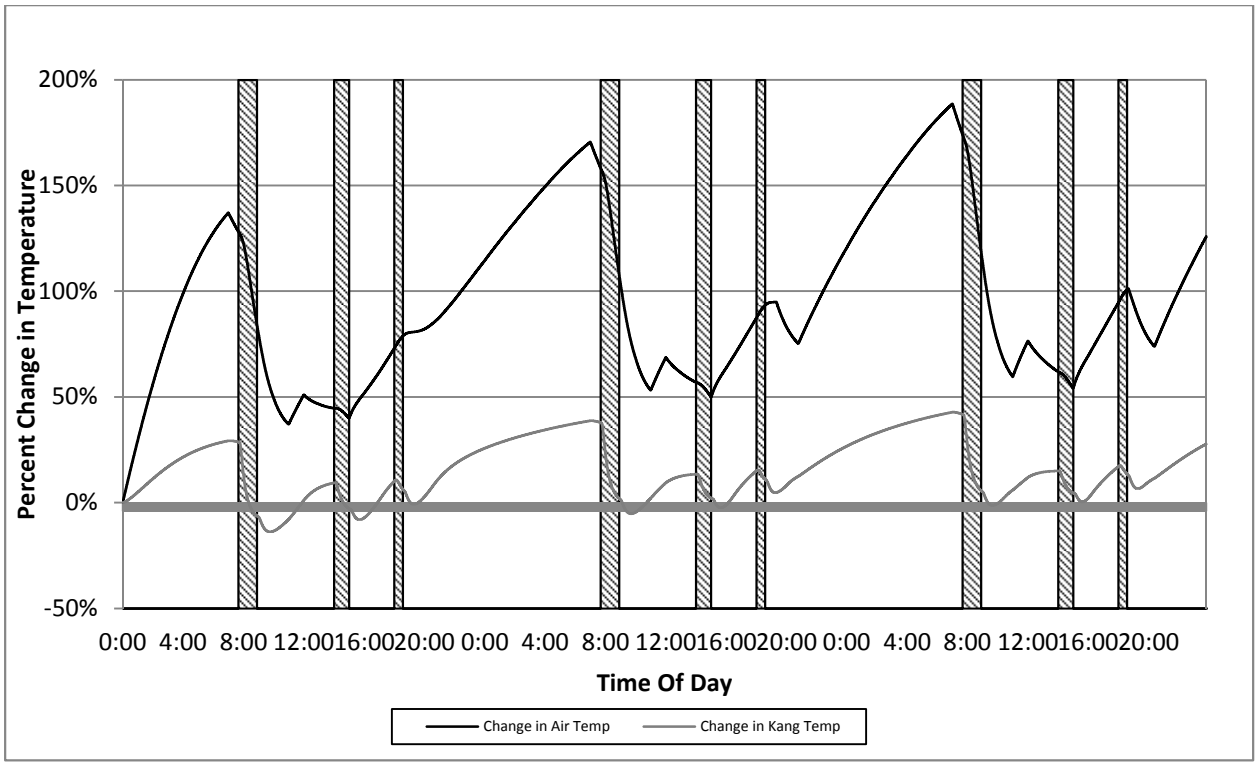

Figure 63 - Improvement Effectiveness - Heat Exchanger – Room Radiator – Elevated Living Set Point – SHW - Increased Tank Size - Improved Building Insulation

Table 20 - Scenario 9 Results

Scenario 9	Air	Kang
Average	126.58%	26.20%

Table 20 shows the air temperature increased 126% over that of the base case and the kang's temperature rose 26%. These results are markedly improved over other scenarios.

Scenario ten investigates the effect of using the radiant heat system in the kang and adding improved insulation to the building. The results are shown in Figure 64 and Figure 65.

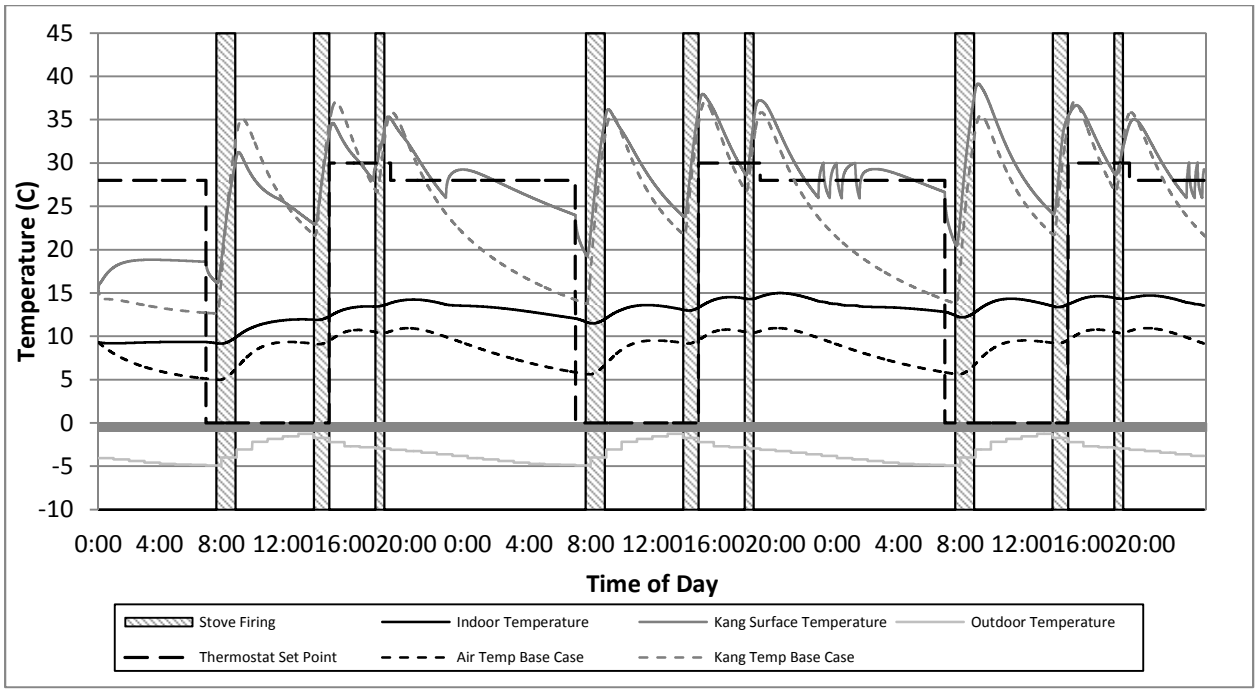

Figure 64 - Heat Exchanger – Kang Radiator – Constant Set Point- - Improved Building Insulation

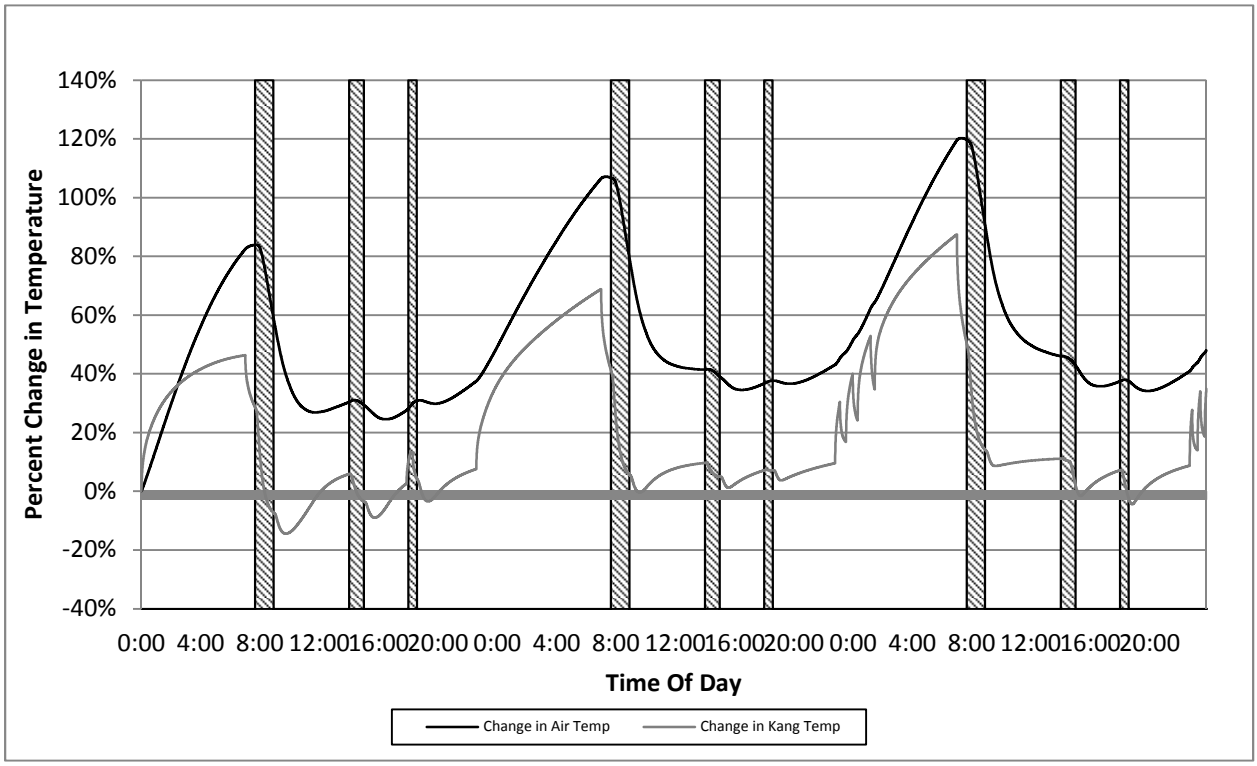

Figure 65 - Improved Effectiveness - Heat Exchanger – Kang Radiator – Constant Set Point- - Improved Building Insulation

The temperature of the kang increases under scenario ten more than it did under any pervious scenario, an average 36% increase. The air temperature increased significantly over the base case scenario but not much over scenario six where only improved insulation was tested on its own. Scenario ten produces satisfactory results as the kang's surface temperature is the warmest of any scenario tested. Table 21 shows the component percent increase in temperature.

Table 21 - Scenario 10 Results

Scenario 10	**Air**	**Kang**
Average	64.70%	36.36%

Scenario eleven investigates the effects of adding a phase change material to the surface of the kang. The PCM does not add any energy to the system, functioning only as a thermal battery that can store heat that can be released at a later time. Figure 66 and Figure 67 show the effects of adding 70 kilograms of PCM to the surface of the kang. The melting point of the PCM is set at 28℃ and is not exceeded during the simulation. 70 kilograms of PCM are required to achieve thermal saturation. Less than 70 kilograms results in the PCM's temperature increase above 28℃.

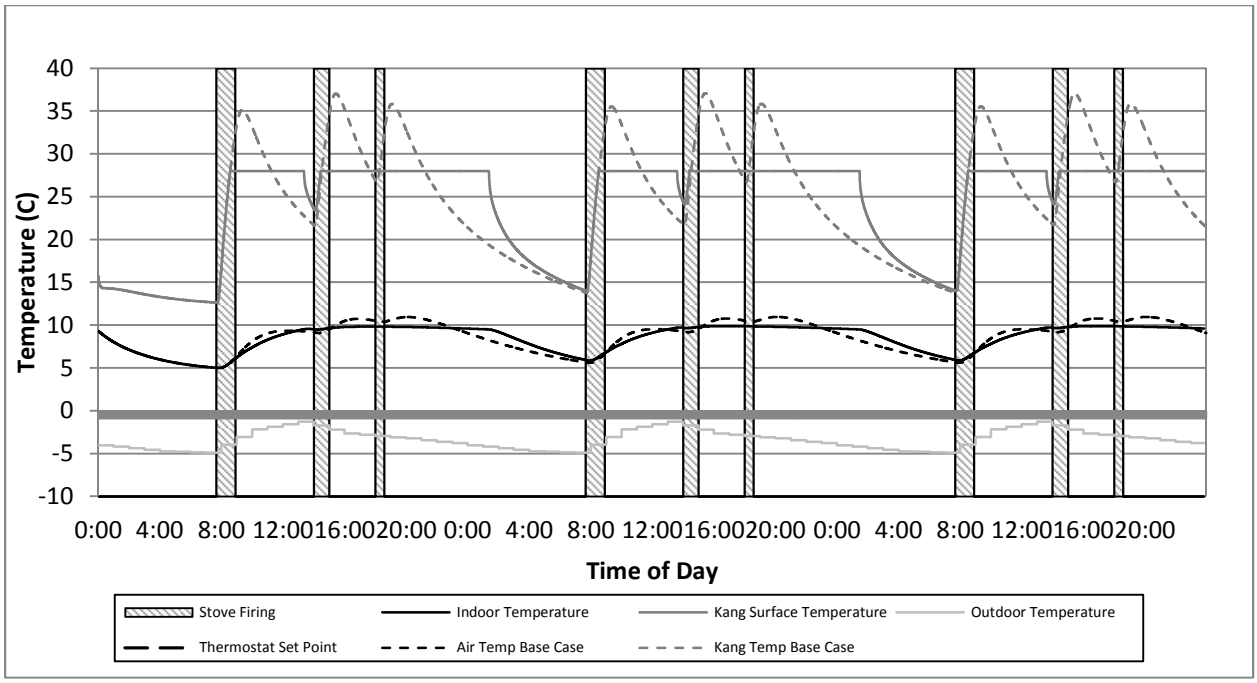

Figure 66 - PCM

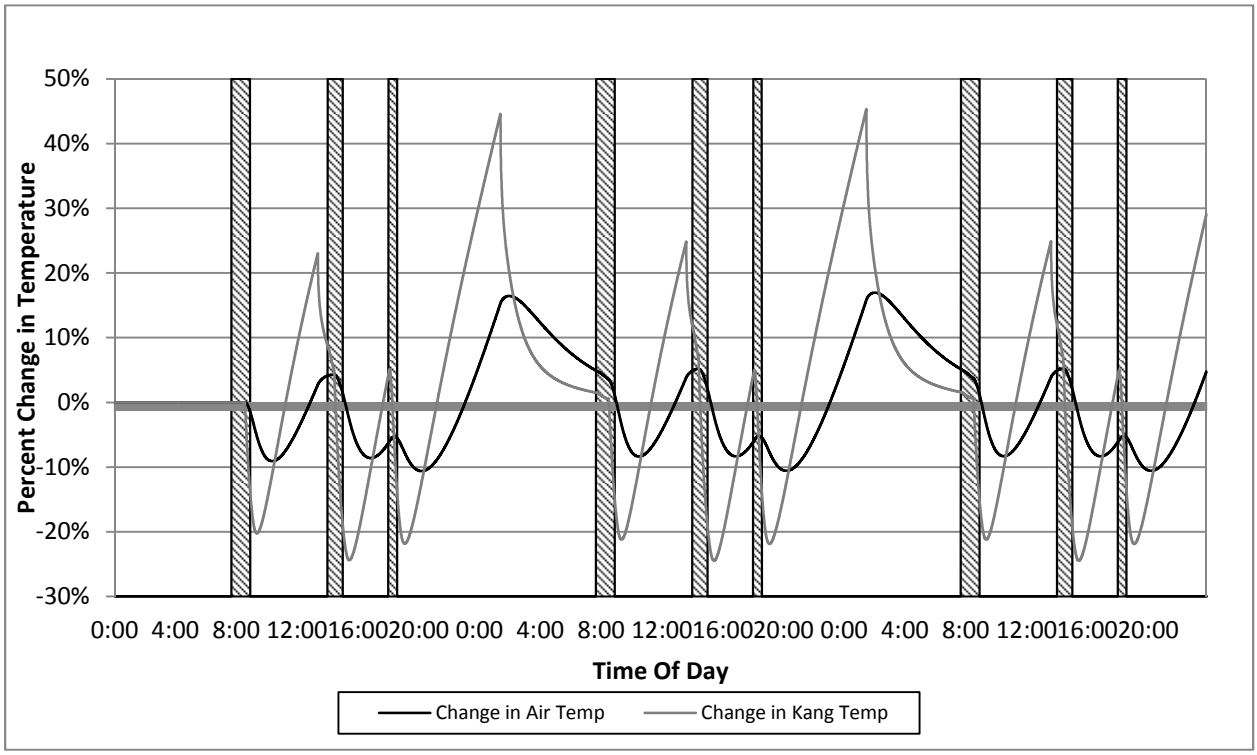

Figure 67 - Improved Effectiveness - PCM

Table 22 displays the percent increase in air and kang temperature due to the use of PCM. While the percent increase is not much, the kang temperature is more uniform which is a desirable characteristic.

Table 22 - Scenario 11 Results

Scenario 11	Air	Kang
Average	2.85%	7.73%

Scenario twelve returns to scenario nine and adds PCM. The simulation was run several times with the intention of flattening the kang temperature curve. The amount of PCM required to keep the kang surface temperature from falling below 28℃ is 100 kg. Even this large amount of PCM becomes saturated. However, it is able to store and release enough energy to keep the kang surface temperature from falling below 28℃. The resulting component temperature profiles are charted in Figure 68 and Figure 69.

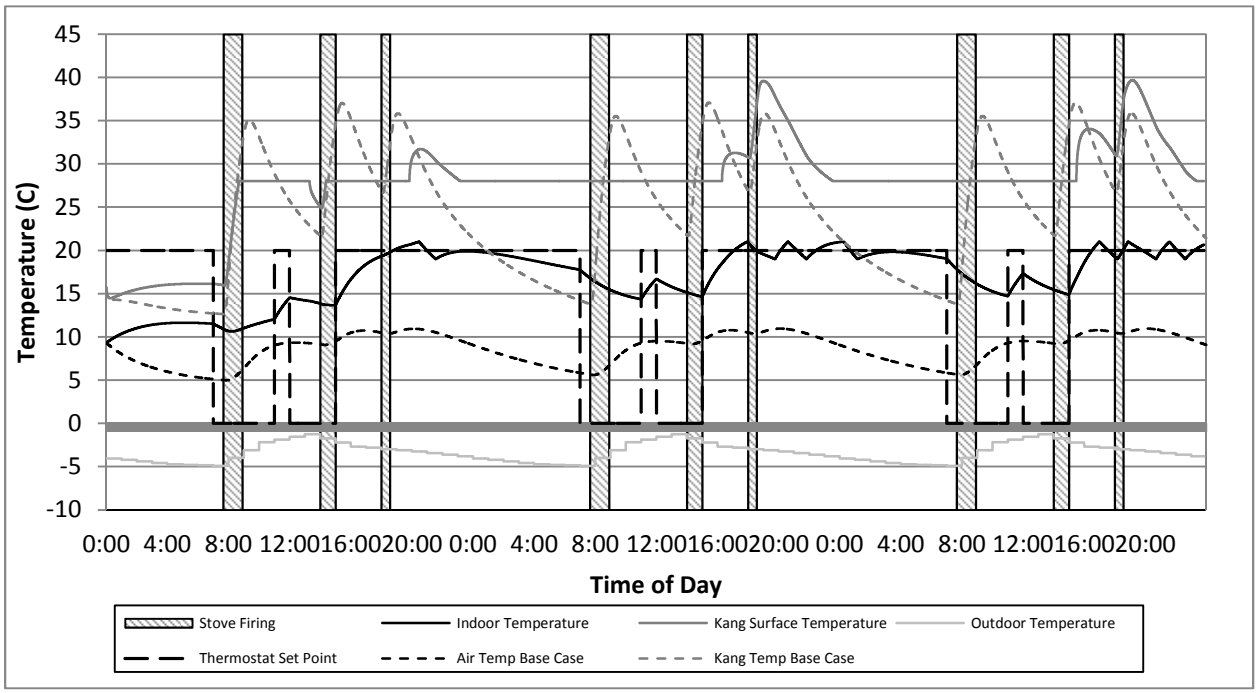

Figure 68 - Heat Exchanger – Room Radiator – Elevated Living Set Point – SHW - Increased Tank Size - Improved Building Insulation - PCM

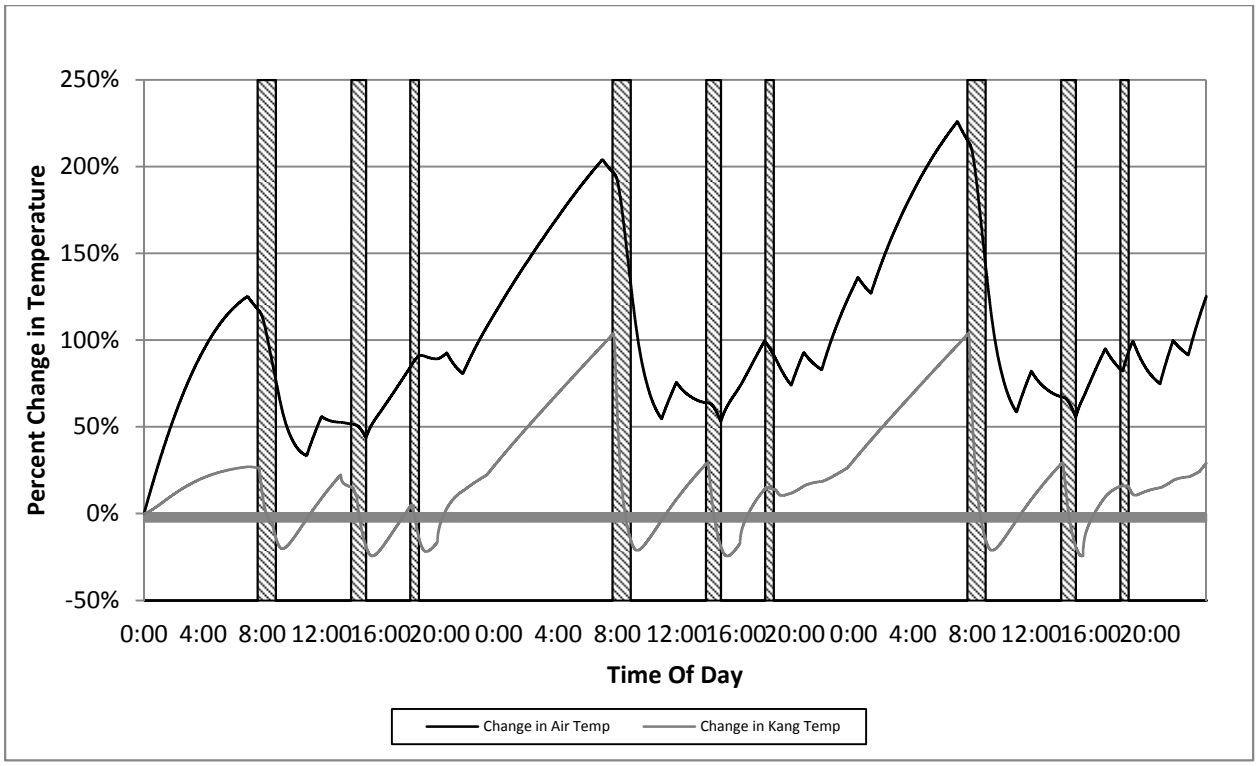

Figure 69 - Improvement Effectiveness - Heat Exchanger – Room Radiator – Elevated Living Set Point – SHW - Increased Tank Size - Improved Building Insulation – PCM

Table 23 displays the increase in component temperature, 135% for the air and nearly 43% for the kang. The air temperature is only slightly greater than that of scenario nine, but the kang's temperature is 16% higher. More so, the kang's temperature is flatter, cooler in the late morning and afternoon and warmer during the sleeping hours. The addition of PCM can provide improved comfort to the building's residents.

Table 23 - Scenario 12 Results

Scenario 12	Air	Kang
Average	135.62%	42.59%

Scenario 13 investigates the effect of adding a bathing load to scenario two. Four showers, each consisting of 25 liters of 40°C water, are taken during the hours of 17:00-18:00. Figures Figure 70 and show the results below.

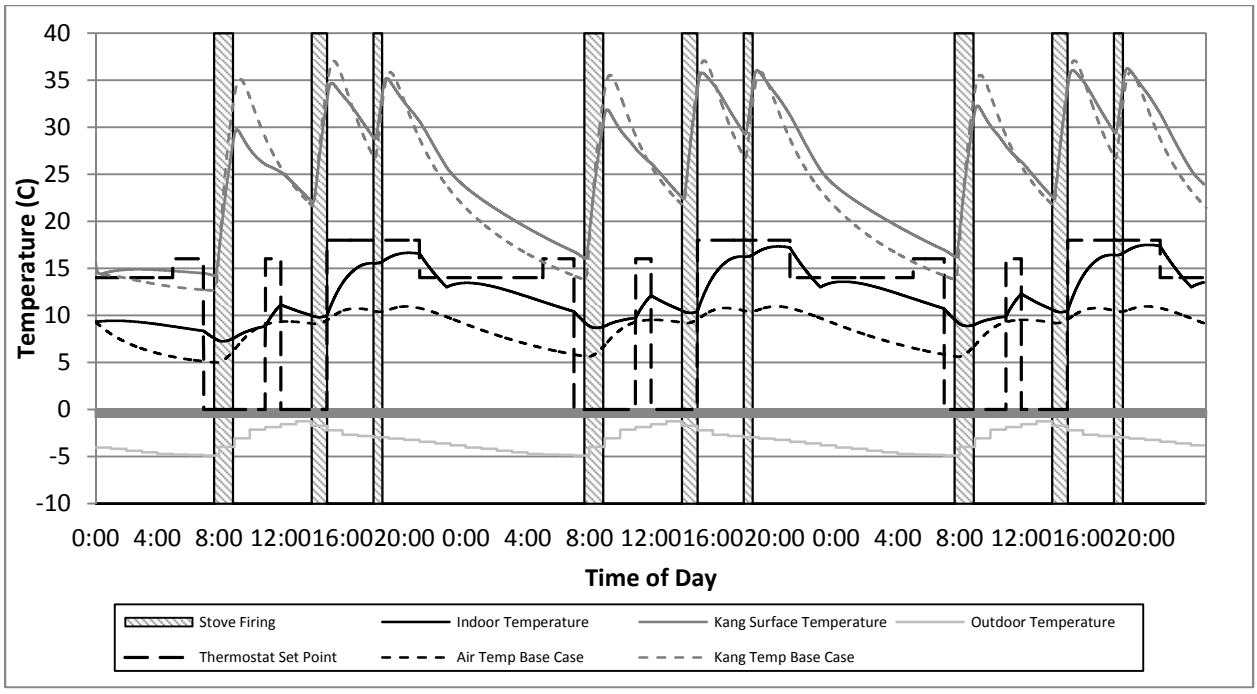

Figure 70 - Improvement Effectiveness -Heat Exchanger – Room Radiator – Living Set Point - Bathing Load

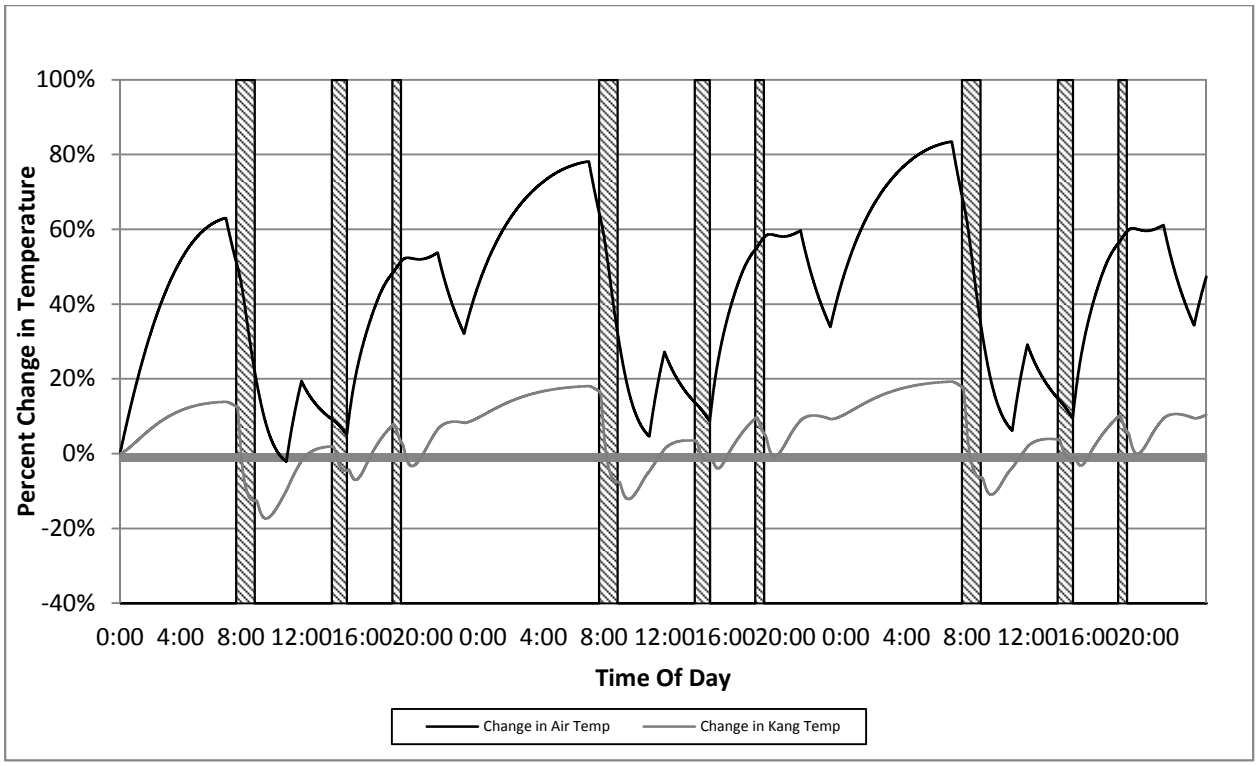

Figure 71 - Improvement Effectiveness -Heat Exchanger – Room Radiator – Living Set Point - Bathing Load - Improvement Effectiveness

Table 24 - Scenario 13 Results

Scenario 13	Air	Kang
Average	60.75%	11.70%

Table 24 shows the effect on the air and kang temperature from the residents withdrawing hot water from the system for bathing purposes. The air temperature decreases from over 67% to under 61% and the kang's temperature falls from 13.75% to 11.70%. Scenario five, adding SHW to scenario two, increases the air and kang temperatures more than the bathing load decreases them. This implies the SHW is capable of supplying hot water for bathing purposes in a separate system, even during the coldest months. This is supported by community interviews that stated their independent and individual SHW systems functioned well during the winter.

Table 25 displays possible scenarios with different improvements active during the simulation. There are several observations from the resulting data. The radiator and heat exchanger system can provide added comfort to the building residents. The location of the radiator is important; using kang radiant heating produces less desirable results regarding room air temperature but warmer temperatures of the kang's surface plates. The solar hot water heater adds little energy to the system but could function well as a separate system for bathing purposes. However, the model simulates the month of January; more favorable results would be produced if months with more daylight hours, e.g. from September to March, were simulated. Insulation can raise the temperature of the home significantly. The number of air shifts per hour has a large effect on the amount of heat the homes loses. The PCM does not increase the temperature of the kang or air significantly. It does flatten the kang's temperature curve which would make the surface more comfortable for residents. It should not be ruled out as a possible tool to improve occupant comfort.

Table 25 – Analysis of Improvements

Scenario	**Improvement**	**Average Percent Increase**	
		Air	Kang
1	Heat Exchanger – Room Radiator - Constant Set Point	58.74%	6.69%
2	Heat Exchanger – Room Radiator – Living Set Point	67.67%	13.75%
3	Heat Exchanger – Kang Radiant – Constant Set Point	19.49%	35.27%
4	Heat Exchanger – Kang Radiant – Living Set Point	18.82%	33.19%
5	Heat Exchanger – Room Radiator – Living Set Point - SHW	72.83%	15.29%
6	Improved Building Insulation	48.87%	10.71%
7	Heat Exchanger – Room Radiator – Living Set Point- Improved Building Insulation	88.15%	17.86%
8	Heat Exchanger – Room Radiator – Living Set Point- Improved Building Insulation - SHW	88.14%	17.97%
9	Heat Exchanger – Room Radiator – Elevated Living Set Point – SHW - Increased Tank Size - Improved Building Insulation	126.58%	26.20%
10	Heat Exchanger – Kang Radiant – Constant Set Point- - Improved Building Insulation	64.70%	36.36%
11	PCM	2.85%	7.73%
12	Heat Exchanger – Room Radiator – Elevated Living Set Point – SHW - Increased Tank Size - Improved Building Insulation - PCM	135.62%	42.59%
13	Improvement Effectiveness -Heat Exchanger – Room Radiator – Living Set Point - Bathing Load	60.75%	11.70%

Chapter V: Community Assessment

5.1 Introduction

Three separate communities in rural northeast China were visited during the summer of 2012: Pulandian, Dandong and Chende. A map showing the three communities is displayed in Figure 73.

Figure 73- Map of studied communities

Figure 72 - Traditional stove and corn stalks used for fuel

During each visit, information regarding the Kang system was gathered. The method used varied. In Pulandian and Dandong, rural residents were informally interviewed. A focus group was conducted in Chengde with roughly 10 villagers.

Pulandian

Five homes were visited in Pulandian. The first home was the site of the previous DUT studies. This was an important visit as the kang system that was to be modeled could be seen and understood. Two

traditional houses were visited. Both had unimproved ground kang systems. Neither home had domestic hot water. Both homes were built in the 1980s.

Figure 74 - Traditional home in Pulandian, China

A modern home, built in the last few years, was also toured. The modern house had elevated kang systems. However, it had modern radiators which were used more often than the kang system for heating. The modern home also had a hot water system. The final home visited had several different kang systems: ground kangs, elevated kangs and an elevated water kang. The water kang had no chamber, only a large slab functioning as the bed platform. Water pipes were plumbed inside the slab where water heated by a connected boiler would exchange heat. The system of running water pipes through the kang slab is similar to the kang radiator system discussed above. The home had access to indoor hot water. The large central boiler used coal to heat the water.

Residents of each home in Pulandian were interviewed about their kang system. Generally, they felt their current setup is satisfactory. Many of the homes visited used coal fired boilers in conjunction with wall mounted radiators to provide supplemental heating during the coldest months. Residents stated the price of coal was expensive. Cornstalk was readily available and abundant; the price of the cornstalk was not considered an issue. Most of the kang systems in Pulandian had hot wall chambers. A hot wall is a secondary firing chamber that allows the kang to be operated outside of cooking times.

Figure 75 - Rural resident in her kitchen. A traditional stove is to the left. The small opening in the wall is where fuel for the kang's hot wall is burned.

Only the modern homes had domestic hot water available. All hot water systems used passive solar arrays located on the roof. All residents without hot water systems stated they desired access. However, some of the traditional homes' structure could not support a solar heater. Cost of a solar heater was also an issue, a typical water heating system costs ¥ 5,000 ($800).

The residents did not like the idea of using a modern stove. A modern stove is more efficient but is smaller and cannot accommodate traditional large woks that are used in the region for cooking. Meals that are typically prepared require the large woks and cannot be made using smaller pots and pans. Additionally, food for pigs that are raised on each farm is cooked. Many of the homes visited had two stoves, one was used to cook food for the residents, and the other was used to cook for the pigs. Residents stated the pigs' food required the large woks to be prepared.

Dandong

The second community visited was near the city of Dandong, China. Only one home was toured in this community. The community is geographically close to Pulandian, slightly more than 200 km to the northeast. However, culturally the regions vary. Less corn is grown around Dandong and the homes use more wood as a fuel source. The home visited near Dandong was a modern home. It had two elevated kangs, domestic hot water, and a biogas reactor.

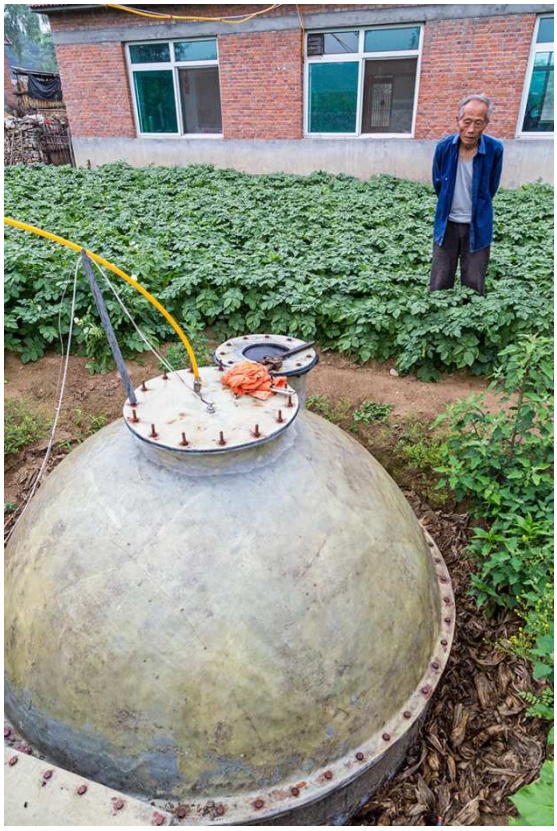

Figure 76 - A biogas reactor at a farm near Dandong, China

Using the reactor, crop and animal waste are converted into methane gas which is used for cooking. The reactor supplies enough gas for the household cooking needs year round. A solar hot water heater was used to keep the contents of the reactor warm and facilitate the conversion of organic waste to methane. The reactor requires cleaning every six months. Livestock is required to make the reactor functional; if only crop waste is used the reactor does not produce enough gas. The reactor doesn't produce enough gas to heat the household, for which the traditional stove and kang system is still used. The residents used the traditional stove to cook food for their pigs. They liked their modern stove and did not feel the need to use large traditional woks to prepare their meals.

Figure 77 - A farmer talks about his kang system. Both a kang platform and modern bed are present in the room

Chengde

The village of Chengde in Hebei province, northeast of Beijing was visited. Several homes were toured. The homes ranged from traditional to modern. Ground and elevated kangs were used. Only the modern homes had access to domestic hot water systems. The homes that had hot water used passive solar heaters on their roofs.

Residents of Chengde participated in a focus group to evaluate their feelings regarding their current kang systems. Initially, plans were developed to interview men and women separately. However, due to time and organizational constraints, men and women participated in the focus group together. Roughly eight members of the community partook in the focus group. Though some members left halfway through and others arrived after it had begun to socialize with the gathered group.

Figure 78 - Participants in the focus group in Chengde, China

Questions were asked of the participating villagers, staring with basic information. See Appendix E for the full set of questions. Basic and general questions were discussed first. The results of the questions are discussed below. Most villagers have lived in Chengde their whole life and have no plan to leave. The focus group participants felt their homes' current heating systems were satisfactory. However, they knew things could be improved. Some rooms were not used during the winter in order to keep the rest of the home warm. Generally, the current kang systems were liked and not many residents felt the desire to improve them. It was stated that the younger generations prefer modern beds. Most residents wanted domestic hot water but stated the passive solar heaters were too expensive.

Handouts displaying possible technical heating solutions were given to the focus group participants and their opinions were expressed; refer to Appendix D for diagrams. A poorly insulated home with leaky windows and a ground kang and traditional stove was presented as a base case scenario. Improvements to the base case were displayed pictorially as possible solutions: replacing the ground kang with an elevated kang system (case 1), improved home insulation & modern windows (case 2), added domestic hot water using passive solar heating (case 3), radiant heating using water heated using the stove (case 4), a water kang system that uses radiant heating (case 5), a biogas and modern stove system for

cooking as well as compressed fuel briquettes to be used for heating and cooking (case 6). Each case was presented as an addition on the previous case's technological solutions.

Figure 79 - Residents of Chengde review a diagram of possible technical solutions

The focus group's reaction to each case is as follows: Case 1 was well received but the associated costs were concerning. Many felt their current ground kangs functioned adequately. Case 2 was desired but thought to be too expensive. Many residents would buy new windows and insulation if they could afford the costs. Case 3 was also desired but costs were a large concern, additionally the possibility of water pipes freezing in the winter was worrisome. Case 4 was intriguing; many residents liked the idea of using the stove to heat water that could exchange heat to the room through a radiator. All the homes visited in Chengde had radiators but used coal boilers to heat the water. The residents stated the cost of coal was very high. Case 5 was not well received. Some of the residents knew of systems in use and said leaks could be problematic. They also worried about water freezing in the pipes when the kang was not in use. Case 6 was also not popular. The villagers knew of abandoned biogas reactors in the area that never worked as promised. They stated there were not enough animals to create the required waste to make the reactors function. The abandoned reactors became too cold during the winter and wouldn't function. The villagers were intrigued by the addition of a passive solar heater to the reactor system that

would allow the reactor to function throughout the winter. Members of the focus group were not dissuaded by using a modern stove. Some homes had both modern and traditional stoves. Most residents stated they were not comfortable only using a modern stove, and that a traditional stove was still required to cook for their pigs and to make certain dishes.

Further investigation is required pertaining to what the residents define as comfort and how they prioritize certain amenities. It is known that the room air is too cold, but it is not understood if it is more desirable to increase the air temperature at the expense of lessening the temperature of the surface of the kang. Additionally, it is unknown if the residents place a higher priority on obtaining improvements that allow for bathing over increasing the temperature of the air. More in depth questionnaires and interviews with the community members should be developed to answer these and other questions.

Chapter VI: Economic Analysis

Previously, the technical and cultural feasibility of each solution were assessed. Now the cost of each solution will be analyzed. This will allow for each solution to be evaluated on three separate criteria and an optimal solution recommended.

To compare each improvement equally, the costs of each component were calculated as an annuity. To do this, the lifespan of each item must be known along with the discount rate of the future. For this analysis a discount rate of 7% was used. Many households use large quantities of coal, typically around 2 tons per year in the northeast (Yang, 2010). Currently the price for thermal coal is $166 per ton (China Coal Resource) implying an average household spends $332 per year on coal. This is the annual baseline cost to which other improvements will be compared.

To implement an improvement a household would have to pay capital upfront whereas the benefits provided by the improvement will occur over time. The capital recovery factor (CRF) for each improvement can be calculated using the following equation, where i is the discount rate and n is the life span of the improvement.

$$CRF = \frac{i(1+i)^n}{(1+i)^n-1} \quad 61$$

Multiplying the CRF by the initial capital investment of the improvement produces a uniform annuity. This annuity allows each improvement to be equally compared as an annual cost. Table 26 - Annualized Cost Data below overviews the cost and life cycle details for each improvement.

Table 26 - Annualized Cost Data

Improvement	Initial Cost	CRF	Annual Cost	Life Cycle
Insulation	$2,500.00[1]	0.08	$201.47	30
Tank - 500 L	$700.00[2]	0.08	$56.41	30
Tank - 1,000 L	$1395.00[3]	0.08	$112.42	30
Heat Exchanger	$200.00[4]	0.11	$21.96	15
Radiator	$350.00[5]	0.11	$38.43	15
Pump, controls, valves gauges	$560.00[6]	0.11	$61.48	15
Thermostat	$98.50[6]	0.11	$10.81	15
Kang Piping	$25.00[6]	0.11	$2.74	15
Tank HX Installation (12 hrs)	$133.00	0.11	$14.60	15
Kang Piping Installation (18 hrs)	$133.00	0.11	$14.60	15
SHW	$800.00	0.11	$87.84	15
PCM – 100kg - 10,000 cycles	$770.00[7]	0.24	$187.80	5
PCM Installation (12 hrs)	$133.00	0.24	$32.44	5

The cost for each item was obtained from literature and current market prices for comparable items currently for sale. The life span of each item was researched. The cost of certain components can be added to determine the total annual cost for a given improvement system. This is displayed in Table 27

Table 27 – Annual Improvement Cost

Improvement System	Annual Cost
Insulation	$201.47
Room Radiator - 500 L Tank	$203.70
Room Radiator - 1,000 L Tank	$259.71
Kang Radiator - 500 L Tank	$189.98
Kang Radiator - 1,000 L Tank	$245.98
SHW	$87.84
PCM	$220.23
Coal	$332.00

[1] (Li M. , 2011)
[2] (Alibaba.com)
[3] (SolarOZ)
[4] (Hydronic Heating Supplies)
[5] (Amazon.com)
[6] (Radiant Floor Company)
[7] (Kosny, 2010)

Home insulation was determined to last the life span of the home or thirty years. The cost includes insulating a rural Chinese home with 0.75 mm thick foam insulation with a U value of 0.38. The cost includes installation and maintenance of insulation over the walls and roof of the domicile.

The radiator system includes the cost of the water tank, heat exchanger, pump & controls, thermostat, and the installation of each item. It was assumed that the installation would take 12 hours (Homwyse). The installation cost was calculated using a value of $1,000 for labor to install a comparable system in the US and then dividing by 5, the difference between US and Chinese construction labor rates (Worldsalaries.org, 2008).

The kang radiant system has the same components as the room radiator system without the radiator. The cost of the kang piping was added and the cost to install the kang system is higher due to the installation of pipes inside the kang. The solar hot water was evaluated separately to determine its incremental cost. The lifecycle of all components for both the room radiator and the kang radiant systems was set at 15 years. The SHW panels do not offer enough energy to heat the home and it wouldn't make technical sense to have a tank, SHW, radiator system that does not capture energy from combusted coal or fuel..

The phase change material cost includes material and insulation costs. Insulation would require reconstructing the top surface of the kang. It was assumed this job would take 12 hours and the costs were calculated similarly to installation costs for the room radiator system. The PCM's life cycle is much lower than other systems. A typical PCM can last 10,000 phase changes (Wilson, 2009). If the PCM melts and freezes during each firing, that is 6 phase changes each day. This makes the life span of the PCM roughly 5 years. At the end of 5 years, new material would have to be purchased and re-installed. If a PCM with longer life was implemented, the annual cost for the PCM would be less.

6.2 Recommendations

Each improvement can have its technical effectiveness compared to its annualized cost to determine which solution is most cost effective at increasing the air and kang temperature. Table 28 shows each scenario's resulting increase of component temperature along with the annualized cost. The table also displays the percent increase in component temperature per dollar of annualized cost. The higher this value the more the scenario is able to increase the air or kang temperature per unit of capital invested.

Table 28 - Improvement Cost Effectiveness

Scenario	Improvement	Average Percent Increase			Average Percent Increase / Annualized Cost	
		Air	Kang	Improvement Annualized Cost	Air	Kang
2	Heat Exchanger – Room Radiator – Living Set Point	67.67%	13.75%	$ 203.70	0.33%	0.07%
3	Heat Exchanger – Kang Radiant – Constant Set Point	19.49%	35.27%	$ 189.98	0.10%	0.19%
4	Heat Exchanger – Kang Radiant – Living Set Point	18.82%	33.19%	$ 189.98	0.10%	0.17%
5	Heat Exchanger – Room Radiator – Living Set Point - SHW	72.83%	15.29%	$ 291.54	0.25%	0.05%
6	Improved Building Insulation	48.87%	10.71%	$ 201.47	0.24%	0.05%
7	Heat Exchanger – Room Radiator – Living Set Point- Improved Building Insulation	88.15%	17.86%	$ 405.17	0.22%	0.04%
8	Heat Exchanger – Room Radiator – Living Set Point- Improved Building Insulation - SHW	88.14%	17.97%	$ 493.00	0.18%	0.04%
9	Heat Exchanger – Room Radiator – Elevated Living Set Point – SHW - Increased Tank Size - Improved Building Insulation	126.58%	26.20%	$ 549.01	0.23%	0.05%
10	Heat Exchanger – Kang Radiant – Constant Set Point- - Improved Building Insulation	64.70%	36.36%	$ 391.44	0.17%	0.09%
11	PCM	2.85%	7.73%	$ 220.23	0.01%	0.04%
12	Heat Exchanger – Room Radiator – Elevated Living Set Point – SHW - Increased Tank Size - Improved Building Insulation - PCM	135.62%	42.59%	$ 769.24	0.18%	0.06%

Figure 80- Chart of Improvement Cost Effectiveness plots the right most columns of Table 28 - Improvement Cost Effectiveness. From the chart it is clear that scenario two, the room radiator by itself,

adds the most improvement to the air temperature for the least amount of invested capital. Scenario three, just the radiant heating within the kang, increases the kang's temperature the most per dollar of capital invested. Improving the building's insulation, scenario six, does not increase the room's air temperature more per dollar invested than adding a room radiator.

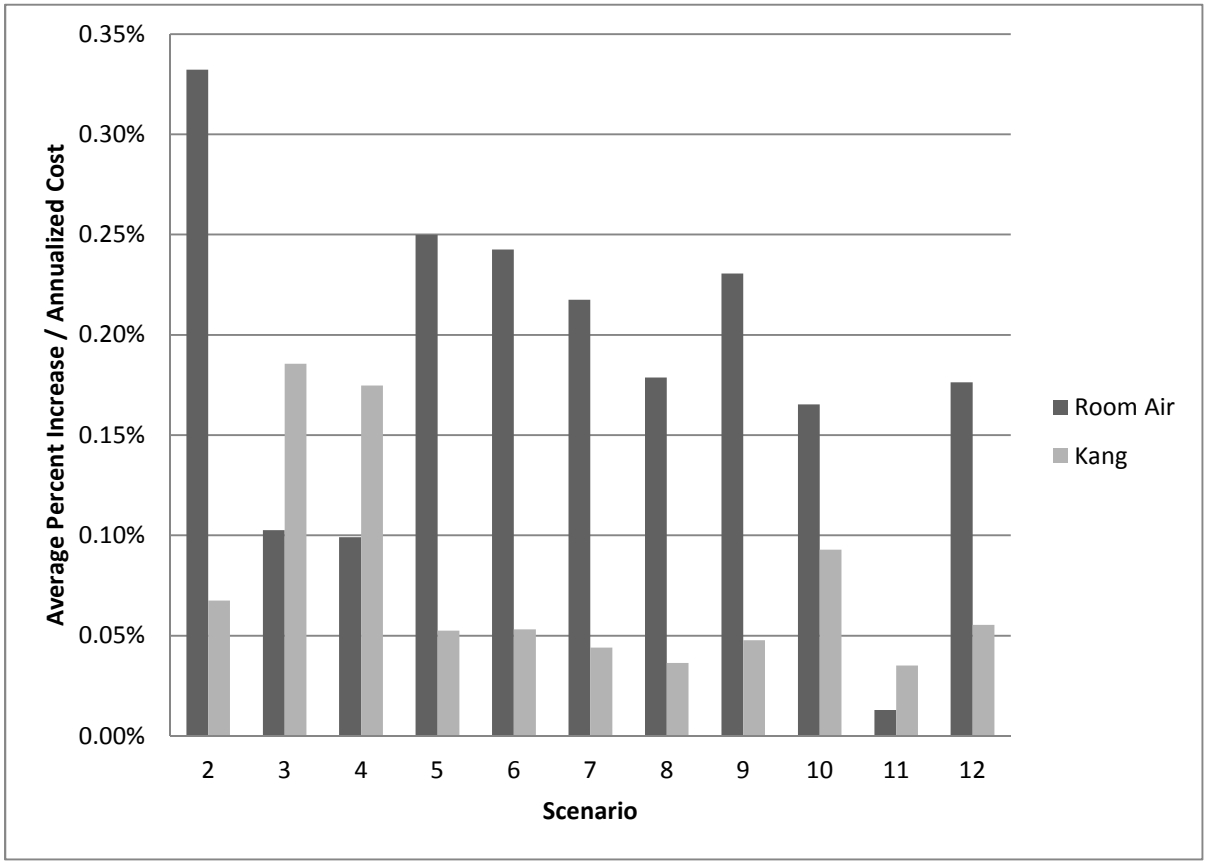

Figure 80- Chart of Improvement Cost Effectiveness

Finally, a decision matrix can be created to determine the technical, economic and cultural feasibility of each improvement. Each improvement is considered independently and is assessed in three categories: technical, economic and cultural feasibility. In each category a value is assigned based on how well the improvement meets the requirements of the category. Only three possible values are available and are represented by three distinct circles.

For the technical category, the improvement's performance was assessed regarding how well it increased the air and kang temperature and whether it is capable of providing an option for bathing. If the improvement was able to fully meet the living set point of the thermostat, the improvement was given a full mark. If the improvement was capable of significantly increasing the component's temperature over that of the base case, but not able to meet the living set point of the radiator, it was given half a mark. If the improvement was not capable of increasing the component's temperature significantly over that of the base case it was given an empty mark.

The economic scores were calculated based on the percent of the cost of coal the improvement would cost. That is, the insulation's annual cost is 40% less than the annual cost of coal. Therefore it is receives a half filled mark, falling in the category of 33-67%. A full mark is anything with an annual cost of 67-100 % less than the annual cost of coal and an empty mark is given to any improvement with an annual cost of 0-33% less than the annual cost of coal.

The cultural category is scored based of information gleaned from the community assessments. A filled mark is considered acceptable by the community. A half mark implies the community's views regarding the improvement are unknown. An empty mark means the community has expressed dissatisfaction with the improvement.

Table 29 - Improvement Feasibility Matrix

Improvement	**Improvement Feasibility**				
	Technical			Economic	Cultural
	Air	Kang	Bathing		
Insulation	◑	○	○	◑	●
Room Radiator - 500 L Tank	◑	○	●	◑	●
Kang Radiator - 500 L Tank	○	●	●	◑	○
SHW	○	○	●	●	●
PCM	○	●	○	◑	◑
Coal	●	○	○	○	○

The matrix provides a guide regarding the tested solutions. None satisfy every criterion perfectly, but some are clearly better than others and all present a better alternative to the continued use of coal. A more detailed decision analysis could be conducted if each category was ranked by desirability by the affected community members. For instance, residents could rank their desire for each category to be satisfied and these ranks could then weight the scores of each category. This would allow each solution to have an individual score rather than a series of separate marks. However, to carry out this more detailed decision analysis, further discussion with the local community members is required.

Chapter VII: Conclusion

China is developing very quickly. Factors such as climate change and high cost of fuel make increasing living standards through increased energy use alone difficult. Heating issues are still a problem in the countryside and many rural residents have adapted their lifestyles to accommodate the harsh winter environment. Technical solutions currently exist that can provide more comfortable living conditions without straining residents' pocketbooks or negatively impacting the environment.

Both the output of the model and the local residents indicated that improving the building's insulation is a high priority. However, the cost of insulation compared to the added benefit is less than that of installing a room radiator water system. Many homes already have radiator systems installed. Currently they are coupled to a coal boiler. However, it would be feasible to install a heat exchanger in the stove and reconfigure the existing radiator system to work in conjunction with a stove heat exchanger. Doing so would sever the residents' reliance on coal, which is currently used to heat the water in the radiator system. This approach would also be cheaper than what is implied in the economic analysis as some of the equipment required for the room radiator system is already present.

Local residents didn't like the idea of the water kang due to difficulties with maintenance and repairs and instances of pipes freezing when the system was not in use. The output model showed the radiant heating as a viable technical solution. Much work would be required to implement this improvement as there are cultural barriers that need to be overcome. Behavior Change Communication (BCC) could be used to work with the home's occupants to develop a behavioral program to lessen water kang failures.

The solar hot water panel was shown to not add significant energy to the heating system. More panels could be used but cost quickly becomes prohibitive. Many residents expressed their desire for domestic

hot water, particularly for bathing. While a solar hot water heater might not be practical for heating purposes, it should not be ruled out for domestic use.

Further questionnaires and interviews need to be conducted with the targeted communities to assess their definition of comfort. If bathing is considered a more important priority over increasing the temperature of the air, resources should be focused towards solutions that permit bathing to occur.

These solutions require further investigation to ensure they are implemented properly. The development of the system model is an important step in selecting appropriate technical solutions. The improvements tested and discussed here are few, and several alternate combinations of solutions can be configured and optimized. Furthermore, many possible technical solutions are constrained by cultural habits and behavior. Older generations still use the Kang system, but many young Chinese prefer a traditional bed. It is possible that a solution to the kang system might involve removal of the kang or its complete reconfiguration. Slight cultural differences will require custom solutions for each distinct region, and it is important to work with each local community to make sure their needs and concerns are expressed and considered.

Bibliography

Alibaba.com. (n.d.). *OEM free 80 to 500 Liters water tank*. Retrieved 1 29, 2013, from Alibaba.com: http://www.alibaba.com/product-gs/703546383/OEM_free_80_to_500_Liters.html

Amazon.com. (n.d.). *DD24.40DBL Wall Panel Radiator 24"H x 40"L - 8,240 BTU*. Retrieved 1 29, 2013, from Amazon.com: http://www.amazon.com/DD24-40DBL-Wall-Panel-Radiator-quot/dp/B005M50R1K

Apricus Solar Hot Water. (2011, 08 17). *Submittal Data Information - AP-20C Solar Collector*. Retrieved 1 29, 2013, from http://184.106.137.17/en/america/products/solar-collectors/ap-30c-buy-american-collector/

Chen, B. (2007). Field survey on indoor thermal environment of rural residences with coupled Chinese kang and passive solar collecting wall heating in Northeast China. *Solar Energy*, 781-790.

China Coal Resource. (n.d.). *China Coal Prices, China Coal Production, China Coal Market, Coal Index, Coal News & Analysis - China Coal Resource*. Retrieved 1 29, 2013, from China Coal Resource: http://en.sxcoal.com/

Guangyu, C. (2011). Simulation of the heating performance of the Kang system in one Chinese detached house using biomass. *Energy and Buildings*, 189-199.

Hirman , S. (2003). Characterization of Alkalanes and Paraffin WAkex for Application as Phase Change Energy Storage MEdium. *Energy Sources*, 117-128.

Homwyse. (n.d.). *Cost to Install Radiant Floor Heat - 2013 Cost Calculator*. Retrieved 1 29, 2013, from Homwyse: http://www.homewyse.com/services/cost_to_install_radiant_floor_heat.html

Hydronic Heating Supplies. (n.d.). *Water To Air Heat Exchangers*. Retrieved 1 29, 2013, from Hydronic Heating Supplies: http://www.northlanddistrib.com/Water-To-Air-Heat-Exchangers_c_423.html

Jabbar N. Khalifa, A. (2011). EXPERIMENTAL STUDY OF TEMPERATURE STRATIFICATION IN A THERMAL STORAGE TANK IN THE STATIC MODE FOR DIFFERENT ASPECT RATIOS. *ARPN Journal of Engineering and Applied Sciences*, 53-60.

Jiangjiang, W. (2011). Influence analysis of building types and climate zones on energetic, economic and environmental performances of BCHP systems. *Applied Energy*, 3097-3112.

Kosny, J. (2010). *Understanding Potential for Phase Change Material Applications in ResidentialBuildings.* Denver: U.S. Department of Energy's Building America Program.

Li, M. (2011). *Sustainable Design Optimization of Rural Houses in North China.* West Lafayette, IN: Purdue University.

Li, Y. (2009). Chinese kangs and building energy consumption. *China Science Bulletin*, 993-1002.

Merriott Design Radiators. (2012). *Merriott Radiators - Products*. Retrieved 1 29, 2013, from Merriott Radiators: http://www.merriott-radiators.com/downloads/QUINNHPR.pdf

Pachauri, S. (2008). *The Household Energy Transition in India and China.* Laxenburg, Austria: International Institute for Applied Systems Analysis.

Qian, H. (2010). Surface Temperature Distribution of Chinese Kangs,. *International Journal of Green Energy*, 347-360.

Radiant Floor Company. (n.d.). *Radiant Heat From Radiant Floor Company - Prices and Quotes*. Retrieved 1 29, 2013, from Radiant Floor Company: http://www.radiantcompany.com/prices/prices.shtml

Sharma, A. (2009). Review on thermal energy storage with phase change. *materials and applications*, 318-345.

SolarOZ. (n.d.). *Tanks - 1000L Stainless Tank - SolarOz | Solar Hot Water Systems Australia | DIY Solar Hot Water Installation*. Retrieved 1 29, 2013, from SolarOz: http://solaroz.com.au/shop/tanks/1000l-stainless-tank/prod_168.html

Standardization Administration of the People's Republic of China. (2000). *Air quality guidelines for Europe 2000 - Second Edition WHO.* WHO Regional Publications.

US Department of Energy. (n.d.). *iomass Program: Biomass Feedstock Composition and Property Database*. Retrieved 1 29, 2013, from Use Department of Energy: Energy Efficiency & Renewable Energy: http://www.afdc.energy.gov/biomass/progs/search1.cgi

Wang, Y. (2006). *Economic Analysis of Solar Water Heaters in GuangZhou.* Guangzhou, China: School of Architecture, South China University of Technology .

Weber, T. (2004). *A Calculation Method for Air Infiltration Energy Loss Based on Climatic Data.* Stockholm, Sweden: Royal Institute of Technology, Division of Building Technology.

Wei, H. (2013). A study on thermal performance, thermal comfort in sleeping environment and solar energy contribution of solar Chinese Kang. *Energy and Buildings*, 66-75.

WHO. (2000). *Air quality guidelines for Europe 2000 - Second Edition .* WHO Regional Publications.

Wilson, A. (2009, 11 24). *Storing Heat in Walls with Phase-Change Material*. Retrieved 1 29, 2013, from Green Building Advisor: http://www.greenbuildingadvisor.com/blogs/dept/energy-solutions/storing-heat-walls-phase-change-materials

Worldsalaries.org. (2008). *Construction Sector Average Salary Income - International Comparison<*. Retrieved 1 29, 2013, from Worldsalaries: http://www.worldsalaries.org/construction.shtml

Yang, X. (2010). Energy and IAQ in Chinese Rural Housing: Sustainable Strategies and Demonstration Projects. *International Conference on Indoor Air Quality, Ventilation and Energy Conservation in Buildings*, (pp. 1-66). Syracuse.

Zhai, Y. (2009). *Thermal Performance of Heating System of Hot-wall Kang.* Dalian, China: Dalian University of Technology.

Zhu, B. (2011). Adoption of renewable energy technologies (RETs): A survey on rural construction in China. *Technology in Society*, 223-230.

Zhu, J. (2010). *Study on Rural heating systems which Based on Hot-wall Kang.* Dalian, China: Dalian University of Technology.

Zhuang, Z. (2007). A mathematical Model For A House Integrated With An Elevated Chinese Kang Heating System. *Building Simulation*, 64-70.

Zhuang, Z. (2008). Measured Heat Transfer and Smoke Flow Performance of a Typical Elevated Chinese Kang. *Energy and Buildings*.

Zhuang, Z. (2009). Chinese kang as a domestic heating system in rural northern China—A review. *Energy and Buildings*, 111-119.

Zhuang, Z. (2010). Thermal and energy analysis of a Chinese kang. *Energy Power Eng. China*, 84-92.

Appendix Reference

Appendix A: Kang Diagram

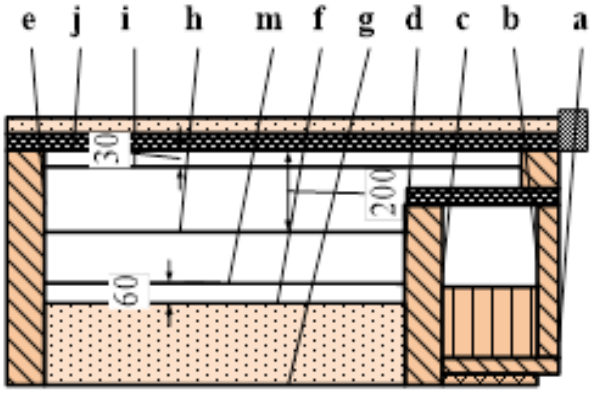

a: Outer surface of exterior of hot-wall
b: Inner surface of exterior of hot-wall
c: Inner surface of interior hot-wall
d: Outer surface of interior of hot-wall
e: Inner surface of outer Kang wall
f: Surface of substrate
g: 10mm deep in the mud
h :middle part of smoke
i: top part of smoke
j: Interior of Kang plates
k: Kang surface
m: low part of smoke

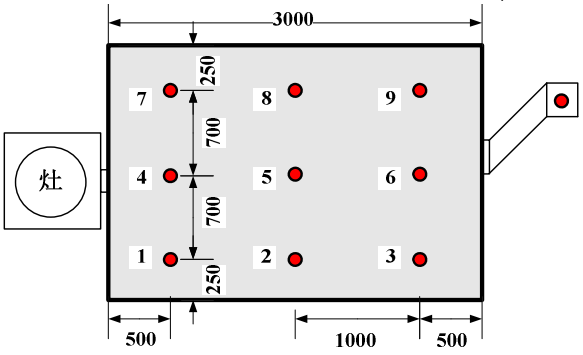

Kang surface

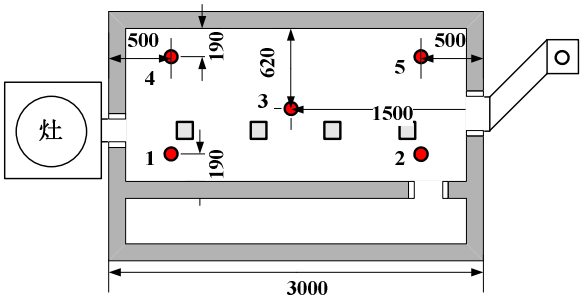

f,g,m plane

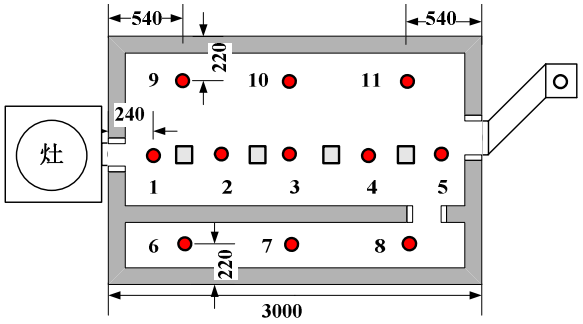

i,j plane

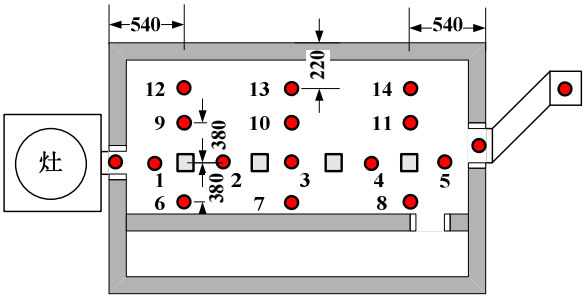

h plane

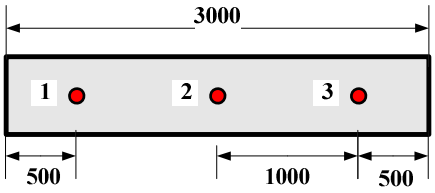

a plane

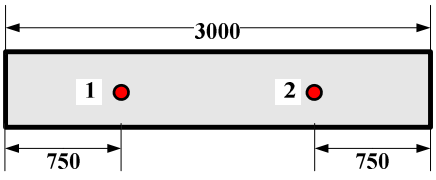

b,c,d plane

Appendix B: Model Sensitivity Charts

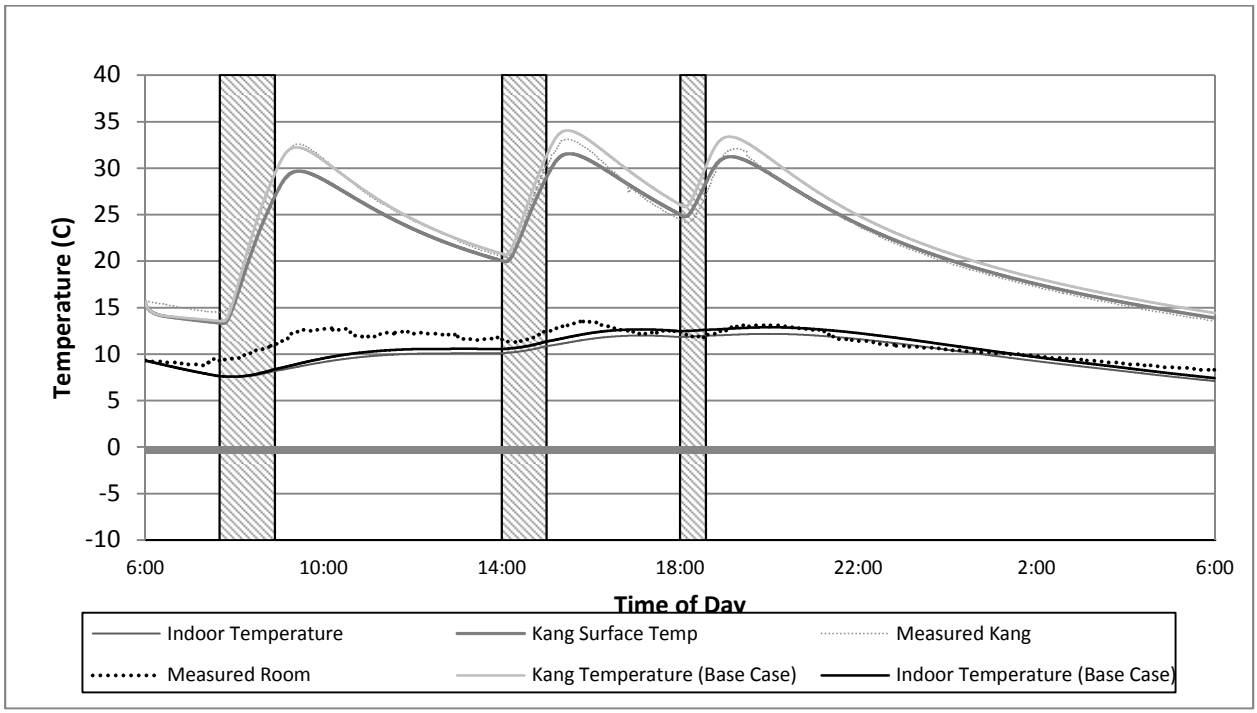

Figure 81 - Component Temperature Profile - h Kang Chamber (-20%)

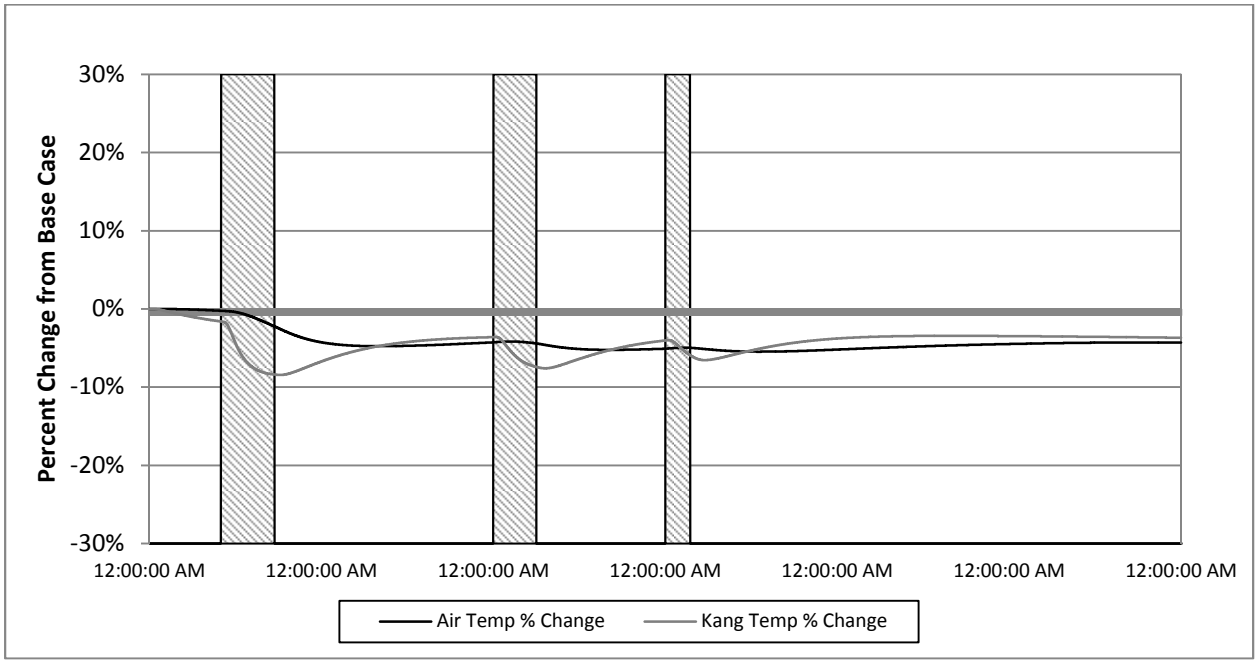

Figure 82 - h Kang Chamber (-20%)

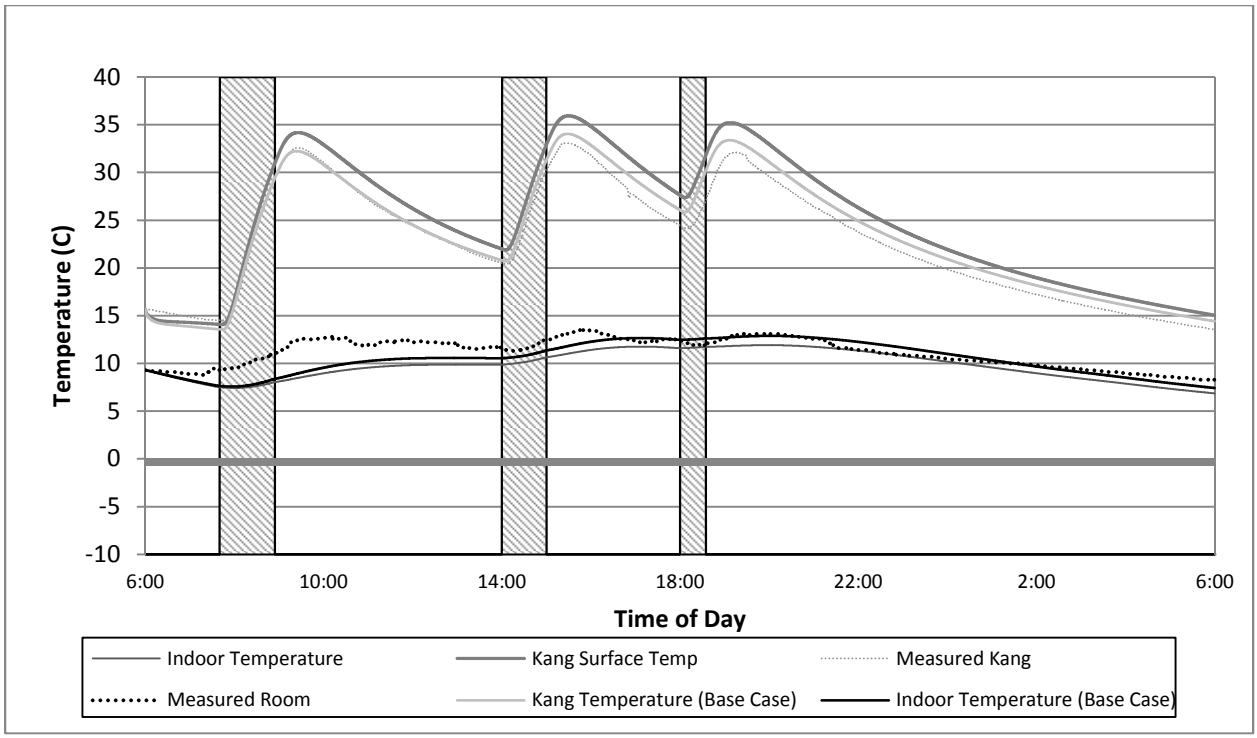

Figure 83 - Component Temperature Profile - h Kang Surface (-20%)

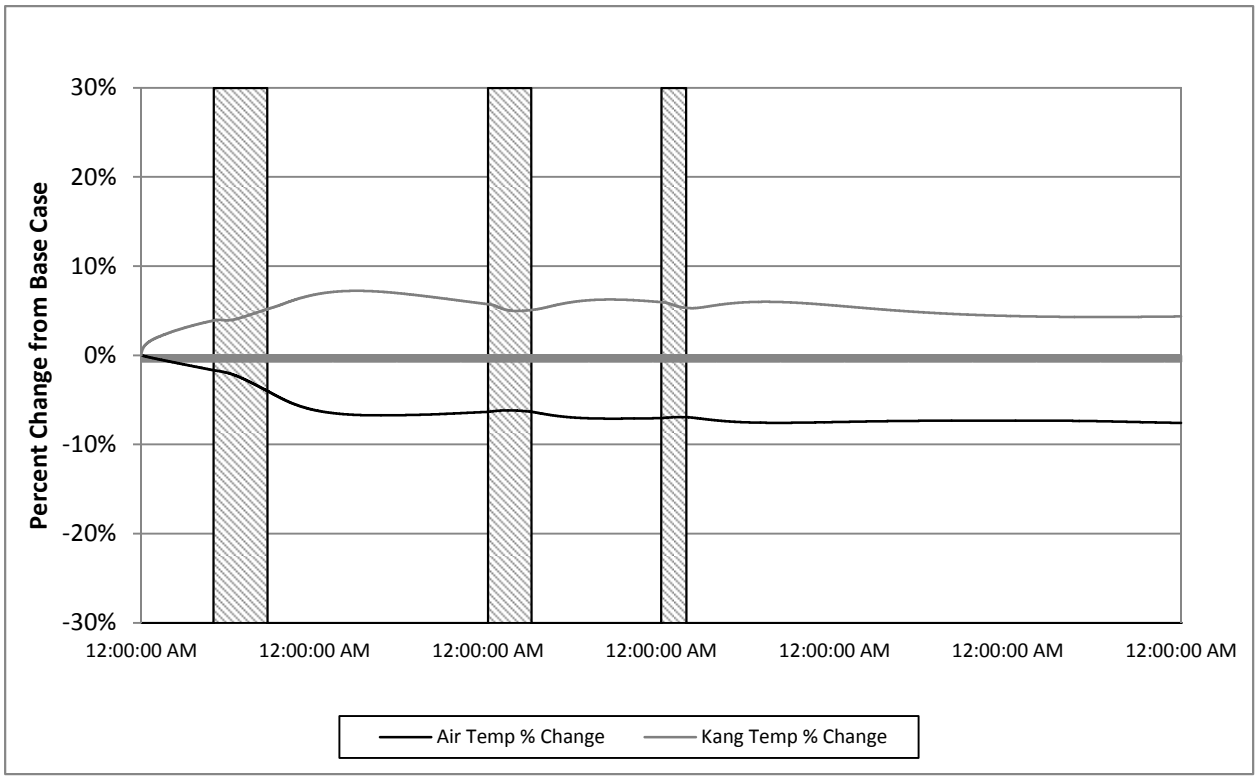

Figure 84 - h Kang Surface (-20%)

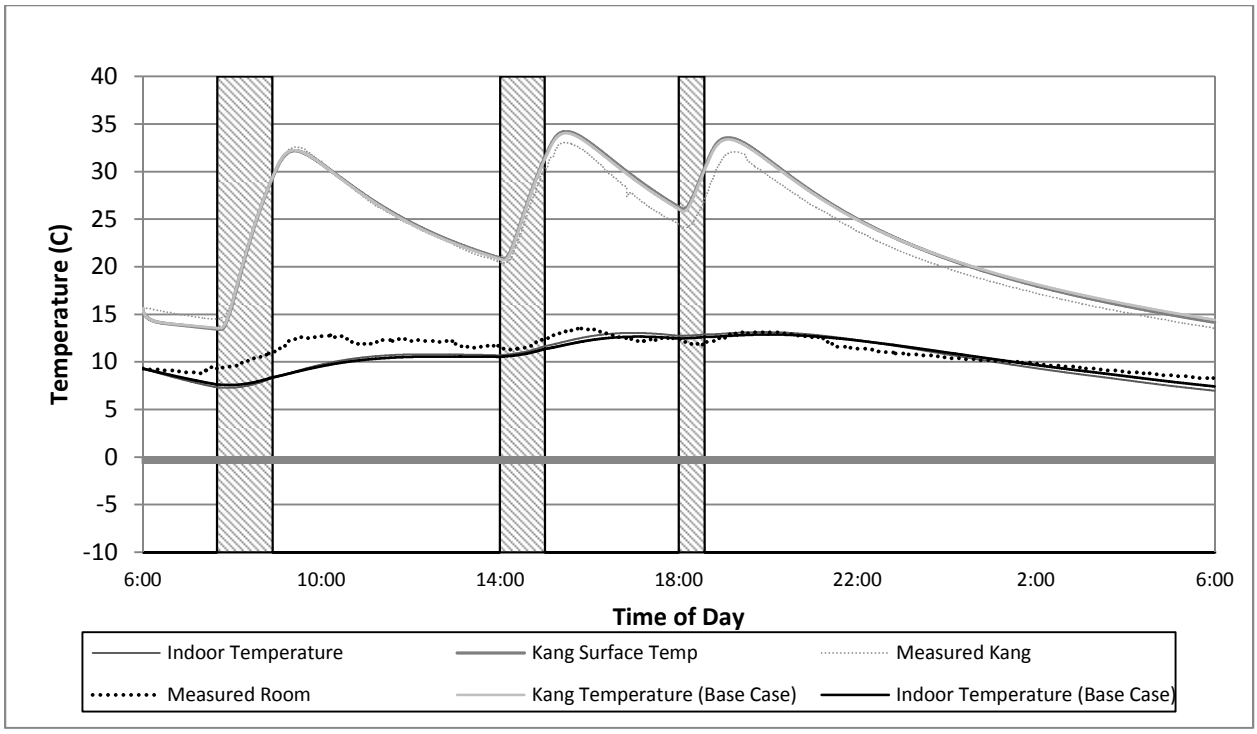

Figure 85 - Component Temperature Profile - Additional Thermal Mass (-20%)

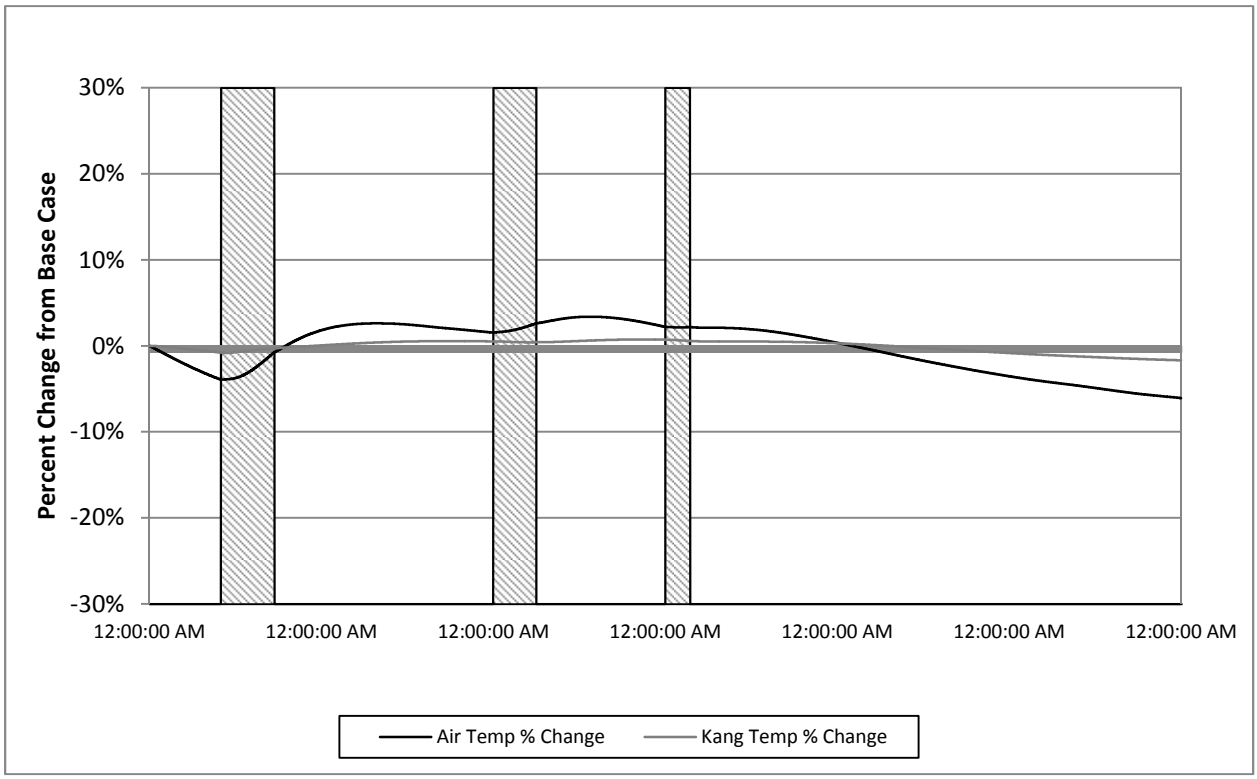

Figure 86 - Additional Thermal Mass (-20%)

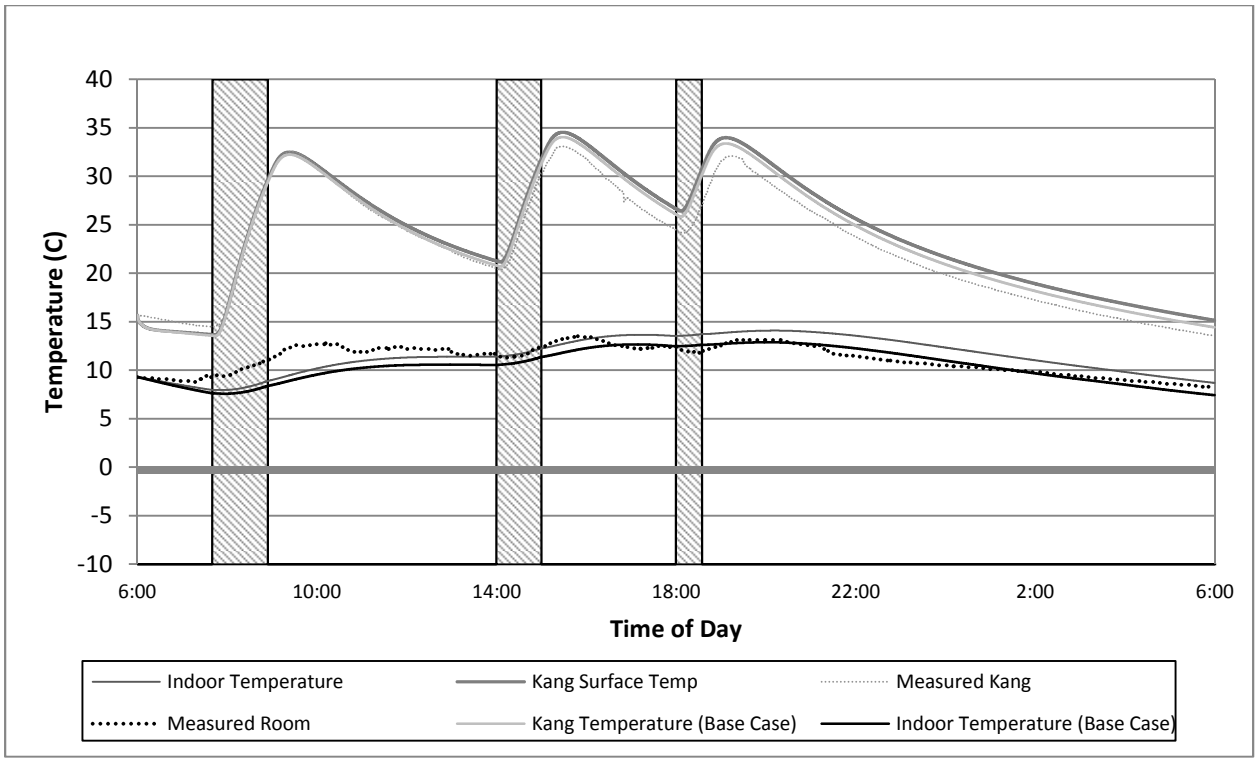

Figure 87 - Component Temperature Profile Air Shifts per Hour N (-20%)

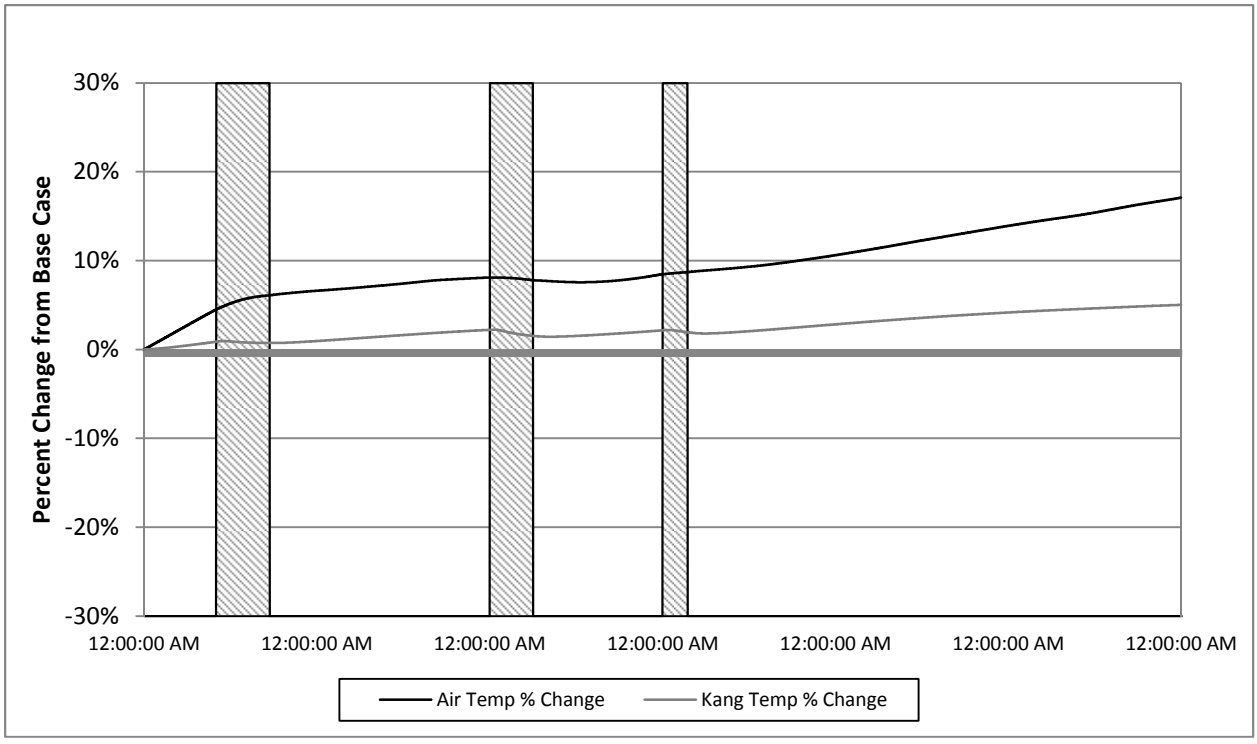

Figure 88 - Air Shifts per Hour N (-20%)

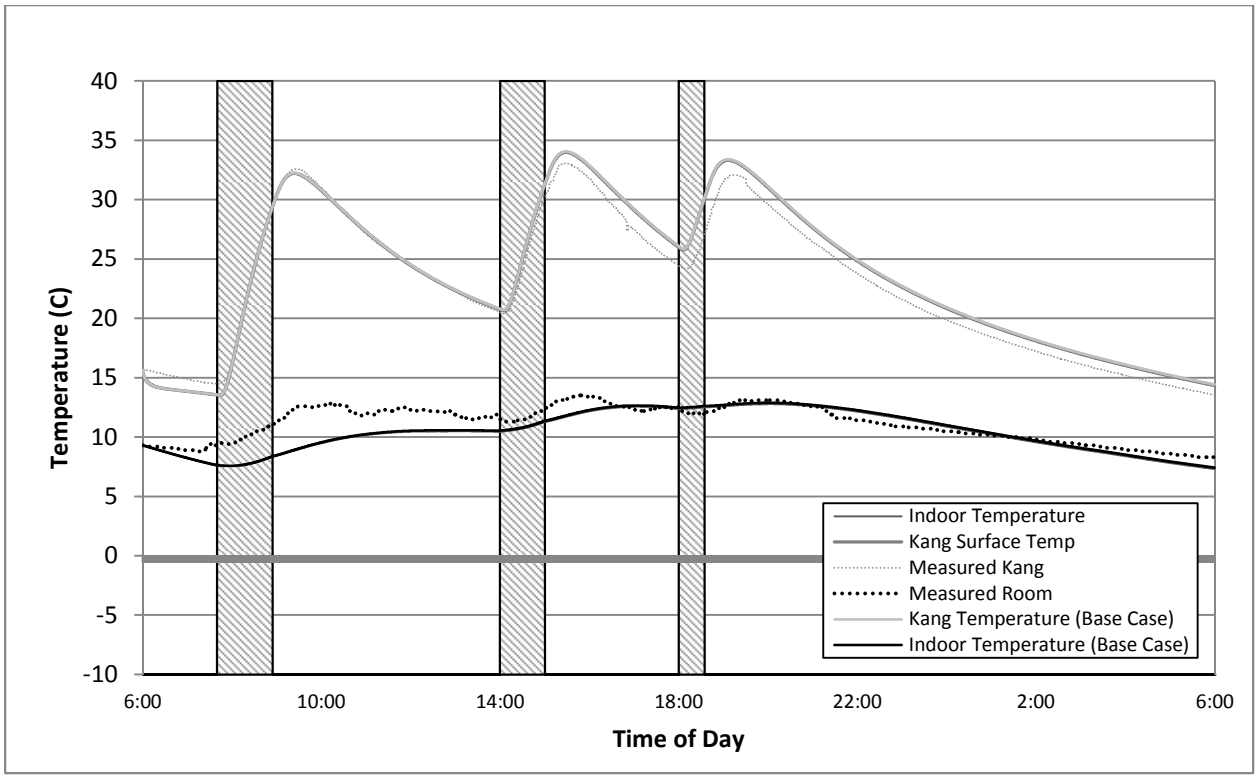

Figure 89 - Component Temperature Profile - Adjacent Room Temperature (-20%)

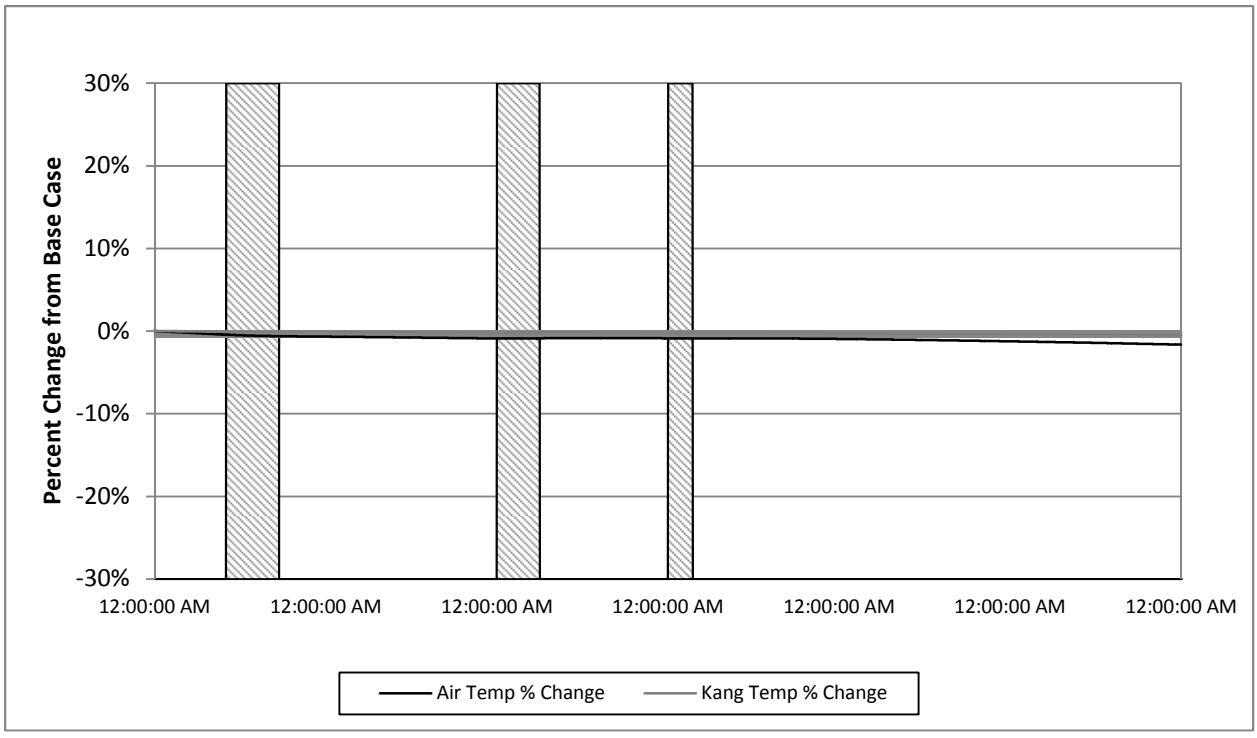

Figure 90 - Adjacent Room Temperature (-20%)

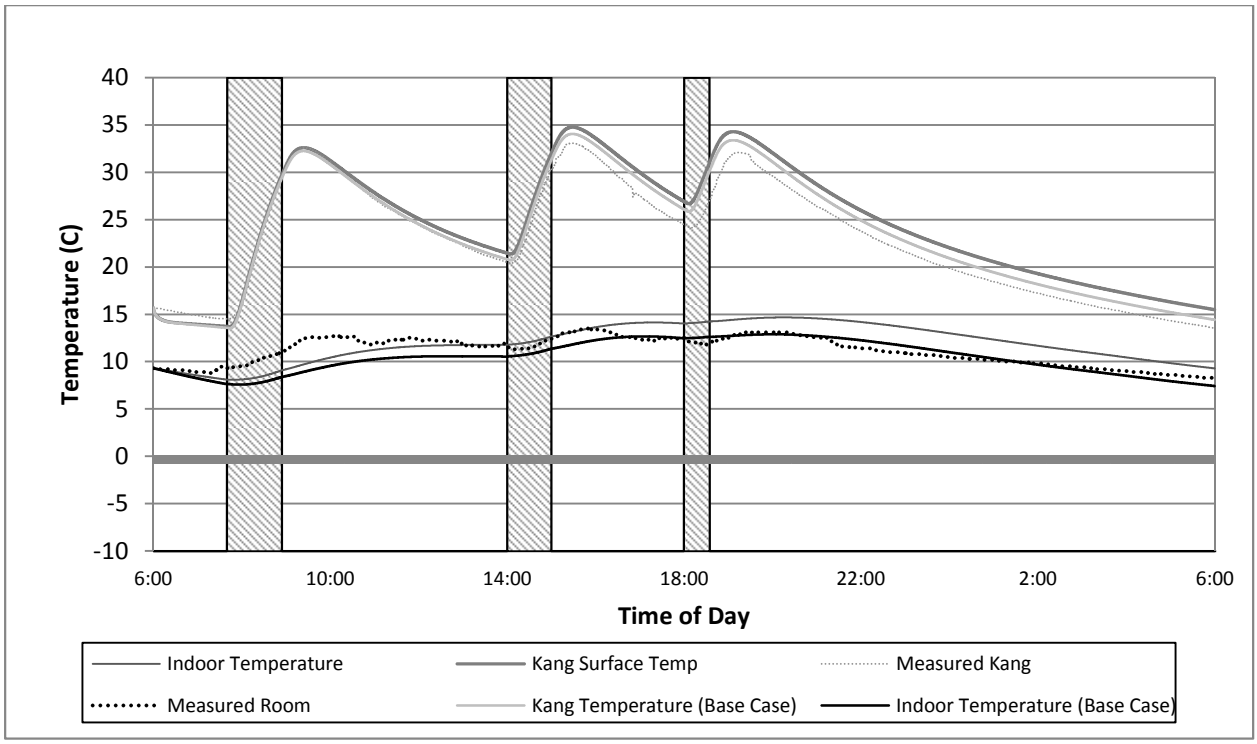

Figure 91 - Component Temperature Profile - BLC (-20%)

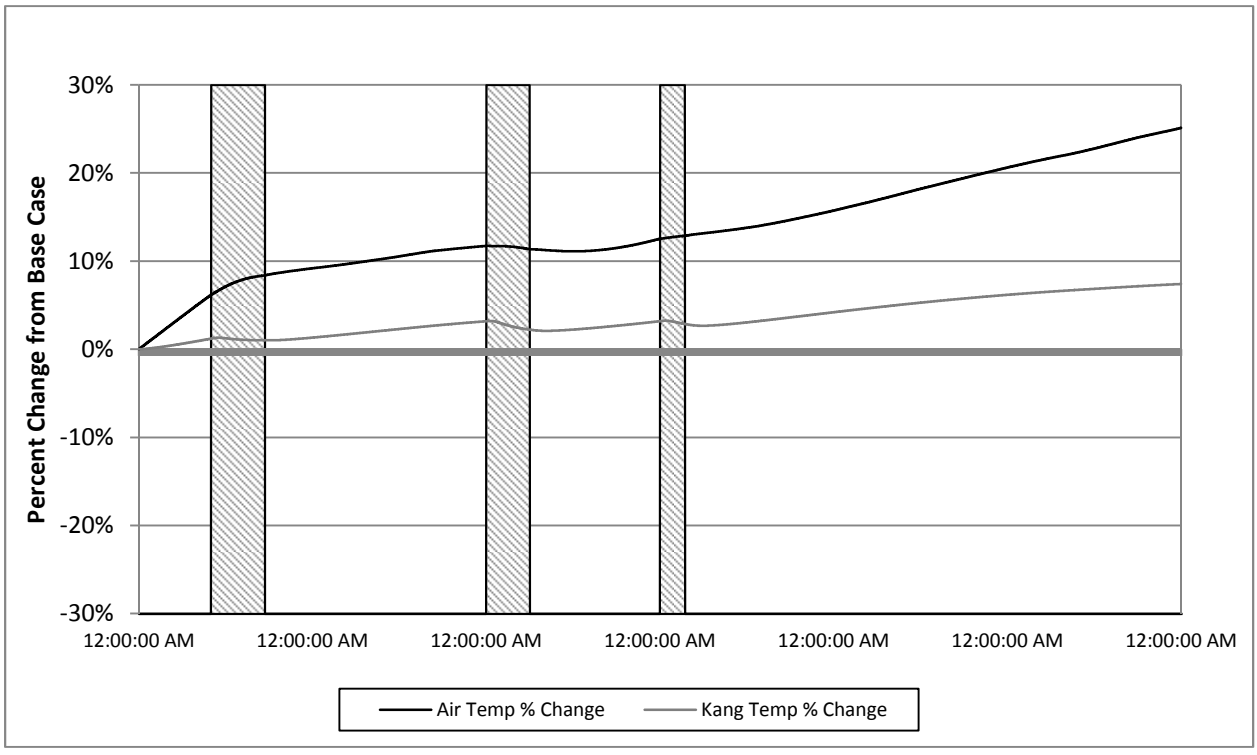

Figure 92 - BLC (-20%)

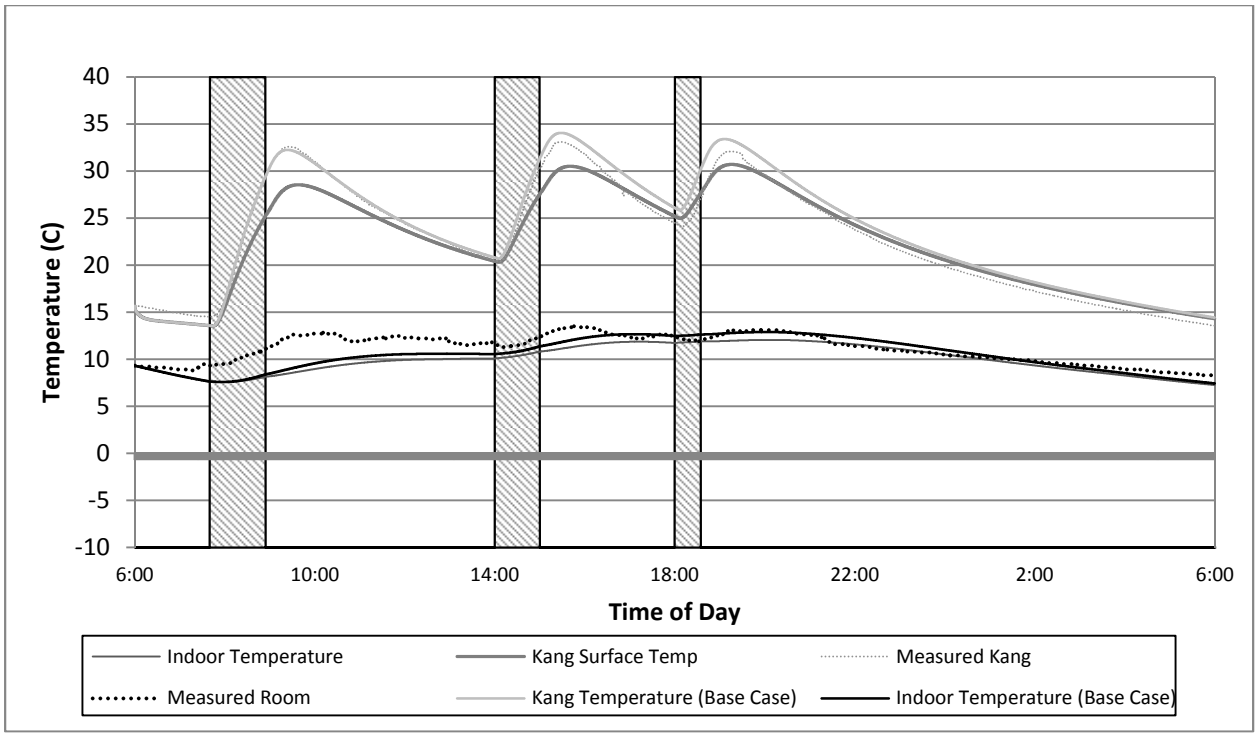

Figure 93 - Component Temperature Profile - Smoke Temp (-20%)

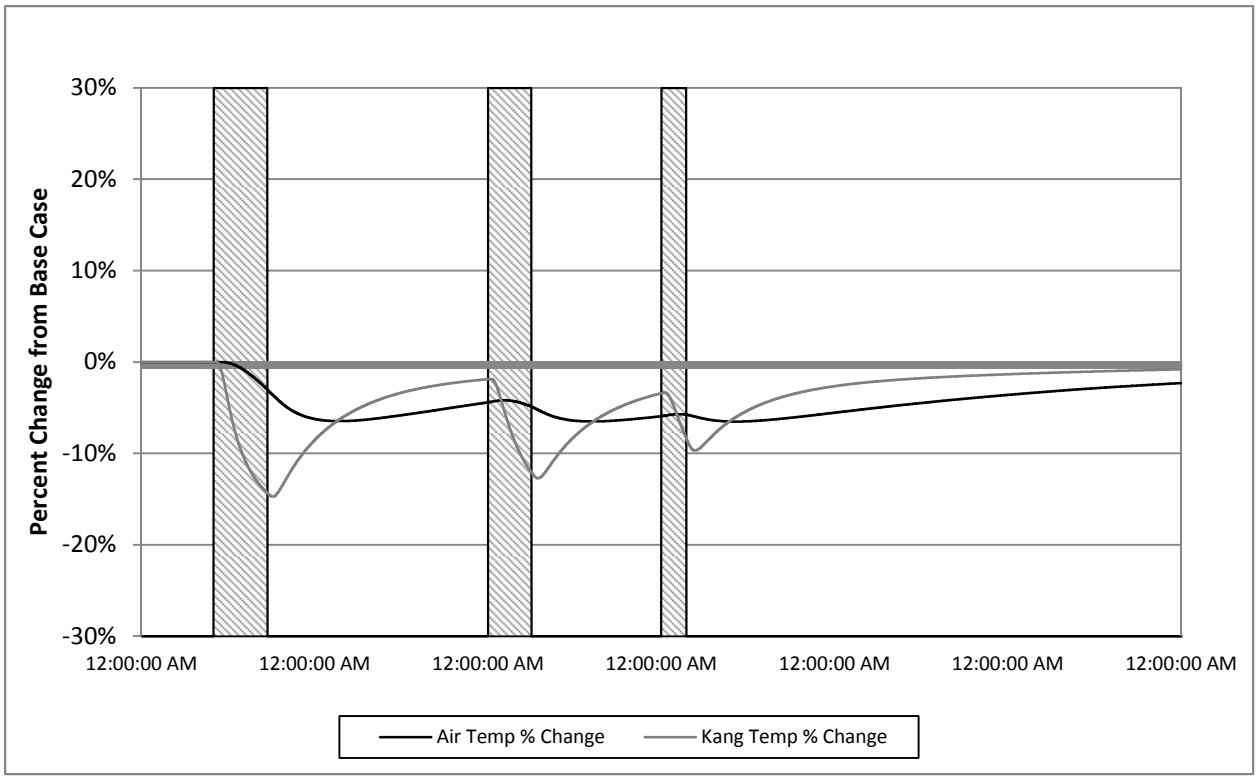

Figure 94 - Smoke Temp (-20%)

Appendix C – Program Inputs

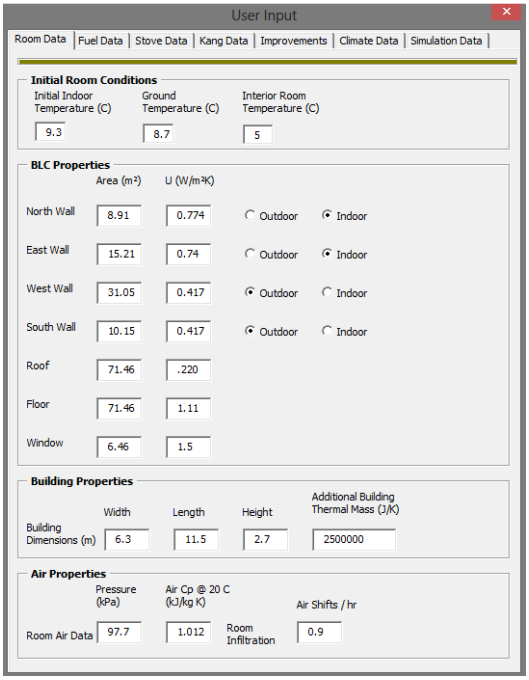

Figure 95 - Room Data Tab

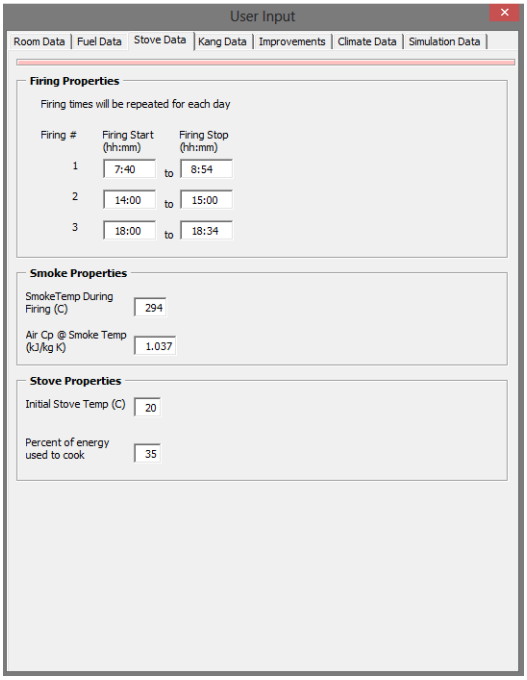

Figure 97 - Stove Data Tab

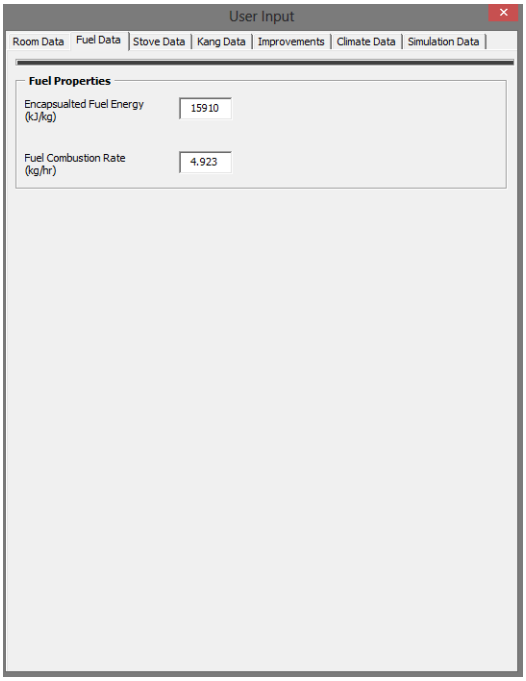

Figure 96 - Fuel Data Tab

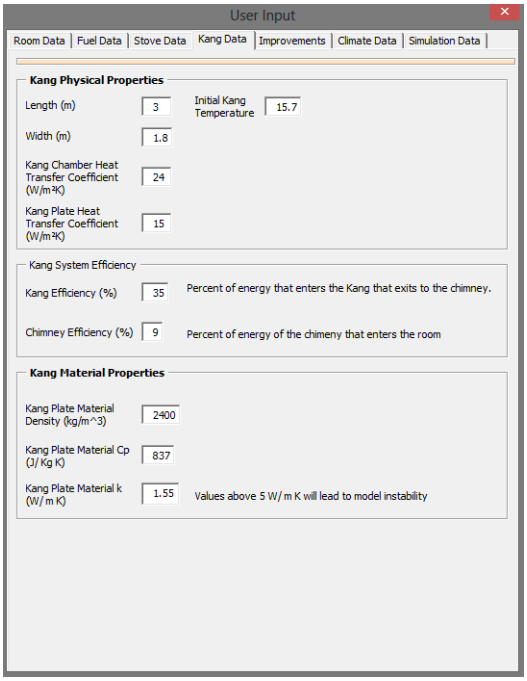

Figure 98 - Kang Data Tab

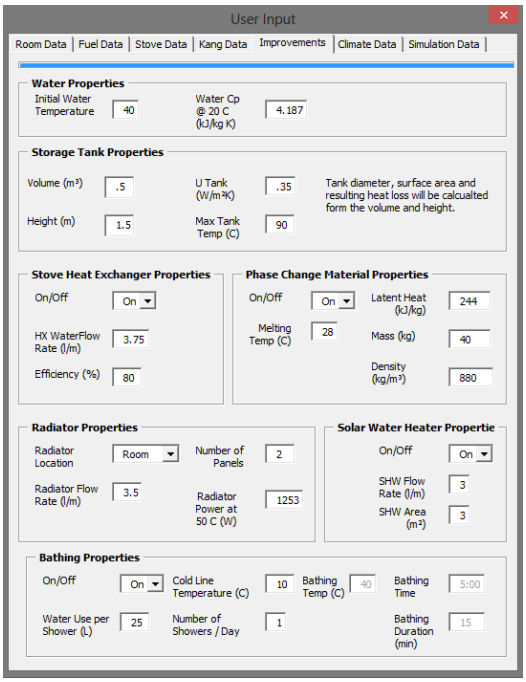

Figure 99 - Improvement Tab

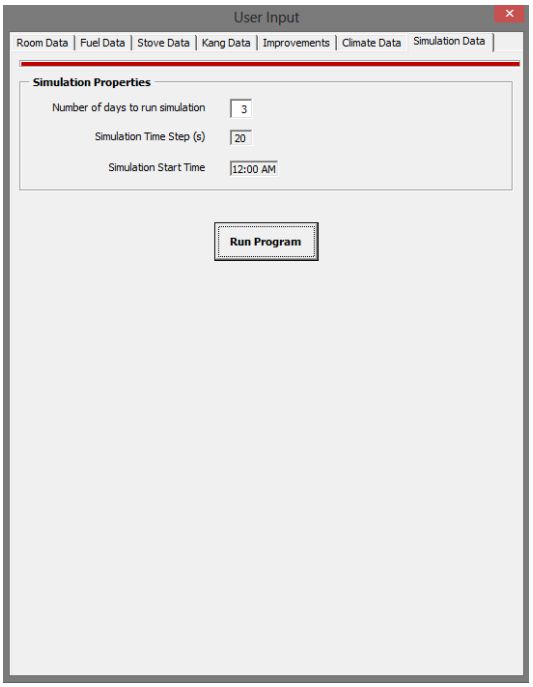

Figure 101 - Simulation Tab

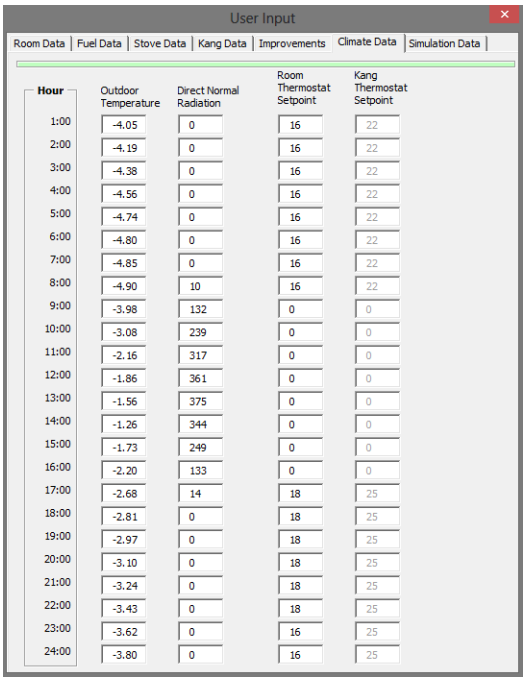

Figure 100 - Climate Data Tab

Appendix D – Diagrams of possible domestic improvements

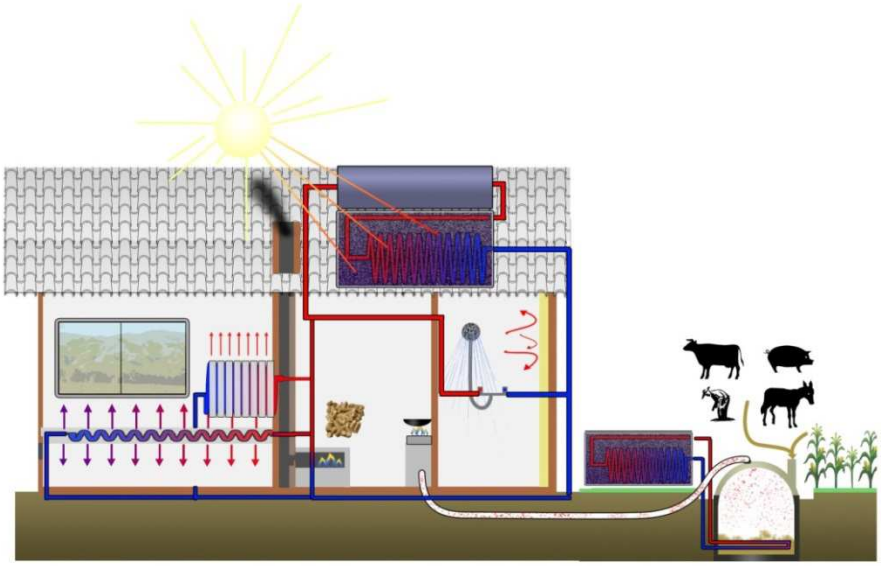

Figure 102 -Traditional home with water Kang, improved windows, building insulation, domestic hot water system, biomass-fired boiler based radiative heating, modern gas stove and biogas reactor

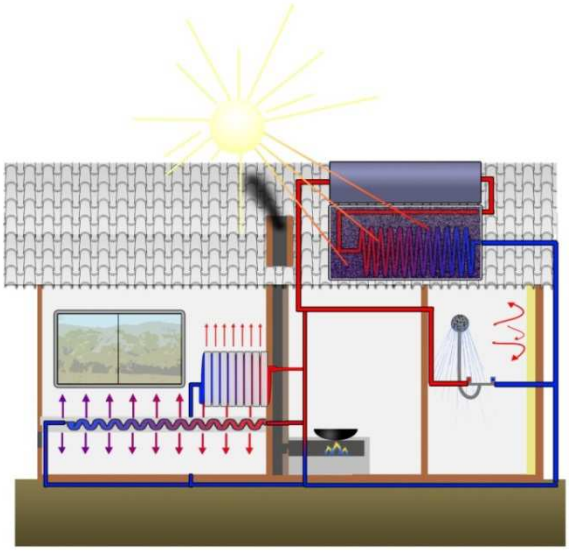

Figure 103- Traditional home with water Kang, improved windows, building insulation, domestic hot water system stove based radiative heating

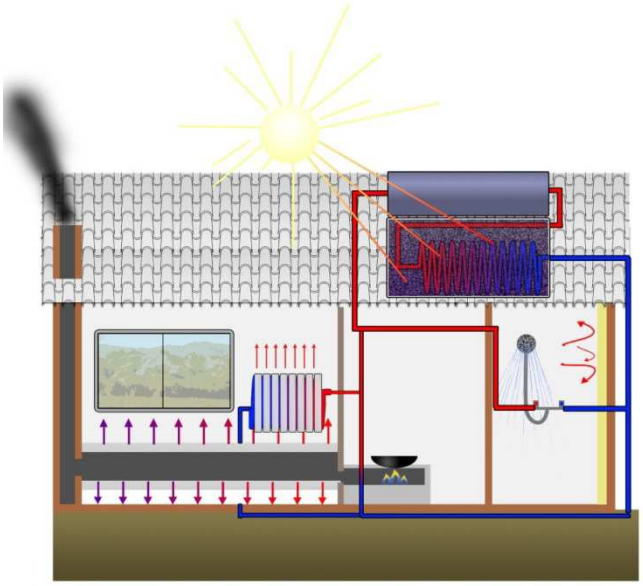

Figure 104 -Traditional home with elevated Kang, improved windows, building insulation, domestic hot water system and stove based radiative heating

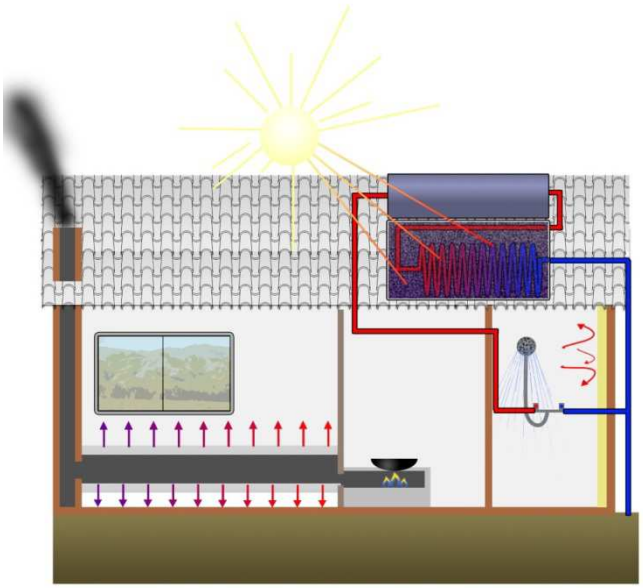

Figure 105 -Traditional home with elevated Kang, improved windows, building insulation and domestic hot water system

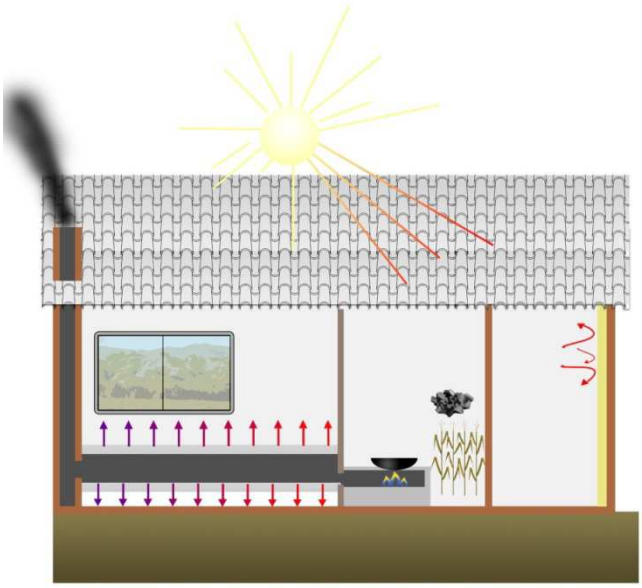

Figure 106 - Traditional home with elevated Kang, improved windows and building insulation

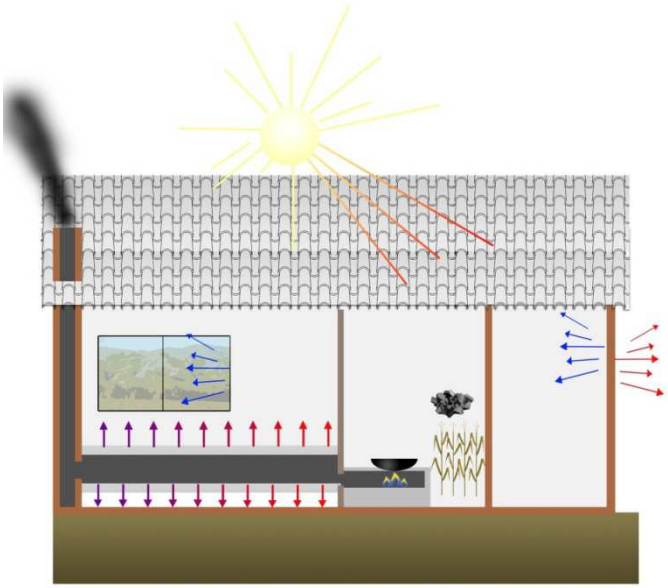

Figure 107 - Traditional home with elevated Kang

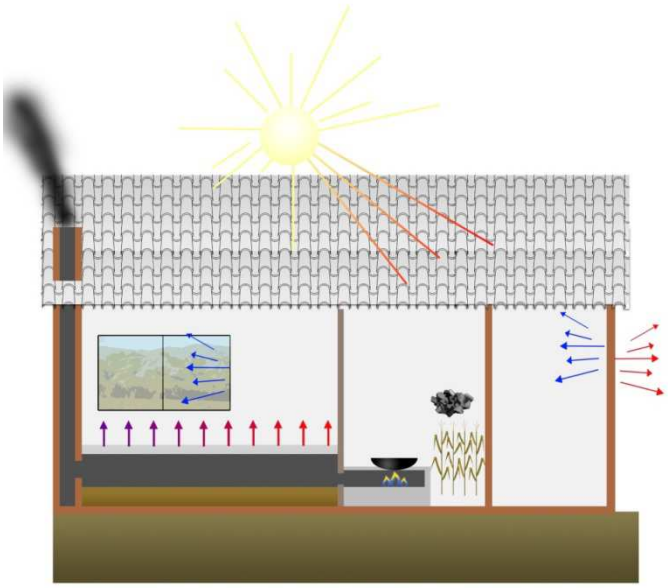

Figure 108 - Traditional home with ground Kang

Appendix E– Questions for Chengde Residents

Basic Data

How long have you lived in this area?

How long have you lived in this house?

Do you plan on staying in this house for a long time?

Can you generally describe your daily routine?

General Data

What is your general feeling about your home?

What is the greatest difficulty or frustration regarding your home?

Is your home comfortable?

How is the temperature inside during the winter?

How is the air quality inside during the winter?

How often are you in your house? During the winter? During the summer?

Technical Data

What do you think about your stove? Kang? Do they work well?

What can you tell me about the fuel you use? Is it expensive? Is it abundant? Is it dirty?

How do you feel about changing items in your home? Would you like new technology if it made you more comfortable?

Would you be willing to change your habits and routines if you had new technology?

Do you have money to buy improvements? If the government assists, would you be interested in buying improvements